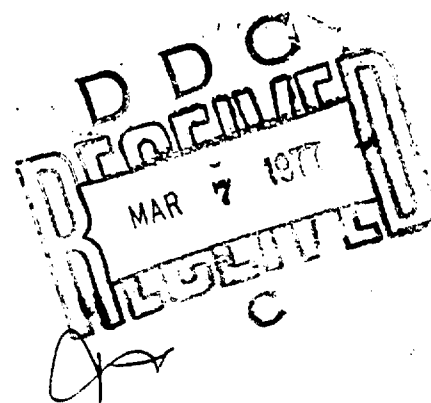


ADA 037035

MOST Project 72
NRL TRANSLATION NO. 130

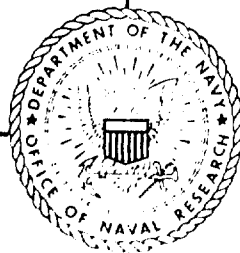
(1)

HANDBOOK FOR THE CALCULATION OF SOUND PROPAGATION PHENOMENA



COPY AVAILABLE TO THE PUBLIC DOES NOT
PERMIT FULLY LEGIBLE PRODUCTION

DISTRIBUTION STATEMENT A
Approved for public release;
Distribution Unlimited



NAVAL RESEARCH LABORATORY

WASHINGTON, D.C.

Best Available Copy

14) NRL-Trans ~~XXXXXXXXXX~~ -130

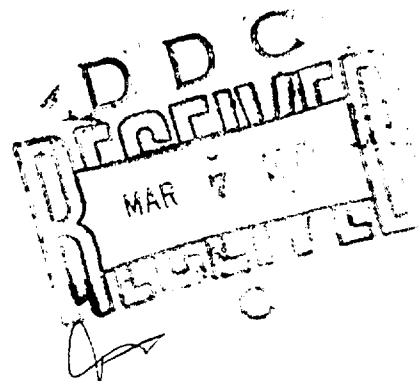
11) NOV 47

12) 141 p.

6) HANDBOOK FOR THE CALCULATION OF SOUND
PROPAGATION PHENOMENA,

by

10) Dr. Heinrich Stenzel



21) Translated November, 1947 by A. R. Stickley from
Leitfaden zur Berechnung von Schallvorgängen
published by Julius Springer, Berlin, (1939)

~~Property of the U. S. Navy. To be~~

~~used for Governmental purposes only~~

DISTRIBUTION STATEMENT A

Approved for public release,
Distribution Unlimited

Naval Research Laboratory
Washington, D. C.

Best Available Copy

251 950

Translator's Acknowledgements

Because of the appearance of certain inconsistencies in this handbook, it has seemed advisable to add a series of explanatory notes as an aid to the reader. Much help in the preparation of these notes has been furnished by Mr. P. N. Arnold and Mr. B. D. Simmons of the Sound Division who, in numerous cases, suggested clarifying changes in the text and furnished considerable help in working out the English equivalent of the German jargon in this field. Aid in the latter respect has also been furnished by Dr. Elias Klein. Finally, indebtedness is expressed to Mrs. Adele Mayfield of the Transducers Section for her painstaking work in the arduous task of preparing the manuscript for publication.

ACCESSION for		
NTIS	Write Section	<input checked="" type="checkbox"/>
DTIC	Diff Section	<input type="checkbox"/>
UNANNOUNCED		<input type="checkbox"/>
JUSTIFICATION <i>Per ltr.</i>		
<i>on file</i>		
BY		
CONTRIBUTOR/AVAILABILITY CODES		
Dist.	AVAIL. and/or SPECIAL	
<i>A</i>		

PRECEDING PAGE BLANK-NOT FILMED

TABLE OF CONTENTS

Translator's Acknowledgements	Page iii
Introduction	vii

Part One

THE SOUND FIELD AT A GREAT DISTANCE FROM THE RADIATOR

1. Non-directional (Ungebündelte) radiation	1
2. Beamed (Gebündelte) radiation	5
A. The directional characteristic	5
(a) For a definite frequency	5
(b) For a noise	31
(c) with artificial compensation	35
B. The radiation factor	42
(a) At a fixed frequency	42
(b) With artificial compensation	52

Part Two

THE SOUND FIELD IN THE NEIGHBORHOOD OF THE RADIATOR

3. The group of two radiators	58
4. The circular piston membrane	70

Part Three

THE SOUND FIELD OF THE SPHERICAL RADIATOR

5. The simple spherical radiator of definite order	90
6. The compound spherical radiator	96
7. The disturbance of a sound field caused by a rigid sphere	115
(a) The derivation of the general formula	115
(b) The sound reflection on rigid sphere	116
(c) The sound field in the neighborhood of a sphere	120
Tables	127
Literature	133

Introduction

The complete calculation and representation of sound fields involves considerable difficulties even in the cases of simple radiator arrangements. For this reason, no systematic treatment of the subject is available to the author's knowledge. In the following treatment, an attempt is made to develop the basic formulae and concepts and to apply them practically in a series of simple examples. Due to the extraordinary simplification, it appears justifiable at first to confine the calculation to a region at a great distance from the radiator. With this limitation, the transition from the non-directional to the directional radiator is made very simply when the formulae for the non-directional sound emitter are modified by an additional factor designated as the directional characteristic or the radiation factor. Also, with this simplification, the calculation of the sound field of membranes (which, in contrast to the piston membrane, do not need to have constant vibration amplitudes and may possess nodal lines) then encounters no particular difficulties.

The second part treats the representation of the sound field in the immediate neighborhood of the radiator. The case first investigated, that of two point radiators, shows that even here substantially more complicated circumstances exist. One is therefore forced to describe the sound field at every point. This is done most simply when the constant pressure amplitude curves are drawn. In the case of the circular piston membrane, which is of considerable practical significance, the values on the normal axis and also in the immediate neighborhood of the membrane can be very plainly stated. From the fact that, with diameters increasing in relation to the wavelength, an ever increasing number of null values and maximum values result on the axis, it follows that the piston membrane with increasing radius produces no sound field even in the axis neighborhood comparable with a plane sound wave. In the cases where the diameter is not too great in relation to the wave length, the calculations of the sound field can generally be carried out at nearby points. The graphical representation of the curves of constant pressure amplitude provides a simple conspectus of such sound fields.

The spherical radiators which are treated in Part Three have a particular significance. For sound velocity amplitudes given on the sphere, the sound field can be calculated even for nearby field points. It is shown in a series of examples that the formulae, which at first appear involved, are quite useful for practical calculation.

In order to avoid a complicated appearance of the text, the theoretical derivations are given only in so far as is necessary for comprehension, and references are given to the existing literature for the remainder. Also, for simplicity, the calculation and representation of the sound velocity amplitudes are avoided and only the pressure amplitude is used to describe the sound field. Thereby the use of the velocity potential is completely avoided since the concept possesses mainly a mathematical significance and according to experience provides no pleasure for the practical physicist.

All considerations are based on a given velocity amplitude of the vibrating membrane; or, what amounts to the same thing, a definite sound velocity amplitude immediately before the membrane (imagined stationary) is prescribed.

Part One

THE SOUND FIELD AT A GREAT DISTANCE FROM THE RADIATOR

1. Nondirectional radiation

We start with radiators of zero order, i.e., with radiators whose radiating surface moves cophasally outwards and inwards.

The simplest case is a breathing or pulsating sphere (Fig. 1-a). Here the velocity amplitude is the same for all points of the radiating surface. In general, the motion of the radiating surface is described by the behavior of the velocity amplitude $w = w \cdot e^{i\omega t}$ of the membrane. w will in general be different at different points of the radiating surface.

It is advantageous to introduce the velocity amplitude w instead of the displacement amplitude a (for which the relation $w = 2\pi n a$ exists) since the latter achieves a particular significance only in very infrequent cases.

We first consider the series of radiator forms represented in Fig. 1. The radiators 1-a to 1-d are rotationally symmetric about a vertical axis through the center. The radiators 1-e to 1-g are likewise rotationally symmetric or have a rectangular cross section like 1-h. The rest position of the membrane is indicated by a heavy broken line, the position of maximum displacement is dotted, and the rigid supporting wall is indicated by a solid line. The maximum amplitudes of the periodically (sinusoidally) moving membrane are indicated by the greatly enlarged arrows. The linearity of the general wave equation depends on the assumption that the pressure and velocity amplitudes of the sound field be small. This assumption is fulfilled in practice except for unusually strong pressure variations (e.g., explosion waves). Furthermore, the separation of those membranes vibrating symmetrically with respect to the middle plane (e.g., in Figs. 1-e and 1-f) is assumed so small that the membrane zero position can be regarded as practically coincident with this middle plane.

It then turns out that the sound field can be very simply determined if the two following assumptions are fulfilled:

- A. The dimensions of the radiator in every direction are small compared to the wave length.

B. The field point lies at a sufficiently great distance from the radiator.

From the general formulae (to be explained later) it then follows that the behavior of the sound pressure is represented in the simple form:

$$p_0 = p_0 e^{i(\omega t - kr + \pi/2)} \quad (1)$$

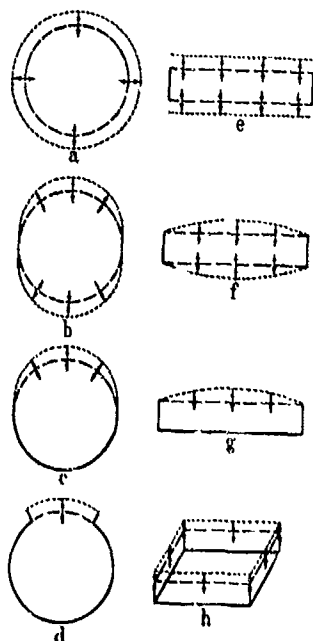
where the sound pressure amplitude p_0 is given by

$$p_0 = \frac{c \cdot \sigma \cdot F \cdot w_m}{2\lambda r} \quad (2)$$

and the total radiated sound power L_0 by

$$L_0 = (p_0^2 / 2c\sigma) 4\pi r^2 = \frac{1}{2} c \cdot \sigma \pi \cdot \frac{F^2 \cdot w_m^2}{\lambda^2} \quad (3)$$

We see that the pressure amplitude is described in a very simple manner by the standard quantities and that each of these quantities appears linearly. The significance of the various symbols is as follows:



- σ is the density of the medium
- c is the velocity of sound in the medium
- F is the total radiating surface¹
- w_m is the mean velocity amplitude of the radiating surface
- r is the distance of the field point from the center of the radiator
- λ is the wave length
- k is the wave number ($2\pi/\lambda$) and
- ω is the circular frequency $2\pi\nu$.

The product $c \cdot \sigma$ is termed the specific acoustic resistance. For plane waves its magnitude is determined by the ratio of the sound pressure amplitude to the sound velocity amplitude. For the two values with which we are principally concerned, those for air and water, we have 43 and 1.5×10^5 absolute C.G.S. units respectively as the value of $c \cdot \sigma$.

Fig. 1 Simple radiators

In the general case the velocity amplitude $w(x, y, z)$ varies for the individual points of

¹ For membranes which vibrate in a rigid wall we will denote the surface radiating into the half space by F so that the "2" in the denominator of equation 2 drops out.

the membrane. In this case w_m is given by

$$w_m = \frac{1}{F} \int w(x, y, z) dF. \quad (4)$$

The influence of the membrane is given by the product $F \cdot w_m$. If we define the volume swept by the oscillating surface during each half period as the deformation volume of the radiator, then two radiators of equal frequency have equal deformation volumes if the product $F \cdot w_m$ has the same value for both. This is so since the displacement amplitude $a(x, y, z)$ differs from the velocity amplitude $w(x, y, z)$ only by a constant factor ($w = 2\pi n \cdot a$).

From the fact that the quite varied vibration forms of Figs. 1-a to 1-h produce the same sound field for equal values of $F \cdot w_m$, we will quite generally conclude: For radiators which are small compared to the wave length and whose membrane motion takes place in phase, the sound field at a comparatively great distance is determined by the formulas (1), (2), and (3). This means that under assumptions A and B two sound radiators for which the frequency and the product $F \cdot w_m$ are identical, produce the same sound field, independently of the separate values of displacement amplitude and radiating surface. In Fig. 2 three different radiators corresponding to Fig. 1-e and 1-f are represented with equal deformation volumes, i.e., equal values of $F \cdot w_m$.

The shaded surfaces represent the maximum amplitudes in one direction of the vibrating membranes in two mutually perpendicular planes. The velocity amplitude corresponding to that of Fig. 2-b is given by $w = (1 - q^2/q_0^2)^{1/2}$. Then for the three (3) cases of Fig. 2 the equal values

$$\frac{1}{3} q_0^2 \pi, 2\pi \int_0^{q_0} (1 - q^2/q_0^2)^{1/2} q dq = \frac{1}{3} q_0^2 \pi, \frac{a^2 \pi}{6} = \frac{1}{3} q_0^2 \pi. \quad (4a)$$

result for $F w_m$.

It is advantageous to set up a simple example as a standard form since from it the sound pressure can be specified under quite general conditions because of the linear influence of all of the independent variables. As such a standard form we consider a piston membrane in a rigid wall which produces a sound pressure amplitude of 1 dyne/cm² at a frequency of 800 cps on the normal axis at 100 cm distance (which corresponds to the sound pressure amplitude for normal speech immediately in front of the mouth of the speaker). We thus find that with a velocity amplitude of 10 cm/sec the surface radiating into the half space must be 10 cm². It is to be particularly noted that formula 2 is valid for all plane beamed radiator arrangements if the field point lies on the normal axis at a sufficient distance from the radiator.

This will be explained in the next chapter. Therefore a radiating surface of 100 cm^2 also produces a sound pressure amplitude of 1 dyne/cm^2 at a field point 10 m distant on the normal axis. Finally, the formula is likewise valid² for a spherical radiator of zero order for a sufficient distance of the field point.

The corresponding sound power per cm^2 for the standard form is (according to 3)

$$\frac{L_0}{4\pi r^2} = \frac{1}{2 \cdot 43} = 1,16 \cdot 10^{-2} \text{ erg/sec cm}^2 = 1,16 \cdot 10^{-9} \text{ Watt/cm}^2. \quad (4b)$$

In water the sound pressure amplitude $p_n = 800 \text{ dynes/cm}^2$ results for the same assumptions (with the same frequency - therefore a different wave length) and the sound power becomes

$$\frac{L_0}{4\pi r^2} = \frac{8^2 \cdot 10^4}{2 \cdot 1,5 \cdot 10^6} = 2,13 \text{ erg/sec cm}^2 = 2,13 \cdot 10^{-7} \text{ Watt/cm}^2. \quad (4c)$$

One thus sees what a decisive influence the "sound resistance" (specific acoustic resistance) exerts. In order for the membrane to impress the same velocity amplitude in water as in air at the same frequency 184-fold power must be produced. On the other hand for a membrane which is to radiate at an equal wave length the same power in air as in water it follows that

$$\frac{w_l}{w_w} = \sqrt{\frac{1,5 \cdot 10^6}{43}} \sim 60, \quad (4d)$$

i.e., the velocity amplitude w_l of the membrane in air is then 60 times as great as the velocity amplitude w_w in water while the displacement amplitude of the membrane in air is about 13 times as great as that in water.*

² This is so with the provision of Note 1.

* That the number $13(60/4.5)$ should be changed to $270(60 \cdot 4.5)$ is shown by the following:

Using the statement made at the end of the paragraph following eq. 4, one has from eq. 4d:

$$\frac{w_l}{w_w} = \frac{2\pi n_l a_l}{2\pi n_w a_w} \approx 60 \quad \text{or} \quad \frac{a_l}{a_w} \approx \frac{n_w}{n_l} \cdot 60$$

Since λ is to be constant for the two cases, we have $\lambda = \frac{c_w}{n_w} = \frac{c_l}{n_l}$ or $\frac{n_w}{n_l} = \frac{c_w}{c_l} = 4.5$. Hence $\frac{a_l}{a_w} \approx 60 \cdot 4.5 = 270$.

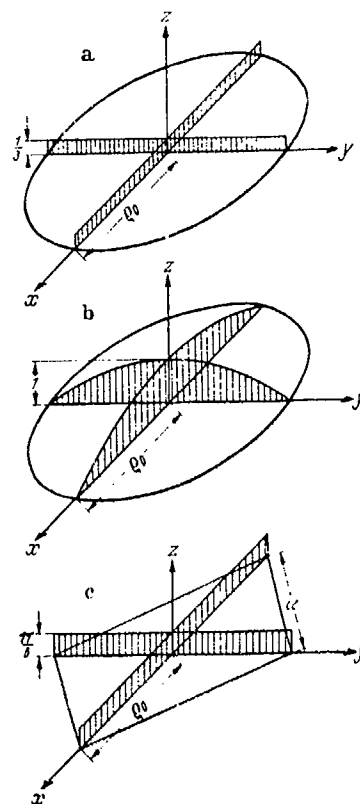


Fig. 2. Radiators with equal deformation volumes.

2. Beamed Radiation

A. The directional characteristic

(a) For a definite frequency

We now drop assumption (A) but impose instead the condition that the membrane vibrates as a double membrane cophasally toward the two sides - the middle plane at every moment of the vibration being the symmetry plane. Examples of such membranes are represented in Figs. 1-e and 1-f. Since the whole process above the symmetry plane represents the process below the symmetry plane, a rigid wall can be introduced at the position of the symmetry

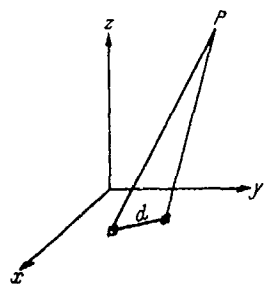


Fig. 3. Nondirectional radiation.

plane without changing the sound process in any way. In place of the double-sidedly acting membrane, one can then just as well imagine the one half of the sound field produced by a simple membrane vibrating in a rigid wall. This is significant since a membrane vibrating in a large rigid wall appears in practice rather frequently. Without particular emphasis in every case it is assumed in the following examples that the radiating surface consists of such double membranes vibrating symmetrically to the central plane or of membranes vibrating in a rigid wall for which only the one half space is considered which is cut off by the rigid wall and into which the one half of the membrane with the surface F radiates. If we imagine that the elementary waves produced by the individual elements of the radiator act together (as point sources) at the field point, it is then clear that the concurrent action in uniform phase at far distant field points prevails for all directions as long as the individual elements are at a distance d from one another which is small compared to λ .³ Otherwise, the elementary waves arrive at the field point with a phase difference which is no longer negligible (Fig. 3) with a resulting lack of spherical symmetry. We can take account of the latter conditions

³ The qualifying condition here would rather seem to be that the over-all dimension of the radiating ensemble be small compared to λ . The statement in the text could be construed to mean this if d were taken to represent the distance between any two elements (including the two most distant elements) instead of being merely the distance between two adjacent elements as is shown in Fig. 3.

by applying the directional characteristic \mathfrak{R} . hence in place of (2) we have the formula

$$p = p_0 \cdot \mathfrak{R}, \quad (5)$$

wherein p_0 has the value given by (2) while \mathfrak{R} is defined as the integral over the surface F :

$$\mathfrak{R} = \frac{1}{w_m \cdot F} \int_F w(x, y) \cdot e^{ik(x \cos \alpha + y \cos \beta)} dF. \quad (6)$$

Here the rigid wall with the membrane (in the position of rest) is thought to be in the plane of the coordinate system. Since the XY-plane is the symmetry plane for the sound field, we can confine our considerations to the space lying above the XY-plane and therefore disregard the symmetrically downward oscillating part of the double membrane (Fig. 4).

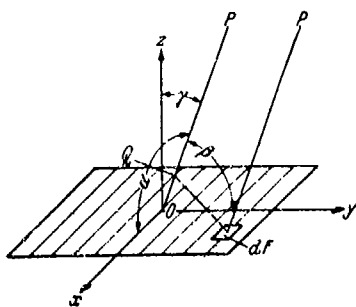


Fig. 4. Beamed radiation.

Let α , β and γ be the direction angles for the corresponding field point line, x and y the coordinates of the point belonging to the element of integration dF , $w(x, y)$ the corresponding velocity amplitude and let $k = 2\pi/\lambda$. We note that if the wave length λ is great compared to x and y - i.e., great compared to the dimensions of the membrane - the exponent under the integral approaches zero so that

$$\mathfrak{R} = \frac{1}{w_m \cdot F} \int_F w(x, y) dF \quad (6a)$$

and therefore by (4) becomes equal to 1 as was to be expected. As has already been indicated, it is essential to note that \mathfrak{R} likewise becomes 1 for a large F if the field point line coincides with the Z -axis (since $\alpha = 90^\circ$ and $\beta = 90^\circ$).

The validity of (5) results from the general basic relation (for a surface F on an infinite plane) given by Rayleigh⁴:

⁴ The Theory of Sound, Sec. 278.

$$\varphi = -\frac{1}{2\pi} \int_F \frac{\partial \varphi}{\partial n} \frac{e^{-ikr}}{r} dF. \quad (7)$$

When we introduce the pressure

$$p = -\sigma \frac{\partial \varphi}{\partial t} \quad (8)$$

in place of the velocity potential φ and replace the normal velocity $\frac{\partial \varphi}{\partial n}$ by

$$w = w(x, y) e^{i\omega t} \quad (9)$$

we immediately obtain

$$p = \frac{i \cdot c \cdot \sigma}{\lambda} e^{i\omega t} \int_F w(x, y) \frac{e^{-ikr}}{r} dF. \quad (10)$$

We will now consider the sound field at a great distance from the radiating surface and accordingly assume that the field point P is at a sufficient distance R from O so that the connecting lines from it to the individual radiator elements dF can be regarded as parallel. (A more accurate formulation will be given later (p. 59).) If we then drop a perpendicular from dF which is determined by the coordinates (x, y) to OP intersecting OP at Q then $OQ = x \cos \alpha + y \cos \beta$ and $r = R - (x \cos \alpha + y \cos \beta)$.

Since $R \gg x \cos \alpha + y \cos \beta$ we can replace r by R in the denominator and obtain:

$$p = \frac{i c \sigma}{\lambda R} e^{i(\omega t - kR)} \int_F w(x, y) e^{ik(x \cos \alpha + y \cos \beta)} dF \quad (11)$$

and from this, considering (2), (4), and (6), there results the formula (5).

⁵ Here the symbol r designates the distance from the field point to the surface element whereas the same symbol, as employed in equations (1) and (2), signifies the distance from the field point to the center of the radiator (see the list of definitions on p. 2).

We shall assume for what follows that the radiating surface or the radiating system possesses a point of symmetry, which coincides with the coordinate origin, such that $w(x, y) = w(-x, -y)$. (That is, two membrane points situated in image fashion with respect to the membrane point of symmetry have the same amplitude and phase.) The integral (11) may then be written in the real form:*

$$\Re = \frac{1}{w_m F} \int_F w(x, y) \cos[k(x \cos \alpha + y \cos \beta)] dF. \quad (11a)$$

We will furthermore confine the field point line to a definite plane (the measuring plane (die Peilebene)) which is to coincide with the ZY-plane. Then since $\alpha = 90^\circ$ and $\beta + \gamma = 90^\circ$ (Fig. 4)

$$\Re = \frac{1}{w_m F} \int_F w(x, y) \cos[ky \sin \gamma] dF. \quad (12)$$

In many cases, interest in the behavior of \Re does not extend to the whole measuring plane but, particularly with sharply beamed radiators, only to the immediate neighborhood of the principal maximum at $\gamma = 0^\circ$.

For this range $\cos[ky \sin \gamma]$ can be replaced by $1 - \frac{1}{2} k^2 y^2 \sin^2 \gamma$ and it is found that

$$\Re = 1 - \frac{k^2 \sin^2 \gamma}{2 w_m F} \int_F w(x, y) y^2 dF. \quad (12a)$$

If we imagine the radiating surface element dF at the point (x, y) of the membrane replaced by an element of mass

$$dm = \frac{w(x, y)}{w_m F} dF \quad (12b)$$

then

$$T_z = \frac{1}{w_m F} \int_F w(x, y) y^2 dF = \int_F y^2 dm \quad (12c)$$

denotes the moment of inertia with respect to the X-axis of the stationary membrane thus covered with mass (total mass 1), and for small values of γ we can write

* Apparently this is the real form of eq. 6 instead of eq. 11.

$$\mathfrak{R} = 1 - \frac{1}{2} k^2 \sin^2 \gamma \cdot T_z. \quad (13)$$

This formula is often suitable for a quick determination of the directivity (die Peilschärfe) of radiator arrangements.

As an example we will investigate four simple radiator arrangements (Fig. 5):

1. Two point sources
2. The circular line densely filled with radiators
3. The rectangular piston membrane
4. The circular piston membrane

We find the moment of inertia T and the corresponding approximation formulae without difficulty:

$$\begin{aligned} 1. \quad T_1 &= r^2, & \mathfrak{R}_1 &= 1 - \frac{1}{2} k^2 \sin^2 \gamma \cdot r^2, \\ 2. \quad T_2 &= \frac{r^2}{2}, & \mathfrak{R}_2 &= 1 - \frac{1}{2} k^2 \sin^2 \gamma \cdot \frac{r^2}{2}, \\ 3. \quad T_3 &= \frac{r^2}{3}, & \mathfrak{R}_3 &= 1 - \frac{1}{2} k^2 \sin^2 \gamma \cdot \frac{r^2}{3}, \\ 4. \quad T_4 &= \frac{r^2}{4}, & \mathfrak{R}_4 &= 1 - \frac{1}{2} k^2 \sin^2 \gamma \cdot \frac{r^2}{4} \end{aligned} \quad (13a)$$

For these four cases the directional characteristics may be generally calculated by carrying out the integration in Eq. (6)⁷. There results (see Fig. 5)⁸:

$$\mathfrak{R}_1 = \frac{e^{ikr \sin \gamma} + e^{-ikr \sin \gamma}}{2} = \cos \left[\frac{2\pi r}{\lambda} \sin \gamma \right], \quad (14)$$

Fig. 5. Calculation of the directional characteristic

$$\begin{aligned} \mathfrak{R}_2 &= \frac{2}{2\pi r} \int_0^{2\pi} e^{ik(x \cos \alpha + y \cos \beta)} ds \\ &= \frac{1}{2\pi} \int_0^{2\pi} e^{ikr \sin \gamma \cos \varphi} d\varphi = J_0 \left(\frac{2\pi r}{\lambda} \sin \gamma \right), \end{aligned} \quad (15)$$

⁷ Electr. Nachr. Techn., Vol. 4 (1927), pp. 239-253.

⁸ From equations (13a), the following meanings of r are to be inferred:
 r = one-half distance between elements, for two point sources,
 r = radius, for ring and piston,
 r = one half the side of the square piston membrane.

$$\mathfrak{R}_3 = \frac{1}{2r} \int_{-r}^{+r} e^{ik y \sin \gamma} dy = \frac{\sin\left(\frac{2\pi r}{\lambda} \sin \gamma\right)}{\frac{2\pi r}{\lambda} \sin \gamma}, \quad (16)$$

$$\mathfrak{R}_4 = \frac{1}{r^2 \pi} \int_0^r \rho d\rho \int_0^{2\pi} e^{ik \rho \sin \gamma \cos \varphi} d\varphi = \frac{2}{r^2} \int_0^r \rho d\rho J_0(k \rho \sin \gamma) = 2 \cdot \frac{J_1\left(\frac{2\pi r}{\lambda} \sin \gamma\right)}{\frac{2\pi r}{\lambda} \sin \gamma}. \quad (17)$$

With the abbreviation $\frac{2\pi r}{\lambda} \sin \gamma = \frac{\pi d}{\lambda} \sin \gamma = x$, it is found that

$$\mathfrak{R}_1 = \cos x, \quad \mathfrak{R}_2 = J_0(x), \quad \mathfrak{R}_3 = \frac{\sin x}{x}, \quad \mathfrak{R}_4 = \frac{2J_1(x)}{x}, \quad (17a)$$

where $J_0(x)$ or $J_1(x)$ signify Bessel's functions of the zero or first order respectively. By the well-known series development the correctness of the approximation formulae may be immediately confirmed. One thus obtains

$$\cos x = 1 - \frac{x^2}{2} + \dots, \quad J_0(x) = 1 - \frac{x^2}{4} + \dots, \quad \frac{\sin x}{x} = 1 - \frac{x^2}{6} + \dots, \quad (17b)$$

$$\frac{2J_1(x)}{x} = 1 - \frac{x^2}{8} + \dots$$

In order to obtain a general measure for the directivity we will inquire as to the angle φ in the measuring plane (ZY) which the field point line forms with the Z-axis when the sound energy is reduced to half the maximum value, (i.e., the amplitude is reduced from 1 to $1/\sqrt{2}$) (Fig. 6).

We will denote this angle as the half-value beam width in this measuring plane⁹. A simple calculation then yields with sufficient accuracy for practical purposes the following simple relations:

⁹ It is here assumed that there is some directivity so that the half-value width amounts at most to 30° .

$$\begin{aligned}
\varphi_1 &= 15^\circ \lambda/d \text{ for two point sources} \\
\varphi_2 &= 20^\circ \lambda/d \text{ for the circular line} \\
\varphi_3 &= 25^\circ \lambda/d \text{ for the rectangular piston membrane} \\
\varphi_4 &= 30^\circ \lambda/d \text{ for the circular piston membrane.}
\end{aligned} \tag{18}$$

The error here is less than 1° for $\lambda = d$ and decreases proportionally for smaller values of λ .

The angles 15° , 20° , 25° , and 30° are then characteristic of the directivity. We will emphasize this by a special term - the directivity coefficient (das Peilmass). The directivity coefficient is in general different for every measuring plane. In order to obtain the directional characteristic for a measuring plane completely, the characteristic functions will be plotted as a function of x and a variable scale will be placed below the x -axis, which permits reading off the directional characteristic for each value of d/λ and each angle γ . Thus the complete behavior of the directional characteristic as a function of γ in the above four examples and for all values of d/λ which lie between 0 and 8 can be immediately ascertained from Fig. 7. If, for example, the directional characteristic for the densely covered circular line

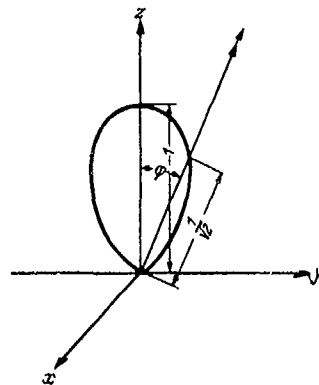


Fig. 6. Definition of the beam sharpness.

$R = J_0\left(\frac{\pi d}{\lambda} \sin \gamma\right)$ is desired for $d/\lambda = 3$, and $\gamma = 40^\circ$, one follows the line $d/\lambda = 3$ to its intersection with the 40° line and reads off the corresponding ordinate on curve 2. It is thus found that $R = +0.15$ (see the broken line in Fig. 7).

As an additional example, we mention the straight line group which consists of a number of uniform nondirectional individual radiators arranged at equal intervals on a straight line. Due to its special significance in practice, we will investigate this arrangement very closely. Let the radiators lie on the Y -axis at a distance d from each other and let them have the coordinates:

$$y_p, y_{p-1}, \dots, y_{(p-1)}, y_{-p}, \tag{18a}$$

Here the coordinate origin is to coincide with the middle radiator for an odd number of radiators ($n = 2q + 1$) and is to lie midway between the middlemost radiators for an even number of radiators ($n = 2q$). In the first case one would then set $p = q + 1$, $p - 1 = q - 2$ etc., while in the second case one would set $p = q + \frac{1}{2}$, $p - 1 = q - \frac{3}{2}$, etc., (Fig. 8).

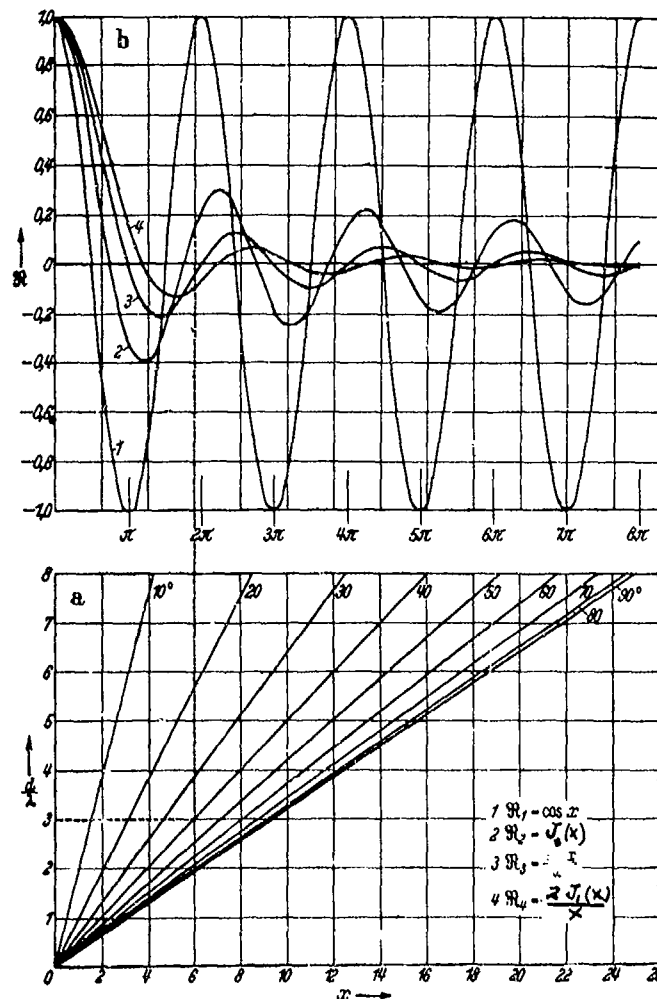


Fig. 7. General representation of the directional characteristic.

1. Directional characteristic of the system consisting of two radiators (Distance d).
2. Directional characteristic of the densely covered circular line (Diameter d).
3. Directional characteristic of the densely covered rectangular surface (Length d) in the symmetry plane.
4. Directional characteristic of the densely covered circular surface (Diameter d).

In general, then, for an arbitrary index l , the relation $y_l = ld$ is valid. If, for abbreviation, we set

$$e^{ikd \sin \gamma} = z, \quad (18b)$$

we then find the directional characteristic from (6) when we replace the integral by a summation sign

$$\mathfrak{R} = \frac{1}{n} \sum_{m=-p}^{m=+p} z^m \quad (18c)$$

The geometric series on the right may be easily summed and one obtains:

$$\mathfrak{R} = \frac{1}{n} z^{-p} \frac{z^{p+1} - 1}{z - 1} = \frac{1}{n} \frac{z^{p+\frac{1}{2}} - z^{-(p+\frac{1}{2})}}{z^{\frac{1}{2}} - z^{-\frac{1}{2}}}, \quad (18d)$$

from which follows (when $e^{ikd \sin \gamma}$ is again introduced for z)

$$\mathfrak{R} = \frac{\sin \left[\left(p + \frac{1}{2} \right) kd \sin \gamma \right]}{n \sin \left[\frac{kd}{2} \sin \gamma \right]} \quad (18e)$$

Since for odd numbers, $p + \frac{1}{2}$ is replaced by $q - \frac{1}{2} = \frac{n}{2}$ and for even numbers $p + \frac{1}{2}$ is replaced by $q = \frac{n}{2}$, the general result is that

$$\mathfrak{R} = \frac{\sin \left[\frac{n \pi d}{\lambda} \sin \gamma \right]}{n \sin \left[\frac{\pi d}{\lambda} \sin \gamma \right]} \quad (19)$$

- where $k = \frac{2\pi}{\lambda}$ is substituted for k .

In order to obtain a clear understanding of the general behavior of the directional characteristic for different values of d/λ we first consider the function given by

$$r = \frac{\sin n\varphi}{n \sin \varphi} \quad (20)$$

in which \mathfrak{R} has been replaced by r and $\left(\frac{\pi d}{\lambda} \sin \gamma \right)$ by φ . The curve given by (20) in the polar coordinates (r, φ) is now easily understood. The principal maximum is attained at $\varphi = 0$ and $\varphi = \pi$ (and multiples of π). In between lie $n - 2$ secondary maxima which are separated by the zero positions $\varphi = \frac{k\pi}{n}$ ($k=1, 2, \dots, n-1$).

If a straight line is drawn parallel to the ordinate axis at the distance $1/n$, it touches the curve at the points which correspond to the angles

$$\varphi = \frac{\pi}{2n}, \quad \frac{3}{2n}\pi, \quad \dots \quad \frac{2n-1}{2n}\pi \quad (20a)$$

It is seen that the positions of the secondary maxima are, to a good approximation, defined by the angles

$$\varphi = \frac{3}{2n}\pi, \quad \frac{5}{2n}\pi, \quad \dots \quad \frac{2n-3}{2n}\pi \quad (20b)$$

(due to the symmetry with respect to the ordinate axis we can limit ourselves to the values of $\varphi \leq \pi$). Fig. 9 shows the behavior for $n = 6$. Here the broken line curve is an ellipse with the semi-axes 1 and $1/6$ on which lie all the maximum values of

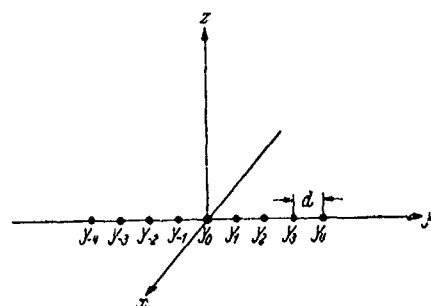


Fig. 8. For the calculation of the straight line group.

$$r = \frac{\sin 6\varphi}{6 \sin \varphi} \quad (20c)$$

The secondary maxima (in the first quadrant) coincide, to a good approximation, with the contact points between the ellipse and the straight line drawn parallel to the ordinate axis at the distance $1/6$.

For a more accurate determination, the equation

$$n \operatorname{tg} \varphi = \operatorname{tg} n\varphi \quad (21)$$

resulting from $\frac{dr}{d\varphi} = 0$ must be solved. This may be done simply if equation (21) is written in the form

$$\varphi = \frac{1}{n} \operatorname{arctg}(n \operatorname{tg} \varphi). \quad (22)$$

The approximation values just found are substituted in the right hand side of (22) and a better approximation is obtained. Then this better approximation is again substituted in the right hand side of (22) etc. If $\varphi_0 = \frac{2m+1}{2n}\pi$ is substituted as a first approximation in the right hand side of (22), $\varphi_0 - \varepsilon_0$ then results as a second

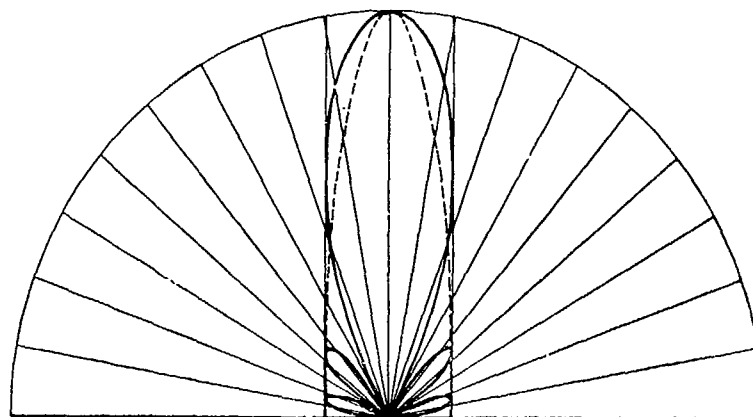


Fig. 9. Marking the positions and magnitudes of the secondary maxima of the directional characteristic for the straight line group of six radiators.

approximation where ε_0 is given by

$$\operatorname{tg} n \varepsilon_0 = \frac{1}{n \operatorname{tg} \varphi_0} \quad (22a)$$

If, e.g., $n = 6$ and $m = 1$ then $\varphi_0 = 45^\circ$ and from

$$\operatorname{tg} 6 \varepsilon_0 = \frac{1}{6} \quad (22b)$$

$\varepsilon_0 = 1^\circ 35'$ so that $\varphi_1 = 43^\circ 25'$. The third approximation yields $\varepsilon_1 = 0^\circ 5'$ and $\varphi_2 = \varphi_1 - \varepsilon_1 = 43^\circ 20'$. Thus $6 \tan \varphi_2 = 5.66$ agrees with $\tan 6 \varphi_2 = 5.67$ to within an error of less than 1%.

If we denote the coordinates for the maximum value by r_m, φ_m then (20) and (21) must be fulfilled simultaneously. Therefore

$$r_m^2 n^2 \sin^2 \varphi_m = \sin^2 n \varphi_m, \quad (23)$$

$$n^2 \operatorname{tg}^2 \varphi_m = \operatorname{tg}^2 n \varphi_m, \quad (24)$$

and dividing (23) by (24):

$$r_m^2 \cos^2 \varphi_m = \cos^2 n \varphi_m \quad (24a)$$

Adding (23) to (24a),

$$r_m^2 [n^2 \sin^2 \varphi_m + \cos^2 \varphi_m] = 1. \quad (24b)$$

That is, the maximum values all lie on an ellipse with the semi-axes 1 and $1/n$. In order to perceive the dependency of the directional characteristic on d/λ and γ , we have only to consider how the discussed r, φ curve is affected by the transformation $\mathcal{R} = r$ and $\varphi = \frac{\pi d}{\lambda} \sin \gamma$ into the r, γ plane.* Due to symmetry, we can confine ourselves to the first quadrant $(0 \leq \gamma \leq \frac{\pi}{2})$ and from the corresponding range $0 \leq \varphi \leq \frac{\pi d}{\lambda}$ can state the positions and number of the principal and secondary maxima. The size is manifestly not changed by the transformation.

If we compare two arbitrary straight line groups I and II where I is characterized by n_1, d_1, λ_1 , and II by n_2, d_2, λ_2 then

$$\begin{aligned} r_1 &= \frac{\sin n_1 \varphi_1}{n_1 \sin \varphi_1}, & \varphi_1 &= \frac{\pi d_1}{\lambda_1} \sin \gamma, \\ r_2 &= \frac{\sin n_2 \varphi_2}{n_2 \sin \varphi_2}, & \varphi_2 &= \frac{\pi d_2}{\lambda_2} \sin \gamma. \end{aligned} \quad (24c)$$

Since one is concerned with only small values of γ in estimating the directivity, $\sin \varphi$ can be replaced by φ . And since, for small values of φ , the inequality

$$\frac{\sin n_1 \varphi_1}{n_1 \varphi_1} > \frac{\sin n_2 \varphi_2}{n_2 \varphi_2} \quad (24d)$$

is fulfilled when and only when $n_1 \varphi_1 < n_2 \varphi_2$, it then follows that the directivity of II is greater than, equal to or less than that of I according as $n_2 d_2 / \lambda_2$ is greater than, equal to or less than $n_1 d_1 / \lambda_1$. With the same frequency and total length the more densely covered group therefore has a smaller directivity (broader beam). And two groups with a different length and a different number of radiators can possess the same directivity.* For example, since $\frac{n_1 d_1}{\lambda_1} = \frac{n_2 d_2}{\lambda_2} = 3$ the groups $n_1 = 18, d_1 = \lambda/6$ and $n_2 = 3, d_2 = \lambda$ have equal directivity while their base lengths have the ratio of 17 to 12.

For a number of directional radiators (in a rigid wall), the calculation is substantially simplified when the radiators are uniform (so that each radiator by itself would produce the same directional characteristic). If we imagine a nondirectional (point-source) radiator in place of each individual directional radiator

* Apparently the \mathcal{R}, γ plane is meant here.

and call the directional characteristic of the system thus composed of nondirectional individual radiators \mathfrak{R}_1 , and the directional characteristic of each individual radiator \mathfrak{R}_2 , then the directional characteristic \mathfrak{R} of the whole arrangement is simply given by the product, i.e., $\mathfrak{R} = \mathfrak{R}_1 \cdot \mathfrak{R}_2$.

For example, the directional characteristic of an arrangement in a rigid wall consisting of two identical circular piston membranes of radius r and with a center-to-center distance a in a rigid wall turns out to be

$$\mathfrak{R} = \cos \left[\frac{\pi a}{\lambda} \cos \beta \right] \frac{2 J_1(kr \sin \gamma)}{kr \sin \gamma}. \quad (25)$$

We prove this theorem, first expressed by Bridge¹⁰, as follows:

Let there be given in the XY-plane a system I of n nondirectional (point-source) radiators with the coordinates

$$(x'_1, y'_1), (x'_2, y'_2) \dots (x'_n, y'_n), \quad (25a)$$

the velocity amplitudes

$$w'_1, w'_2 \dots w'_n \quad (25b)$$

and the radiating surfaces

$$F'_1, F'_2 \dots F'_n, \quad (25c)$$

and for this system, set

$$w'_1 F'_1 + w'_2 F'_2 + \dots + w'_n F'_n = A' \quad (25d)$$

Furthermore suppose a system II of m nondirectional radiators correspondingly characterized by the quantities

$$(x''_1, y''_1), (x''_2, y''_2), \dots (x''_m, y''_m), \quad (25e)$$

$$w''_1, w''_2 \dots w''_m, \quad (25f)$$

$$F''_1, F''_2 \dots F''_m, \quad (25g)$$

$$w''_1 F''_1 + w''_2 F''_2 + \dots + w''_m F''_m = A''. \quad (25h)$$

¹⁰ See H. Poincare, Theorie de la lumiere, p. 158.

Now in place of each radiator of system II, the system I is to be set so that the new system III is correspondingly characterized by the quantities

$$\left. \begin{array}{cccc} (x''_p + x'_1, y''_p + y'_1), (x''_p + x'_2, y''_p + y'_2) \dots (x''_p + x'_n, y''_p + y'_n) \\ w''_p w'_1, & w''_p w'_2, & \dots & w''_p w'_n \\ F''_p F'_1 & F''_p F'_2 & \dots & F''_p F'_n \end{array} \right\} p=1, 2, 3 \dots m. \quad (25i)$$

The directional characteristic \mathcal{R}''' of the system III results then from the general formula (6) where the integral must be replaced by the summation sign. Thus

$$\mathcal{R}''' = \frac{1}{A' A''} \sum_{p=1}^m \sum_{q=1}^n w''_p F''_p w'_q F'_q e^{ik[(x''_p + x'_q) \cos \alpha + (y''_p + y'_q) \cos \beta]}, \quad (25j)$$

while the directional characteristic \mathcal{R}' of I is given by

$$\mathcal{R}' = \frac{1}{A'} \sum_{q=1}^n w'_q F'_q e^{ik[x'_q \cos \alpha + y'_q \cos \beta]} \quad (25k)$$

and the directional characteristic \mathcal{R}'' of II is given by

$$\mathcal{R}'' = \frac{1}{A''} \sum_{p=1}^m w''_p F''_p e^{ik[x''_p \cos \alpha + y''_p \cos \beta]} \quad (25m)$$

From this it follows immediately that $\mathcal{R}''' = \mathcal{R}' \cdot \mathcal{R}''$. This theorem can serve to derive another group arrangement whose directional characteristic possesses a simple form from a simple straight line group arrangement. If we let the directional characteristic of a straight line group which consists of n nondirectional radiators with equal surface placed at equal intervals on the Y -axis with the velocity amplitudes w_1, w_2, \dots, w_n be

$$\mathcal{R} = [w_1, w_2, \dots, w_n], \quad (25n)$$

and denote in particular the directional characteristic of n unit radiators by

$$\mathcal{G}_n = [1, 1, \dots, 1] \quad \frac{\sin nq}{n \sin q}, \quad (26)$$

then

$$\mathcal{G}_2 = [1, 1] \quad \frac{\sin 2q}{2 \sin q} \cos q. \quad (26a)$$

If we now replace each radiator of this group consisting of two elements by the same group, then from the original group

$$\mathcal{G}_2 = \quad \times \quad \times \quad (26b)$$

there manifestly comes the following group

$$\mathcal{G}_2^2 = \quad \times \quad \times \times \quad \times \quad (26c)$$

That is: we obtain a group of 3 elements (1 2 1). The corresponding directional characteristic [1, 2, 1] is then, according to the theorem of Bridge equal to $\cos^2 \varphi$.

Correspondingly, it follows that

$$\mathcal{G}_2^3 = [1, 1][1, 1][1, 1] = [1, 3, 3, 1] = \cos^3 \varphi, \quad (26d)$$

$$\mathcal{G}_2^n = [1, \binom{n}{1}, \binom{n}{2}, \dots, \binom{n}{n}] = \cos^n \varphi. \quad (26e)$$

In order to find the symbolic product

$$\mathcal{M}_a \cdot \mathcal{M}_b = [a_1, a_2, \dots, a_m] [b_1, b_2, \dots, b_n] \quad (26f)$$

i.e., in order to find the directional characteristic of the straight line group which results if each individual radiator of the one group is replaced by an equal and similarly directed group (so that the original radiator and all radiators appearing in its place lie on the same straight line), we form the following rectangular scheme:

	b_1	b_2	b_3	...	b_n
a_1	$a_1 b_1$	$a_1 b_2$	$a_1 b_3$...	$a_1 b_n$
a_2	$a_2 b_1$	$a_2 b_2$	$a_2 b_3$...	$a_2 b_n$
a_3	$a_3 b_1$	$a_3 b_2$	$a_3 b_3$...	$a_3 b_n$
...
a_m	$a_m b_1$	$a_m b_2$	$a_m b_3$...	$a_m b_n$

It is then easily perceived that for the determination of $\mathcal{R}_a \cdot \mathcal{R}_b$, the sums must be formed of the products contained on the diagonals. It then turns out that

$$\mathcal{R}_a \cdot \mathcal{R}_b = [a_1 b_1, a_2 b_1 + a_1 b_2, a_3 b_1 + a_2 b_2 + a_1 b_3, + \dots + a_m b_{n-1} + a_{m-1} b_n, a_n b_m]. \quad (26g)$$

This result may also be explained in a simple manner by considering the product

$$(a_1 x + a_2 x^2 + \dots + a_m x^m) (b_1 x + b_2 x^2 + \dots + b_n x^n) = a_1 b_1 x^2 + (a_2 b_1 + a_1 b_2) x^3 + \dots + a_m b_n x^{m+n} \quad (26h)$$

Of interest is the converse of the question: With a hypothetical straight line group with a fixed number and distance for the receivers, how can the directional characteristic be changed by changing the individual velocity amplitudes, i.e., by changing the sensitivity.

Thus with six radiators which are arranged at a uniform distance d on a straight line the following seven directional characteristics are obtained:

$$\begin{array}{ll} \mathcal{R}_1 = \mathcal{E}_6 = [1, 1, 1, 1, 1, 1] & \left. \begin{array}{l} \sin 6\varphi \\ 6 \sin \varphi \end{array} \right\} \\ \mathcal{R}_2 = \mathcal{E}_5 \cdot \mathcal{E}_2 = [1, 2, 2, 2, 2, 1] & \left. \begin{array}{l} \sin 5\varphi \cdot \sin 2\varphi \\ 5 \sin \varphi \cdot 2 \sin \varphi \end{array} \right\} \\ \mathcal{R}_3 = \mathcal{E}_4 \cdot \mathcal{E}_3 = [1, 2, 3, 3, 2, 1] & \left. \begin{array}{l} \sin 4\varphi \cdot \sin 3\varphi \\ 4 \sin \varphi \cdot 3 \sin \varphi \end{array} \right\} \\ \mathcal{R}_4 = \mathcal{E}_4 \cdot \mathcal{E}_2^2 = [1, 3, 4, 4, 3, 1] & \left. \begin{array}{l} \sin 4\varphi \cdot (\sin 2\varphi)^2 \\ 4 \sin \varphi \cdot (2 \sin \varphi)^2 \end{array} \right\} \\ \mathcal{R}_5 = \mathcal{E}_3^2 \cdot \mathcal{E}_2 = [1, 3, 5, 5, 3, 1] & \left. \begin{array}{l} (\sin 3\varphi)^2 \cdot \sin 2\varphi \\ (3 \sin \varphi)^2 \cdot 2 \sin \varphi \end{array} \right\} \\ \mathcal{R}_6 = \mathcal{E}_3 \cdot \mathcal{E}_2^3 = [1, 4, 7, 7, 4, 1] & \left. \begin{array}{l} \sin 3\varphi \cdot (\sin 2\varphi)^3 \\ 3 \sin \varphi \cdot (2 \sin \varphi)^3 \end{array} \right\} \\ \mathcal{R}_7 = \mathcal{E}_2^5 = [1, 5, 10, 10, 5, 1] & \left. \begin{array}{l} (\sin 2\varphi)^5 \\ 2 \sin \varphi \end{array} \right\} \cdot \cos^5 \varphi \end{array} \quad (27)$$

Here the abbreviation $\varphi = \frac{\pi d}{\lambda} \sin \gamma$ is used.

The corresponding directional characteristics are represented in Fig. 10. According to the moment of inertia theorem it is immediately clear that the directivity of \mathcal{R}_1 is greatest. Since the sensitivity of the receivers becomes more and more concentrated near

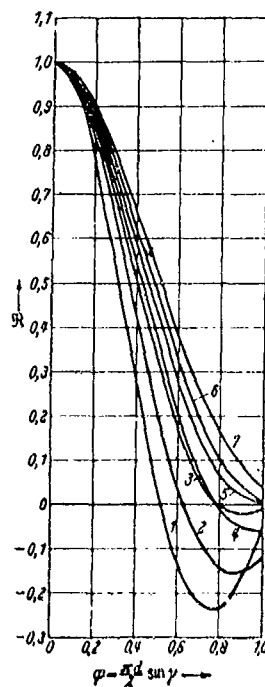


Fig. 10. Directivity of the straight line group of six receivers with different sensitivity.

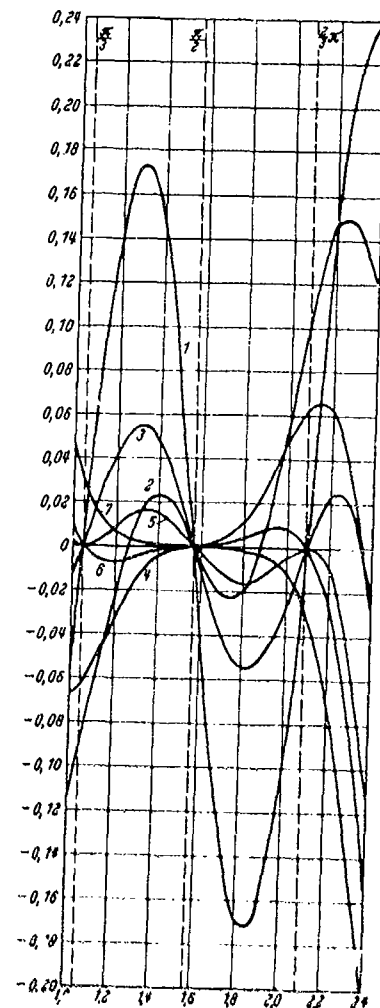


Fig. 11. Secondary maxima of the straight line group of six receivers with different sensitivity.

the center, the directivity must then of necessity decrease more and more. Fig. 10 shows this. It appears of considerable importance that an opposite trend exists for the sizes of the secondary maxima. The part of the curve corresponding to $\varphi > 1$ is greatly enlarged in Fig. 11 in order to show the size of the secondary maxima and

it is evident that, with regard to the size of the secondary maxima, \mathfrak{R}_1 is very unfavorable. Thus, e.g., for \mathfrak{R}_6 sizes of the secondary maxima remain below 1% as compared with 24% for \mathfrak{R}_1 . With a fixed arrangement of radiators we can thus influence the directivity or the sizes of the secondary maxima in the most favorable sense by adjusting the sensitivity (i.e., the amplification) as is necessary.

In order to derive the directional characteristic for the rectangular group, we proceed from the general directional characteristic of the straight line group. Here we substitute $\cos \beta$ for $\sin \gamma$ in Formula (19) in order to show that the relation holds independently of the measuring plane. It was necessary for Formula (19) that the measuring plane coincide with the ZY-plane. We then obtain

$$\mathfrak{R} = \frac{\sin \left[\frac{n\pi d}{\lambda} \cos \beta \right]}{n \sin \left[\frac{\pi d}{\lambda} \cos \beta \right]} \quad (28)$$

If we now imagine each individual radiator replaced by a group

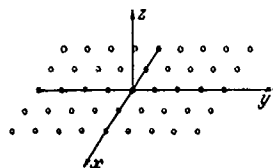


Fig. 12. Rectangular group.

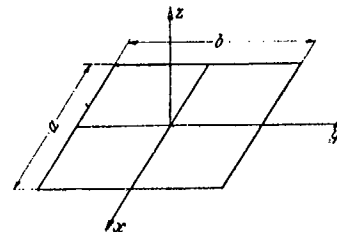


Fig. 13. Rectangular piston membrane.

of m radiators parallel to the X-axis (Fig. 12), according to the rule given above the directional characteristic of this rectangular group then turns out to be:

$$\mathfrak{R} = \frac{\sin \left[\frac{m\pi d_1}{\lambda} \cos \alpha \right] \sin \left[\frac{n\pi d_2}{\lambda} \cos \beta \right]}{m \sin \left[\frac{\pi d_1}{\lambda} \cos \alpha \right] \cdot n \sin \left[\frac{\pi d_2}{\lambda} \cos \beta \right]} \quad (29)$$

If we allow d_1 and d_2 to become smaller and smaller and m and n to increase arbitrarily so that, in the limit, $md_1 = a$ and $nd_2 = b$ (Fig. 13), we then obtain the general directional characteristic for the rectangular piston membrane:

$$\mathfrak{R} = \frac{\sin \left[\frac{a\pi}{\lambda} \cos \alpha \right] \sin \left[\frac{b\pi}{\lambda} \cos \beta \right]}{\frac{a\pi}{\lambda} \cos \alpha \cdot \frac{b\pi}{\lambda} \cos \beta} \quad (30)$$

Here, it must be supposed that the membrane oscillates cophasally on both sides of the XY-plane or that it oscillates in an infinite rigid wall as a simple piston membrane.

In place of the densely filled circular line, a circular group is frequently used in practice which consists of a definite number n of radiators which are arranged equidistantly on a circle of diameter d . \Downarrow If we choose n as an even number ($n = 2m$), then by summing up the response of each pair of diametrically situated radiators, the following relation for the directional characteristic may be easily derived:

$$\mathfrak{R} = \frac{1}{m} \sum_{k=0}^{m-1} \cos \left\{ \frac{\pi d}{\lambda} \sin \gamma \left[\cos \left(\varphi - \frac{\pi k}{m} \right) \right] \right\} \quad (31)$$

Here the field point line is determined by φ and γ (see Fig. 14). For the larger values of m , in particular, calculation by (31) is very time consuming. By the use of Bessel's functions, the sum may be transformed into an infinite series which is considerably more convenient for the calculation. It then turns out that

$$\mathfrak{R} = J_0 \left(\frac{\pi d}{\lambda} \sin \gamma \right) + 2 \sum_{p=1}^{\infty} (-1)^p J_{2pm} \left(\frac{\pi d}{\lambda} \sin \gamma \right) \cdot \cos 2pm\varphi. \quad (32)$$

The practical significance of this relation which, at first, appears complicated, is immediately recognized if it is considered that the first terms in the sum J_{2m}, J_{4m} etc., very rapidly assume a practically negligible value so that it is generally sufficient to consider only the first term J_{2m} .

Moreover, with the aid of (32) the frequently important question can be decided as to how densely a circular line must be covered by the radiators in order that the directional characteristic may be indistinguishable from that of the continuously covered circular line. If we choose, say, four receivers, then the decisive



Electr. Nachr. Tech. Vol. 6 (1929), p. 170, (or the NRL translation (#114) of this paper).

correction term is smaller in absolute value than $\left| 2J_4\left(\frac{\pi d}{\lambda} \sin \gamma\right) \right|$.

If we denote the part from $\gamma = 0$ ($J_0 = 1$) to $\gamma = \gamma_1$ (where γ_1 corresponds to the first zero position) as the principal part of the charac-

teristic of $\mathfrak{R} = J_0\left(\frac{\pi d}{\lambda} \sin \gamma\right)$ then γ_1 is determined by $\frac{\pi d}{\lambda} \sin \gamma_1 = 2,4$ and since $J_4(x) < 0,06$ for $x < 2,4$,

the principal part of the characteristic is then not changed. That is, the directivity of a circular group of four radiators is completely equivalent to the directivity of an arrangement which is densely covered with radiators regardless of how great a radius is chosen for the arrangement. It can likewise be concluded that the complete behavior of the directional characteristic of the circular group can be represented with sufficient

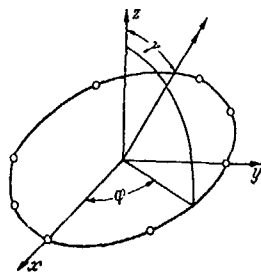


Fig. 14. Calculation of the directional characteristic of the circular group.

accuracy by $J_0\left(\frac{\pi d}{\lambda} \sin \gamma\right)$ if the number n is so large that the condition

$$n \geq \frac{\pi d}{\lambda} + 2 \quad (33)$$

is fulfilled.

Since the circumference of the circle is $\pi d = n \cdot a$ where a is the distance measured on the arc, we can then so formulate the condition (33) that the distance measured on the circle between two neighboring radiators must be somewhat smaller than λ (more precisely $(a/\lambda < 1 - 2/n)$) in order that the circular group directional characteristic may be given by $J_0\left(\frac{\pi d}{\lambda} \sin \gamma\right)$.

Closely connected with the beam sharpness of an arrangement is the matter of the resolving power (Trennschärfe). Then it is a question of when a receiving arrangement is in the position to perceive separately two sound sources placed at a great distance away and at a small distance from each other. If we imagine a sound source placed symmetrically on each side of the perpendicular bisector of a receiver arrangement (sources 1 and 2) and at a great distance r and if we imagine furthermore a circular surface as the receiver arrangement (Fig. 15), being rotated about the X -axis, then the principal maxima produced by each radiator will be perceived

separately if the distance a between the radiators is sufficiently great. If one assumes with Rayleigh that the maxima can then be separated if the maximum of one coincides with the minimum of the other, the necessary condition

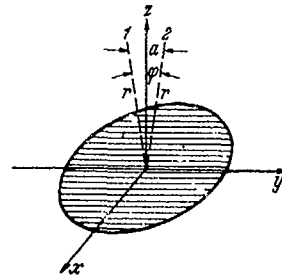


Fig. 15. Resolving power of the circular piston membrane.

$$\frac{\pi d}{\lambda} \sin \varphi \geq 3,83 \quad (33a)$$

then follows from the fact that the equation

$$\frac{2J_1\left(\frac{\pi d}{\lambda} \sin \varphi\right)}{\frac{\pi d}{\lambda} \sin \varphi} = 0 \quad (33b)$$

is fulfilled for $\frac{\pi d}{\lambda} \sin \varphi = 3,83$ Since

$$\sin \varphi \approx \varphi = a/r \quad (33c)$$

it follows that

$$d/\lambda > 1,22 r/a \quad (34)$$

In order, therefore, to be able to separate with an acoustical objective radiators placed at a great distance r from the objective and at a small distance a from each other, the diameter of the objective measured in wave lengths must at least be equal to r/a .

The preceding considerations referred exclusively to the case where all parts of the radiating membrane or radiating system moved with the same amplitude and phase. In practice this is not by any means the case. In general, the force exerted on a membrane is not uniformly distributed over the whole surface but is exerted at the midpoint or along a line. Since there is no absolutely rigid membrane (above all not if, in addition to rigidity, as small a weight as possible is necessary to produce a good efficiency and frequency response), the force acting, say, at the midpoint will, due to the (damped) propagation with finite velocity of the transverse elastic waves, be able to act neither in phase nor with uniform amplitude on, say, the outlying elements as soon as the dimensions of the membrane are no longer small compared to the wave length of this transverse wave. Furthermore, the membrane is generally retarded

in its motion by its support at the boundary. In principle making allowance for a different phase in our formulae will cause no difficulty. We would then need to use the given velocity amplitude $w(x, y)$ as a complex quantity. For simplicity we will confine ourselves to a variable amplitude and accordingly assume $w(x, y)$ as a real function.

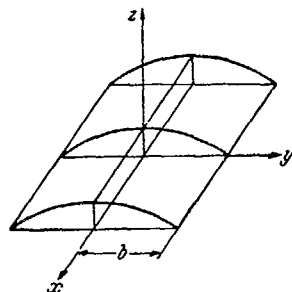


Fig. 16. Vibration form of the rectangular membrane $w(x, y) = 1 - y^2/b^2$.

As the simplest example, we consider the directional characteristic in the ZY-plane of the rectangular membrane represented in Fig. 16 where the membrane is shown at the moment of greatest deflection.

Here w is to be given by $w(y) = 1 - y^2/b^2$. We then find that

$$w_m \cdot F = 2a \int_{-b}^{+b} \left(1 - \frac{y^2}{b^2}\right) dy = 2a \cdot 2b \cdot \frac{2}{3}. \quad (34a)$$

so that

$$w_m = \frac{2}{3}. \quad (34b)$$

and

$$\begin{aligned} \Re &= \frac{2a}{w_m F} \int_{-b}^{+b} e^{ik y \sin \gamma} \left(1 - \frac{y^2}{b^2}\right) dy, \\ \Re &= \frac{3}{u^2} \left(\frac{\sin u}{u} - \cos u \right), \end{aligned} \quad (35)$$

where

$$u = \frac{2\pi b}{\lambda} \sin \gamma \quad (35a)$$

In order to find the directivity coefficient, we have to calculate the value of u for which $\Re = 0.707$. It then results that $u = 1.8$. The directivity coefficient is then equal to $1.8/\pi = 33^\circ$ and the half-value beam width φ is given by $\varphi = 33^\circ \lambda/2b$. Using the approximation formula, we would find that

$$\Re = 1 - \left(\frac{2\pi b}{\lambda} \right)^2 \frac{\sin^2 \gamma}{10}, \quad (35b)$$

and hence that

$$\varphi = 33,5^\circ \cdot \lambda/2b. \quad (35c)$$

As a second example for the rectangular membrane we choose (Fig. 17):

$$w(x, y) = 1 - 2y^2/b^2 \quad (35d)$$

and find $w_m = \frac{1}{3}$.

For the directional characteristic in the ZY-plane, it turns out that

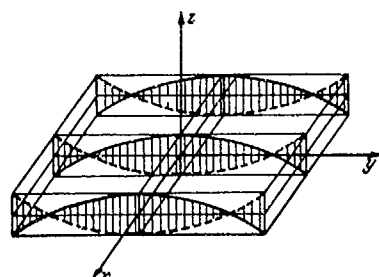


Fig. 17. Vibration form of the rectangular membrane $w(x, y) = 1 - 2y^2/b^2$.

$$\mathcal{R} = \frac{12}{u^2} \left(\frac{\sin u}{u} - \cos u \right) - 3 \frac{\sin u}{u}. \quad (35e)$$

We here determined the directivity coefficient from

$$\frac{12}{u^2} \left(\frac{\sin u}{u} - \cos u \right) - 3 \frac{\sin u}{u} = 0,707, \quad (36)$$

and it hence follows that $u = 4,4$. The directivity coefficient is thus $4,4/\pi = 80^\circ$ while the half-value beam width is $\varphi = 80^\circ \cdot \lambda/2b$ ^{12/}.

Here something new occurs since \mathcal{R} does not possess a maximum but a minimum on the Z-axis. A series development of \mathcal{R} yields:

$$\mathcal{R} = 1 + \frac{u^2}{10} \dots$$

Fig. 18 shows a comparison of the directional characteristics of the rectangular piston membrane of length $2b$ and the two latter membranes. One recognizes how substantial is the change if a membrane with nodal lines is operative in place of the desired piston membrane. On the other hand, this knowledge can be turned to good account if, with a large membrane (which is necessary in order to provide the required energy), it is a question of avoiding a sharp convergence.

As the third example we choose a tightly stretched circular membrane. Here we can generally carry out the calculation for the curves

^{12/} See Note 7.

given by $w(\varrho) = (1 - \varrho^2/r^2)^n$. (Fig. 19 represents the curve $w(\varrho) = (1 - \varrho^2/r^2)^n$ for $n = 0, 2, 4$, and 8 .) Thus we find ¹³

$$w_m = \frac{1}{n+1} \quad \text{und:} \quad \mathcal{R}_n = 2^{n+1} \cdot (n+1)! \frac{J_{n+1}(u)}{u^{n+1}}, \quad (37)$$

wherein $J_{n+1}(u)$ is the Bessel's function of the order $(n+1)$ and $u = \frac{2\pi r}{\lambda} \sin \gamma$.

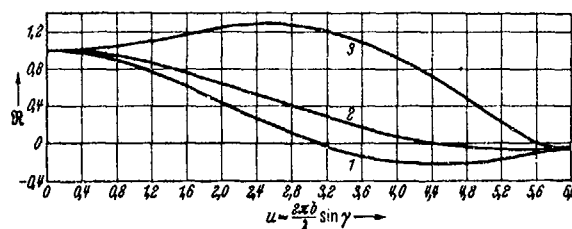


Fig. 18. 1. Directional characteristic of the rectangular piston membrane in the symmetry plane. 2. Directional characteristic of the rectangular stretched membrane in the symmetry plane. 3. Directional characteristic of the rectangular membrane with nodal lines in the symmetry plane.

From the approximation formula calculated with the moment of inertia:

$$\mathcal{R}_n = 1 - \frac{r^2 \pi^2 \sin^2 \gamma}{n+2} \quad (37a)$$

we find the half-value beam width to be

$$\varphi = 15^\circ \cdot \sqrt{n+1} \cdot \lambda/r. \quad (37b)$$

The complete behavior of directional characteristics corresponding

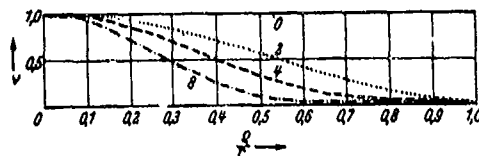


Fig. 19. Vibration forms $w(\varrho) = (1 - \varrho^2/r^2)^n$ for $n = 0, 2, 4, 8$.

¹³ Ann d. Phys., Vol. 7 (1930), n. 972.

to the vibration forms of Fig. 19 is represented in Fig. 20 for $n = 0, 2, 4, 8$. It is to be mentioned, however, that by a linear

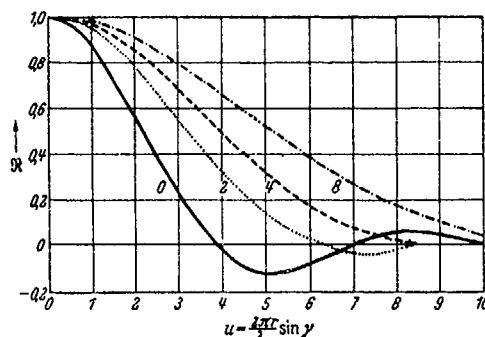


Fig. 20. Directional characteristic of the circular membrane with the vibration form $w(r) = (1 - r^2/r^2)^n$ for $n = 0, 2, 4, 8$.

combination of the vibration forms $(w = (1 - r^2/r^2)^n)$ an arbitrary rotationally symmetric vibration form of the membrane (even with nodal lines) can be represented to an arbitrary degree of approximation.

We can state the directional characteristic corresponding to a general vibration of the membrane

$$w(r) = a_0 + a_1(1 - r^2/r^2) + a_2(1 - r^2/r^2)^2 + \dots + a_n(1 - r^2/r^2)^n. \quad (38)$$

It is

$$\mathfrak{R} = \frac{1}{a_0 + \frac{1}{2}a_1 + \frac{1}{3}a_2 + \dots + \frac{1}{n+1}a_n} \left[2a_0 \frac{J_0(u)}{u} + 2^2 \cdot 1! a_1 \frac{J_2(u)}{u^2} + \dots + 2^{n+1} \cdot n! \frac{J_{n+1}(u)}{u^{n+1}} \right]. \quad (39)$$

An exceptional case arises if the expression in the denominator

$$a_0 + \frac{1}{2}a_1 + \dots + \frac{1}{n+1}a_n \quad (39a)$$

vanishes. Then formula (39) for \mathfrak{R} becomes unusable. However, the difficulty may be immediately removed if the pressure amplitude is calculated directly by equation (11). It then follows that

$$p = \frac{\sigma \cdot \sigma}{\lambda \cdot R} \int_F w(x, y) e^{ik_y \sin \gamma} dF \quad (39b)$$

and for $\gamma = 0$

$$p = \frac{c \cdot \sigma}{\lambda \cdot R} \int_F w(x, y) dF = 0 \quad (39c)$$

This means therefore that since $w_m = 0$ the pressure amplitude at a sufficient distance on the normal axis vanishes. In addition, it

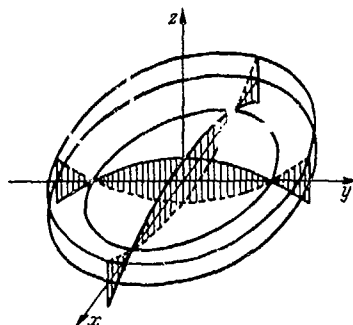


Fig. 21. Circular membrane with the deformation volume zero.

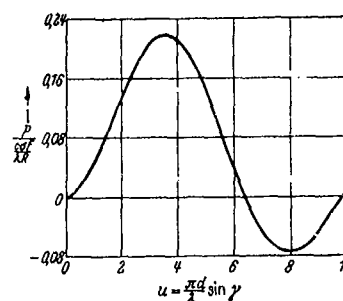


Fig. 22. Relative sound pressure amplitude of a circular membrane with the deformation volume zero.

is clear that the directional characteristic (which represents the ratio of the pressure amplitude in an arbitrary direction to the pressure amplitude on the normal axis) loses its meaning. In other respects, the calculation offers no difficulty.

A suitable example is given by $w = 1 - 2\rho^2/r^2$. Therefore we have $a_0 = -1$, $a_1 = +2$, $a_2 = a_3 \dots = 0$ (see Fig. 21).

Here $w_m = 0$ and p is found from

$$p = \frac{c \cdot \sigma}{\lambda \cdot R} \cdot F[\mathfrak{R}_1(u) - \mathfrak{R}_0(u)] \quad (40)$$

where

$$u = \frac{\pi d}{\lambda} \sin \gamma, \quad \mathfrak{R}_0(u) = \frac{2J_1(u)}{u}, \quad \mathfrak{R}_1(u) = 2^2 \cdot 2 \cdot \frac{J_3(u)}{u^2}. \quad (40a)$$

For small values of u , it is recognized from the series development

$$\mathfrak{R}_1(u) - \mathfrak{R}_0(u) = \frac{u^2}{2^2 \cdot 0!3!} - \frac{u^4}{2^4 \cdot 1!4!} + \frac{u^6}{2^6 \cdot 2!5!} - \dots \quad (41)$$

that even for directions in the neighborhood of the Z-axis the effect of the membrane is extraordinarily small. The complete behavior of $\mathfrak{R}_1(u) - \mathfrak{R}_0(u)$ is represented in Fig. 22.

(b) The directional characteristic for a noise.

In practice, of the sound sources which are to be measured (e.g., underwater), two essentially different types are to be distinguished. Either it is a question of artificial sound sources which are to send out pure tones (light ship transmitters, bells, signal senders on ships) or of more or less natural sound sources which possess a noise-like character and which are generally unintended and undesired (propeller noise, machine noise).

Therefore an investigation to determine how the preceding considerations may be applied in such cases suggests itself. Here we will assume the case occurring most frequently in practice where a noise source is present from whose continuous spectrum a definite frequency range (bounded above and below) is received. As is well known, this may be accomplished without difficulty by an electrical filter. It is additionally assumed that the receiver receives all frequencies of the range in question with equal intensity in the principal direction - i.e., that the transmitter favors no frequency and also that no frequency dependency exists on the path from the transmitter to the receiver in the medium (absorption, reflection). We will, with advantage, define the quadratic mean value

$$\mathcal{G} = \sqrt{\frac{1}{n_2 - n_1} \int_{n_1}^{n_2} \mathcal{R}^2 dn} \quad (42)$$

as the directional characteristic where n_1 and n_2 are the limits of the range and \mathcal{R} is the previously defined directional characteristic dependent on the frequency n .

If we choose as the simplest measuring apparatus two nondirectional receivers separated by the distance d (which is small compared to the wave lengths in question), then

$$\mathcal{G}_1 = \sqrt{\frac{1}{n_2 - n_1} \int_{n_1}^{n_2} \cos^2\left(\frac{n\pi d}{c} \sin \gamma\right) dn}. \quad (42a)$$

Carrying out the integration:

$$\mathcal{G}_1 = \sqrt{\frac{1}{2} + \frac{\sin(x_2 - x_1)}{2(x_2 - x_1)} \cos(x_1 + x_2)} \quad (43)$$

wherein for abbreviation

$$\begin{aligned} n_1 \frac{\pi d}{c} \sin \gamma &= \frac{\pi d}{\lambda_1} \sin \gamma = x_1 \\ n_2 \frac{\pi d}{c} \sin \gamma &= \frac{\pi d}{\lambda_2} \sin \gamma = x_2 \end{aligned} \quad (43a)$$

One sees that for $x_2 = x_1$ formula (43) goes over into the original directional characteristic \mathcal{R}_1 in (14). It is

$$\mathcal{G}_{x_2 = x_1 = x} = \sqrt{\frac{1}{2} + \frac{1}{2} \cos 2x} = \cos x. \quad (43b)$$

We will initially investigate the behavior of the directional characteristic when the pass band is precisely one octave. Here we set

$$x_2 = 2x, \quad x_1 = x = \frac{\pi d}{\lambda} \sin \gamma$$

and obtain:

$$\mathcal{G}_1 = \sqrt{\frac{1}{2} + \frac{1}{2} \frac{\sin x}{x} \cos 3x}. \quad (44)$$

From Fig. 23 we see that the directional characteristic is now substantially different from the previous one (for a single tone, Fig. 7, curve 1). Instead of the zero and unity values appearing periodically with increasing x , there appears here only one principal

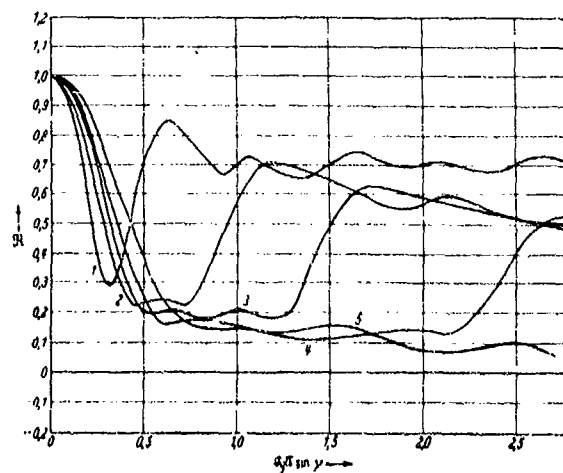


Fig. 23. Directional characteristic of a straight line group (length a) for octave reception:

1. Two receivers, 2. Three receivers,
3. Four receivers, 4. Six receivers,
5. Densely covered.

maximum with the value unity. And for the larger values of x , the curve, oscillating, always approaches the value $\sqrt{\frac{1}{2}}$. In order to investigate the influence of the number of receivers for octave reception, the cases are represented in Fig. 23 when the receiver array consists of 2, 3, 4, 6 and very many receivers - the total length of the array being kept constant and equal to a . One sees how the directivity decreases here also with an increasing number of receivers. Simultaneously a steady decrease occurs in the value which the curve approaches with increasing $\frac{a \cdot \pi}{\lambda} \sin \gamma$. The values corresponding to the receiver numbers 2, 3, 4, and 6 are respectively $\sqrt{\frac{1}{2}}$, $\sqrt{\frac{1}{3}}$, $\sqrt{\frac{1}{4}}$ and $\sqrt{\frac{1}{6}}$ while the value zero corresponds to a large number of receivers.

In general, for a straight line group of n receivers at the same distance d and for a frequency range from ν to $\nu + p\nu$ it is found that

$$G_1 = \sqrt{\frac{1}{n} + \frac{2}{n^2} \sum_{m=1}^{n-1} (n-m) \frac{\sin m p x}{m p x} \cos[(p+2)m x]}. \quad (45)$$

In order to learn the influence of the size of the pass band, the cases $n = 6, p = 0; 0.2; 0.5; 1; 3$ are represented in Fig. 24.

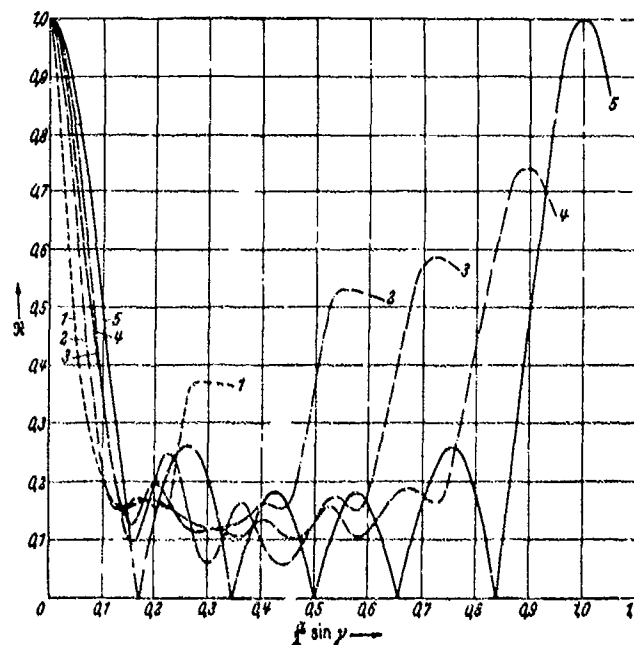


Fig. 24. Influence of the band width on the directional characteristic of a straight line group of six receivers.

It is seen that the size of the pass band determines the amount of the variation above $\sqrt{\frac{1}{2}}$ and that the greater the pass band, the smaller this variation. In Fig. 24,

Curve 1 corresponds to the case $n = 6$ $p = 3$
 Curve 2 corresponds to the case $n = 6$ $p = 1$
 Curve 3 corresponds to the case $n = 6$ $p = 0.5$
 Curve 4 corresponds to the case $n = 6$ $p = 0.2$
 Curve 5 corresponds to the case $n = 6$ $p = 0$.

The values of $\frac{d}{\lambda} \sin \gamma$ are read on the abscissa axis. $a = 5d$ is the length of the base.

As a further example, we consider the noise reception for a dense receiver array on the circular line and on the circular surface. The corresponding directional characteristics are

$$G_2 = \sqrt{\frac{1}{n_2 - n_1} \int_{n_1}^{n_2} J_0^2 \left(\frac{n \pi d}{c} \sin \gamma \right) dn} \cdot \sqrt{\frac{1}{x_2 - x_1} \int_{x_1}^{x_2} J_0^2(x) dx}, \quad (46)$$

$$G_3 = \sqrt{\frac{1}{n_2 - n_1} \int_{n_1}^{n_2} \frac{4 J_1^2 \left(\frac{n \pi d}{c} \sin \gamma \right) dn}{n^2 \left(\frac{\pi d}{c} \sin \gamma \right)^2}} \cdot \sqrt{\frac{1}{x_2 - x_1} \int_{x_1}^{x_2} \frac{4 J_1^2(x) dx}{x^2}}, \quad (47)$$

where again

$$x_1 = \frac{\pi d}{\lambda_1} \sin \gamma \text{ and } x_2 = \frac{\pi d}{\lambda_2} \sin \gamma. \quad (47a)$$

For octave reception ($x_2 = 2x_1 = 2x$; $x = \frac{\pi d}{\lambda} \sin \gamma$):

$$G_2 = \sqrt{\frac{1}{x} \int_x^{2x} J_0^2(x) dx}. \quad (48)$$

This is represented in Fig. 25. For comparison, the ordinary directional characteristics corresponding to the upper and lower limits of the octave are also inserted (curves 1 and 3).

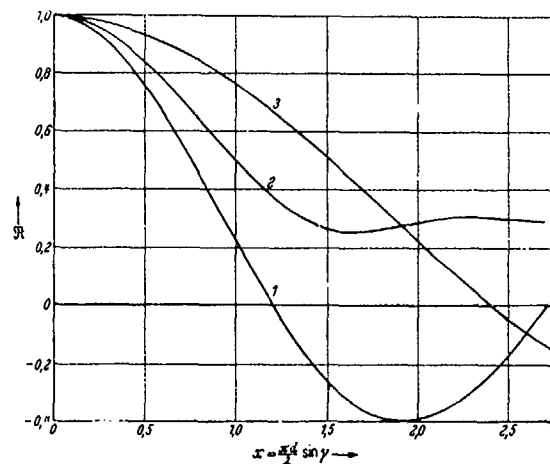


Fig. 25. Directional characteristic of the densely covered circular line.*
 1. For the fundamental (wave length λ). 2. For the octave (wave length λ to $\lambda/2$). 3. For the harmonic (wave length $\lambda/2$).

(c) With artificial compensation

When the position of a sound source is to be determined with a given receiver array, this can be done by rotating the array until the maximum intensity is attained on the indicating instrument (or for the ear). When the elements of the array lie in one plane, this maximum response is obtained when the plane of the array is perpendicular to the sound direction.

However, the same result, which depends on a coincidence of phase, can also be attained by artificial compensation without rotating the array. This is done by variable electrical delay circuits which are inserted between the fixed receiver array and the indicating instrument. Each position of the compensator, which controls the delay time, corresponds to a definite direction in space (in the measuring plane) for which the receiver array is in phase. In order to find the direction of the sound source, leaving the array fixed, one now has only to turn the compensator and read off the corresponding beam angle.

Artificial compensation by electrical delay circuits is quite important for directive reception. Not in the least contributive to its usefulness is the simplicity and accuracy of the operation of the electrical circuits. These generally consist of a number of uniformly constructed sections which contain self-inductance and capacitance and are so assembled that the self-inductance coils are

* Using the indicated argument in this figure, the curves for the fundamental and the harmonic will be identical. If, however, $\sin \gamma$ is used as the argument, curves similar to curves (1) and (3) will be obtained but curve (1) will correspond to the harmonic while curve (3) will correspond to the fundamental frequency.

inserted in series while the condensers are in parallel. If L is the value of the self-inductance and C the capacitance of the condenser, the delay furnished per section of the circuit is \sqrt{LC} .

Furthermore, this delay can be made quite independent of the frequency if one arranges it so that the limiting frequency defined by

$$n = \frac{1}{\pi} \cdot \frac{1}{\sqrt{LC}}$$

is sufficiently far above the frequency range to be passed. In this way one succeeds in imparting a pure time delay per section to a noise signal without changing its character.

If we have an arbitrary receiver array arranged in space then the compensation apparatus can be obtained in a very simple manner for a given measuring plane by a single delay circuit. If we imagine the receivers projected on the measuring plane (XY-plane) and that their coordinates are given by (x_1, y_1) $(x_2, y_2) \dots (x_n, y_n)$ it is then clear that for a compensation in the measuring plane only these projections are of concern. Otherwise expressed, the individual receivers can be arbitrarily displaced perpendicularly to the measuring plane without any change in the compensation action. If, for simplicity, we confine ourselves to three receivers, the natural directional characteristic is then given by

$$\mathcal{R} = \sum_{n=1}^3 e^{ik(x_n \cos \alpha + y_n \cos \beta)}, \quad (49)$$

where α and β are the direction angles of the field point line. If we let the compensation direction in the measuring plane have the direction angles φ and ψ , then, upon applying the delays, the artificial directional characteristic is given by

$$\mathcal{R}_k = \sum_{n=1}^3 e^{ik[x_n(\cos \alpha - \cos \varphi) + y_n(\cos \beta - \cos \psi)]}, \quad (50)$$

If we allow the sound source, i.e., the field point line (α, β) , to shift so that it makes a complete circuit, \mathcal{R}_k assumes its greatest value when the direction of the sound source coincides with the compensation direction. Exactly the same circumstances occur, however, if, with a fixed sound source, we allow the compensation line (φ, ψ) to shift.

If we regard the configuration of Fig. 26 as a scale drawing of the receiver array which can be rotated about the origin O, then in the rotation the correct retardations $x_n \cos \varphi + y_n \cos \psi$ are attained simply as the projections on a fixed line which we will assume to be the X-axis. If we furthermore imagine perpendicular contact bars which are connected with the individual sections of the delay circuit (as is shown in Fig. 26) and place sliding contacts at (x_1, y_1) , (x_2, y_2) , (x_3, y_3) which are constantly connected with the one terminal of the corresponding receiver while the other terminals are connected with a

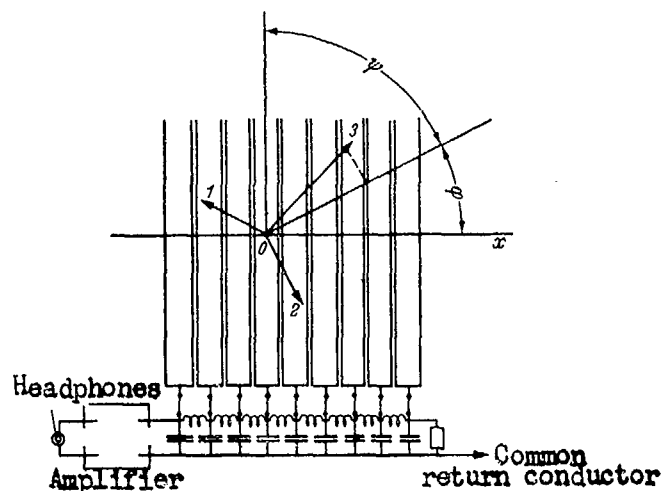


Fig. 26. Compensation apparatus for a group of radiators (1, 2, 3) (small in comparison to the wave length) with an arbitrary arrangement in space.

common return conductor at the circuit input, then each impulse from a receiver reaches the input of the amplifier with the desired delay. At the same time, by an appropriate design of the delay sections the time delays of the circuit are to be made to correspond to the velocity of sound.

For the uncompensated group the directional characteristic is independent of the position of the object to be located. This is not the case, however, with the compensated group. Here the directivity will be so much the more dependent upon the angle the more the pattern of the projections of the receivers on the measuring plane departs from that of a circular array. If we consider the straight line group of Fig. 8, the directional characteristic \mathcal{R}_k for the compensation direction characterized by γ_0 is given by

$$\mathcal{R}_k = \frac{\sin \left[\frac{n\pi d}{\lambda} (\sin \gamma - \sin \gamma_0) \right]}{n \sin \left[\frac{\pi d}{\lambda} (\sin \gamma - \sin \gamma_0) \right]} \quad (51)$$

In Fig. 27 the directional characteristics are represented in polar coordinates for a straight line group ($n = 6$, $d = \lambda/2$) for the compensation directions 0° , 45° , 60° , and 90° ; here the secondary maxima are left out. It is noteworthy here that the directivity is changed only slightly at $\gamma_0 = 45^\circ$. However, for larger angles a decided broadening of the principal maximum arises. Furthermore, the principal maximum no longer lies symmetric to the compensation direction. This has the consequence that too great a value for γ_0 is found if the measurement is undertaken in the usual manner wherein

the compensator positions for equal loudness on both sides of the maximum are determined by ear and the mean of these positions is taken.

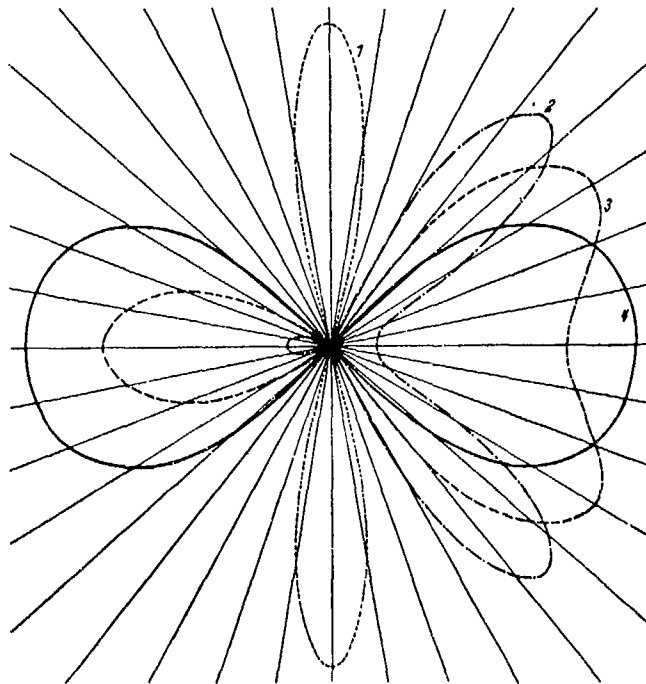


Fig. 27. The directional characteristic of a straight line group of six radiators with compensation.
1. $\gamma_0 = 0^\circ$, 2. $\gamma_0 = 45^\circ$, 3. $\gamma_0 = 90^\circ$, 4. $\gamma_0 = 90^\circ$.

These disadvantages of the straight line group will be avoided if the densely covered circular group is used so that the measuring plane coincides with the receiver plane. If we next calculate the directional characteristic of the circular group compensated for an arbitrary angle $\alpha_0, \beta_0, \gamma_0$ we find that

$$\mathcal{H}_k = \frac{1}{2\pi r} \int e^{ik(x \cos \alpha + y \cos \beta + z \cos \gamma)} d\Omega, \quad (51a)$$

If we let $x = r \cos \varphi$ and $y = r \sin \varphi$ and set

$$\tan \varphi_0 = \frac{\cos \beta + \cos \beta_0}{\cos \alpha + \cos \alpha_0}, \quad (51b)$$

it then follows that

$$\mathfrak{R}_k = \frac{1}{2\pi} \int_0^{2\pi} e^{ikr} [\cos \varphi (\cos \alpha - \cos \alpha_0) + \sin \varphi (\cos \beta - \cos \beta_0)] d\varphi, \quad (52)$$

$$\mathfrak{R}_k = \frac{1}{2\pi} \int_0^{2\pi} e^{ikr} \sqrt{(\cos \alpha - \cos \alpha_0)^2 + (\cos \beta - \cos \beta_0)^2} \cos(\varphi - \varphi_0) d\varphi,$$

and

$$\mathfrak{R}_k = J_0 \left(\frac{2\pi r}{\lambda} \sqrt{(\cos \alpha - \cos \alpha_0)^2 + (\cos \beta - \cos \beta_0)^2} \right)$$

For $\alpha_0 = 90^\circ, \beta_0 = 90^\circ$, \mathfrak{R}_k must become the uncompensated directional characteristic as given by (15); if we let $\cos \alpha_0 = \cos \beta_0 = 0$ in (52) it then follows that

$$\mathfrak{R}_k = J_0 \left(\frac{2\pi r}{\lambda} \sin \gamma \right), \quad (52a)$$

since

$$\sqrt{(\cos \alpha - \cos \alpha_0)^2 + (\cos \beta - \cos \beta_0)^2} = \sqrt{\cos^2 \alpha + \cos^2 \beta} = \sqrt{1 - \cos^2 \gamma} = \sin \gamma, \quad (52b)$$

If the sound source is on the X-axis and the XZ-plane is the measuring plane, then, since $\alpha_0 = 0, \beta_0 = 90^\circ, \beta = 90^\circ$ (see Fig. 28):

$$\mathfrak{R}_k = J_0 \left(\frac{\pi d}{\lambda} \cdot 2 \sin^2 \frac{\alpha}{2} \right) \quad (53)$$

If the sound source is on the X-axis and the XY-plane (receiver plane) is the measuring plane, then, since $\alpha_0 = 0, \beta_0 = 90^\circ, \alpha + \beta = 90^\circ$:

$$\mathfrak{R}_k = J_0 \left(\frac{\pi d}{\lambda} 2 \sin \frac{\alpha}{2} \right). \quad (54)$$

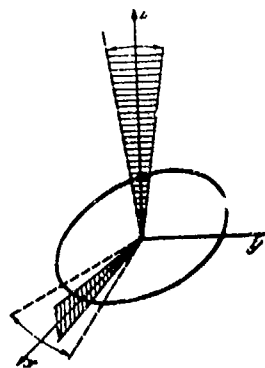


Fig. 28. Different positions of the measuring plane for the compensated circular group.

In practice, this last case, in which the measuring plane and the receiver plane coincide, is of particular significance. From formula (54) we recognize that the directivity of the compensated group agrees with the directivity of the uncompensated group (see formula (15)) so that we again have to choose the angle 20°

as the directivity coefficient. If a definite directivity is required, the ratio of the circle diameter to the wave length is thus determined. If we choose a half value beam width of 13° as an example then from (18)

$$\frac{d}{\lambda} = \frac{20}{13} = 1.5.$$

The remaining question is: how many radiators are necessary in order that no practical difference may exist between the resulting directional characteristic and the directional characteristic of the

densely covered circular group. If, for simplification, we allow the compensation line to go through a radiator, we then find an analogous representation by Bessel's functions¹⁴:

$$\mathcal{R}_k = J_0\left(\frac{2\pi d}{\lambda} \sin \frac{\alpha}{2}\right) + \sum_{p=1}^{\infty} J_{pn}\left(\frac{2\pi d}{\lambda} \sin \frac{\alpha}{2}\right) \cos \frac{\alpha np}{2}.^* \quad (55)$$

From this it also follows that the directivity of the compensated circular group agrees practically completely with the directivity of the group consisting of four radiators. If the complete characteristic is to agree, the inequality

$$n \geq \frac{2\pi d}{\lambda} + 2 \quad (55a)$$

must be fulfilled. Or, the distance a of two neighboring radiators must be somewhat smaller than $\lambda/2$. More precisely

$$\frac{a}{\lambda} < \frac{1}{2} - \frac{1}{n} \quad (55b)$$

In other respects, the formula provides a substantially more simple calculation of the directional characteristic.

As an example we calculate the directional characteristic for $n = 6$, $d = \frac{1}{2}\lambda$ and find the following tables by the approximation formula

$$\mathcal{R}_k = J_0(4.71 \sin \alpha/2) + 2J_6(4.71 \sin \alpha/2) \cos 3\alpha. \quad (55c)$$

α	$4.71 \sin \alpha/2$	$J_0(4.71 \sin \alpha/2)$	$2J_6(4.71 \sin \alpha/2) \cos 3\alpha$	\mathcal{R}_k
0	0.00	1	0	1
10	0.42	0.96	0	0.96
20	0.82	0.84	0	0.84
30	1.22	0.66	0	0.66
40	1.66	0.43	0	0.45
50	1.99	0.23	0	0.23
60	2.36	0.02	0	0.02
70	2.70	-0.14	0	-0.14
80	3.03	-0.27	-0.01	-0.28
90	3.33	-0.35	0	-0.35
100	3.61	-0.36	+0.03	-0.36
110	3.86	-0.40	+0.07	-0.33
120	4.08	-0.39	+0.10	-0.29
130	4.27	-0.37	+0.12	-0.25
140	4.43	-0.34	+0.08	-0.26
150	4.55	-0.31	+0.00	-0.31
160	4.64	-0.29	-0.10	-0.30
170	4.69	-0.27	-0.18	-0.45
180	4.71	-0.27	-0.21	-0.48

¹⁴ Elektr. Nachr.-techn., Vol. 6 (1929), p. 176, (or the NRL translation (#114) of this paper).

* The series called for by the summation sign should be multiplied by the factor 2.

while the direct calculation by the formula

$$\mathfrak{R}_k = \frac{1}{3} \{ \cos[\frac{3}{4}\pi(1 - \cos\alpha)] + \cos[\frac{3}{4}\pi(\cos(\alpha + 60^\circ) - \cos 60^\circ)] + \cos[\frac{3}{4}\pi(\cos(\alpha + 120^\circ) - \cos 120^\circ)] \} \quad (56)$$

yields the following table

α	$\frac{\gamma_1 =}{1 - \cos \alpha}$	$\frac{\gamma_2 =}{\cos(\alpha + 60^\circ) - \cos 60^\circ}$	$\frac{\gamma_3 =}{\cos(\alpha + 120^\circ) - \cos 120^\circ}$	$\cos \frac{3}{4} \pi \gamma_1$	$\cos \frac{3}{4} \pi \gamma_2$	$\cos \frac{3}{4} \pi \gamma_3$	\mathfrak{R}_k
0	0,00	0,06	0,00	1	1	1	1
10	0,02	-0,16	0,14	1	0,93	0,95	0,96
20	0,06	-0,33	0,26	0,99	0,73	0,81	0,84
30	0,13	-0,50	0,37	0,95	0,38	0,64	0,66
40	0,23	-0,67	0,44	0,86	0,00	0,48	0,45
50	0,37	-0,84	0,48	0,67	-0,41	0,41	0,22
60	0,50	-1,00	0,50	0,39	-0,69	0,37	0,02
70	0,66	-1,14	0,48	0,00	-0,90	0,43	-0,14
80	0,83	-1,27	0,44	-0,37	-0,99	0,48	-0,29
90	1,00	-1,37	0,36	-0,71	-1,00	0,66	-0,35
100	1,17	-1,44	0,26	-0,93	-0,97	0,81	-0,36
110	1,34	-1,48	0,14	-1,00	-0,95	0,95	-0,33
120	1,5	-1,50	0,00	-0,92	-0,924	1	-0,28
130	1,64	-1,48	-0,16	-0,76	-0,95	0,93	-0,25
140	1,77	-1,44	-0,33	-0,59	-0,97	0,73	-0,24
150	1,87	-1,37	-0,50	-0,31	-1	0,36	-0,32
160	1,94	-1,27	-0,67	-0,12	-0,99	0	-0,37
170	1,98	-1,14	-0,84	-0,06	-0,90	-0,37	-0,44
180	2,00	-1,00	-1,00	0	-0,69	-0,69	-0,46

In agreement with the general procedure, it is seen that the correction term $2J_0$ has no influence to $\alpha = 60^\circ$. If the requirement

$$n \geq \frac{2\pi d}{\lambda} + 2$$

is not fulfilled, the secondary maximum can assume considerably greater values than the extreme values given by $J_0(x)$.

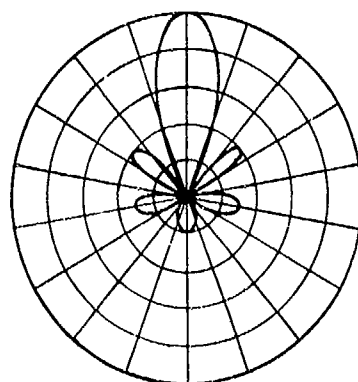


Fig. 29. Directional characteristic of the compensated circular group with a sufficient number of radiators.

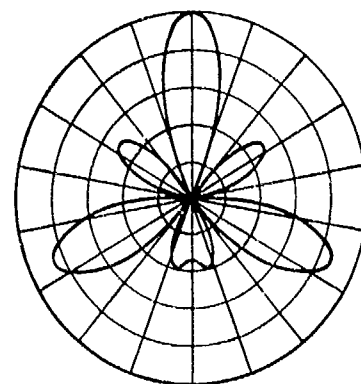


Fig. 30. Directional characteristic of the compensated circular group with an insufficient number of radiators.

As an example, we calculate the case $n=6$, $d/\lambda=1.5$ by the approximation formula (Fig. 30). For comparison the directional characteristic for $n=14$, $d/\lambda=1.5$ which is given simply by $J_0(3\pi \sin \alpha/2)$ is also plotted (Fig. 29). Both directional characteristics agree completely as to their principal parts (i.e., to the first minimum) but then depart considerably in the magnitudes of their secondary maxima.

B. The radiation factor

(a) At a fixed frequency

The directional characteristic has its practical significance when it is a question as to the accuracy with which a beamed receiver system (which, e.g., can be rotated) can locate a distant sound source. Also the behavior of the directional characteristic will determine the freedom from disturbance in certain directions. From the transmission viewpoint, however, beyond the question as to the total power radiated, it is generally a question of concentrating the sound transmission in a certain direction or plane in order to increase the efficiency of the array. Here the question is how great is the sound concentration in the given direction as compared with that for nondirectional sound radiation.

In order to calculate the total power of a beamed radiator, we proceed in a manner similar to that used in introducing the directional characteristic in which we start with formula (3) for the nondirectional system and then calculate the influence of the beaming by the use of a factor \mathcal{G} which we designate as the radiation factor. Thus for the total radiated power L we obtain the relation

$$L = L_0 \mathcal{G} = \frac{1}{2} c \sigma \pi w_m^2 \frac{F^2}{\lambda^2} \mathcal{G}. \quad (57)$$

Here \mathcal{G} is defined by the integral over a sufficiently large sphere K with the radius R :

$$\mathcal{G} = \frac{1}{4\pi R^2} \int_K \mathfrak{R}^2 dK, \quad (58)$$

where \mathfrak{R} is the directional characteristic defined by (6) and dK is the surface element of the sphere with the radius R . Now, with directed sound radiation, the sound energy passing through the unit surface of the sphere with the radius R in the direction defined by the directional characteristic \mathfrak{R} is given by

$$\frac{p^2}{2c\sigma} = \frac{p_0^2 \mathfrak{R}^2}{2c\sigma} = \frac{1}{2} c \cdot \sigma \pi \cdot \frac{w_m^2 F^2}{\lambda^2} \cdot \frac{\mathfrak{R}^2}{4\pi R^2}. \quad (59)$$

On the other hand if the total sound power given by (57) is radiated spherically, the sound energy passing through a unit surface would then be given by

$$\frac{L}{4\pi R^2} = \frac{1}{2} c \cdot \sigma \cdot \pi \cdot \frac{w_m^2 F^2}{\lambda^2} \cdot \frac{1}{4\pi R^2} \quad (60)$$

For each direction characterized by the directional characteristic the ratio of $p^2/2c\sigma$ from (59) to $L/4\pi R^2$ from (60):

$$\frac{p^2}{2c\sigma} : \frac{L}{4\pi R^2} = \frac{\mathcal{R}^2}{\mathcal{C}} \quad (61)$$

states how many times as great the sound energy is in the considered direction as compared with that for spherical propagation. Generally, it is referred to the principal direction for which $\mathcal{R} = 1$.

When this is so we will denote the thus standard quantity $1/\mathcal{C}$ as the condensation factor f .

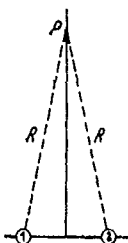


Fig. 31. For illustrating the radiation factor.

We will illustrate the significance of the radiation factor in a simple example. We consider two equal radiators, small compared to the wave length, and assume that the total radiated power of the system consisting of the two radiators is to remain constant while we change the distance between the two radiators. On the basis of symmetry, the power radiated by each of the two radiators then naturally remains constant. We will then find the sound pressure amplitude at a great distance R on the normal axis of the system

(Fig. 31). One could then be led to the following fallacy: Radiator (1) produces the sound pressure amplitude:

$$p_1^0 = \frac{c \cdot \sigma \cdot w_m}{2\lambda R} \cdot F. \quad (61a)$$

Likewise radiator (2) yields the pressure amplitude

$$p_2^0 = \frac{c \cdot \sigma \cdot w_m}{2\lambda R} \cdot F. \quad (61b)$$

Since the signals from the two radiators are in phase on the normal axis, the resultant sound pressure amplitude at P must be equal to twice that due to an individual radiator (independently of the mutual distance of the radiators). But we know that a directional effect dependent on the distance of the two radiators - i.e., a sound condensation variable with the distance of the radiators - exists on the normal axis. The error is due to the fact that, with constant sound radiation of the individual radiator, its

velocity amplitude is by no means independent of the sound pressure produced by the second radiator on its membrane. In addition to the work which the individual radiator must do with an undistorted sound field, it must, in the presence of a second radiator, overcome the pressure exerted by this on its membrane. This additional work will be different with the phase difference, i.e., with the distance between the two radiators. (Quite similar to this is the case where, in a half space cut off by a rigid wall, we bring a radiator of constant sound power nearer and nearer to the wall.) In order to investigate this quantitatively, we calculate the total radiated power of the system consisting of two equal radiators (1) and (2) at the distance d (Fig. 32).

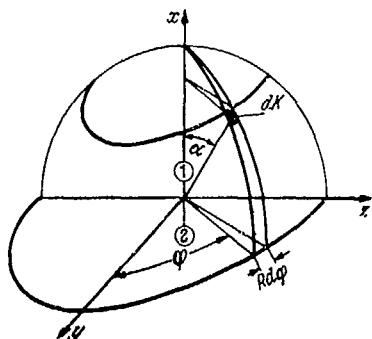


Fig. 32. For calculating the radiation factor.

By (57)

$$L = \frac{1}{2} c \cdot \sigma \cdot \pi w_m^2 \frac{(2F)^2}{\lambda^2} \cdot \mathcal{G}, \quad (62)$$

$$\mathcal{G} = \frac{1}{4\pi R^2} \int_K dK = \frac{1}{4\pi R^2} \int_0^{2\pi} d\varphi \int_0^\pi d\alpha \cos^2\left(\frac{\pi d}{\lambda} \cos \alpha\right) \sin \alpha, \quad *$$

$$\mathcal{G} = \frac{1}{2} \left(1 + \frac{\sin 2\pi d/\lambda}{2\pi d/\lambda}\right). \quad (63)$$

Fig. 33, curve 1, shows the dependence of the radiation factor on d/λ . If we were able to keep w_m for the two radiators constant, according to (62) the radiated power would vary in the same manner as \mathcal{G} in Fig. 33. Conversely, if we keep L constant and vary the distance, w_m^2 must vary with $1/\mathcal{G}$.

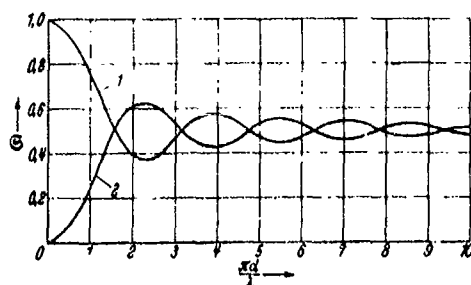


Fig. 33. Radiation factor of a system consisting of two radiators (distance d)

1. In phase. 2. In phase opposition.

* The factor R^2 should also appear in the numerator of the fraction preceding the double integral in the right member of this equation.

radiator, then in the maximum case 2.55-fold sound energy per unit surface can be attained in the symmetry plane as compared with the nondirectional sound radiation. In the same manner, we can inquire as to the maximum condensation factor with arrays of 3, 4, 5, etc. vibrators arranged on a straight line equidistantly and always find one quite definite value of d/λ for which this is the case. This yields the table given below.

n	$f_{\text{max}} = 1/\mathfrak{S}_{\text{max}}$	$\text{int } d/\lambda$
2	= 2,55	= 0,715
3	= 4,25	= 0,77
4	= 5,9	= 0,825
5	= 7,7	= 0,865
6	= 9,5	= 0,90

If we denote the radiation factor for n similarly arranged radiators by \mathfrak{S}_n , there thus results the general formula¹⁵

$$\mathfrak{S}_n = \frac{1}{n^2} \left(n + 2 \sum_{m=1}^{n-1} (n-m) \frac{\sin m 2\pi d/\lambda}{m \cdot 2\pi d/\lambda} \right). \quad (64)$$

For $n = 2, 3, 4, 5, 6$, radiators, $f = 1/\mathfrak{S}_n$ is represented in Fig. 34.

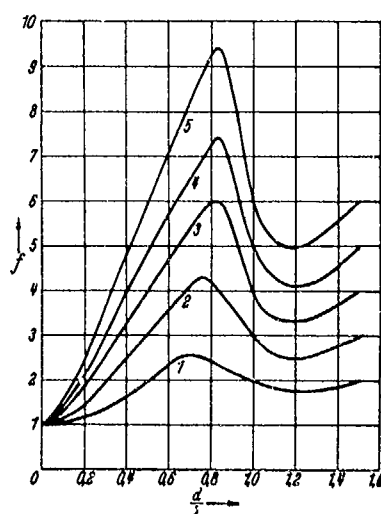


Fig. 34. Condensation factor of the straight line group (d = distance between two radiators).

1. Two radiators. 2. Three radiators. 3. Four radiators. 4. Five radiators. 5. Six radiators.

If d is equal to $\lambda/2$ or an integral multiple thereof, then from (64):

$$\mathfrak{S}_n = 1/n, \quad (64a)$$

i.e., the condensation factor is then equal to $1/n$. This has been pointed out by Lord Rayleigh¹⁶. The calculation of the circular piston membrane is also due to him¹⁷. For this it turns out that

$$\mathfrak{S}_0 = \frac{2}{(\pi d/\lambda)^2} \left[1 - \frac{2J_1\left(\frac{2\pi d}{\lambda}\right)}{2\pi d/\lambda} \right], \quad (65)$$

wherein d is the diameter and J_1 denotes the Bessel function of the first order. From this it results that for large d/λ , the condensation factor f of the circular piston membrane is

$$f = 2\pi F/\lambda^2, \quad (66)$$

where F denotes the surface of the membrane.

¹⁵ Ann. d. Phys., Vol. 7 (1930), p. 964.

¹⁶ On the production and distribution of sound. Phil. Mag., 1903, pp. 289-305.

¹⁷ The theory of sound, sec. 302.

Also, the radiation factors of the circular membrane whose velocity amplitude is

$$w = (1 - \rho^2/r^2)^n \quad (66a)$$

may be calculated with the aid of the Bessel's functions. For $w_1 = 1 - \rho^2/r^2$ there results the radiation factor

$$\mathfrak{E}_1 = 2^2 \cdot 2! \cdot 2! \left(\frac{x^{-4}}{2!} + \frac{x^{-2}}{1! 3!} - \frac{J_2(2x)}{x^6} - \frac{2J_3(2x)}{x^8} \right), \quad (67)$$

and for $w_2 = (1 - \rho^2/r^2)^2$ the radiation factor is

$$\mathfrak{E}_2 = 2^3 \cdot 3! 3! \left(\frac{3x^{-6}}{3!} + \frac{x^{-4}}{1! 4!} + \frac{3x^{-2}}{2! 5!} - \frac{3J_3(2x)}{x^9} - \frac{4J_4(2x)}{x^{11}} - \frac{4J_5(2x)}{x^{13}} \right). \quad (68)$$

In general, by the series development for

$$w_n = (1 - \rho^2/r^2)^n \quad (68a)$$

it turns out that

$$\begin{aligned} \mathfrak{R}_n &= 1 - \frac{(x/2)^2}{n+2} + \frac{(x/2)^4}{2! (n+2)(n+3)} - \frac{(x/2)^6}{3! (n+2)(n+3)(n+4)} + \dots, \\ \mathfrak{E}_n &= 1 - \frac{x^2}{3(n+2)} + \frac{(2n+5)x^4}{2! 3 \cdot 5 \cdot (n+2)^2 (n+3)} \\ &\quad - \frac{(2n+7)x^6}{3! 3 \cdot 5 \cdot 7 (n+2)^3 (n+3)(n+4)} + \dots. \end{aligned} \quad (69)$$

The radiation factors \mathfrak{E}_n , \mathfrak{E}_1 , \mathfrak{E}_2 are represented in Fig. (35).

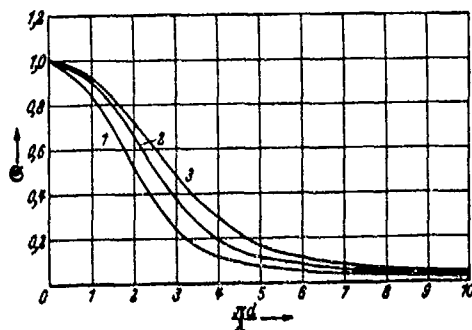


Fig. 35. 1. Radiation factor of the circular piston membrane ($w=1$).
2. Radiation factor of the stretched membrane ($w=1-\rho^2/r^2$).
3. Radiation factor of the stretched membrane ($w=(1-\rho^2/r^2)^2$).



Fig. 36. For the calculation of the radiation factor of the rectangular piston membrane.

For a rectangular piston membrane whose one side (b) is small compared to the wave length while the other side (c) is arbitrary (Fig. 36), the radiation factor

$$\begin{aligned} \mathcal{G} &= \frac{1}{2} \int_0^\pi \frac{\sin^2 \frac{c\pi}{\lambda} (\cos \gamma)}{\left(\frac{c\pi}{\lambda}\right)^2 \cos^2 \gamma} \sin \gamma d\gamma = \frac{1}{2c\pi} \int_{-\frac{c\pi}{\lambda}}^{+\frac{c\pi}{\lambda}} \frac{\sin^2 t}{t^2} dt, \\ \mathcal{G} &= -\frac{\sin^2 c\pi/\lambda}{(c\pi/\lambda)^2} + \frac{1}{c\pi/\lambda} \int_0^{2c\pi/\lambda} \frac{\sin t}{t} dt = -\frac{\sin^2 c\pi/\lambda}{(c\pi/\lambda)^2} + \frac{1}{c\pi/\lambda} Si \frac{2c\pi}{\lambda}. \end{aligned} \quad (70)$$

results.

If one replaces the sine integral

$$Si x = \int_0^x \frac{\sin t}{t} dt \quad (70a)$$

by the approximation

$$Si x = \frac{\pi}{2} - \frac{\cos x}{x} (1 - 2/x^2) - \frac{\sin x}{x}, \quad (70b)$$

one obtains

$$\mathcal{G} = \frac{1}{2x} \left[\pi - 1/x - \frac{\sin 2x}{2x} + \frac{\cos 2x}{2x^2} \right], \quad x = \frac{c\pi}{\lambda}. \quad (71)$$

For larger values of $x (x \geq 2)$, one will be able to use the approximation

$$\mathcal{G} = \frac{\pi}{2x} \quad \text{or} \quad \mathcal{G} = \frac{\pi}{2x} - \frac{1}{2x^2}$$

as is seen in the following table

x	$\frac{\pi}{2x} - \frac{\sin^2 x}{x^2}$	x	$\frac{\pi}{2x} - \frac{\sin^2 x}{x^2}$	$\frac{\pi}{2x} - \frac{1}{2x^2}$
0	1	2.5	0.563	0.548
0.2	0.994	3	0.473	0.467
0.4	0.983	3.5	0.406	0.408
0.6	0.949	4	0.358	0.361
0.8	0.931	4.5	0.323	0.324
1	0.897	5	0.295	0.294
1.2	0.858	5.5	0.271	0.269
1.4	0.813	6	0.249	0.248
1.6	0.766	6.5	0.230	0.230
1.8	0.719	7	0.214	0.214
2	0.673	7.5	0.200	0.200

* The third term in the brackets should be $-\frac{\sin 2x}{x}$. The last term in the brackets should be $\frac{\cos 2x}{2x^2}$.

The maximum condensation factor f then turns out to be $2c/\lambda$ for large values of $c\pi/\lambda$. This therefore means that a narrow rectangular piston membrane (in a rigid wall) with one side equal to 10 wave lengths sends out in the symmetry plane 20 times as much sound energy per unit surface as compared with nondirectional radiation.

If b is not small compared to the wave length \ominus can generally be represented by the following series¹⁸.

$$\ominus = \varphi_0\left(\frac{c\pi}{\lambda}\right) - \frac{1}{2} \cdot \frac{2^3}{4!} \left(\frac{b\pi}{\lambda}\right)^2 \varphi_1\left(\frac{c\pi}{\lambda}\right) + \frac{1}{2} \cdot \frac{3 \cdot 2^5}{4! \cdot 6!} \left(\frac{b\pi}{\lambda}\right)^4 \varphi_2\left(\frac{c\pi}{\lambda}\right) - \dots \quad (72)$$

where

$$\varphi_n(x) = \frac{1}{x} \int_0^x \frac{\sin^2 z}{z^2} \left(1 - \frac{z^2}{x^2}\right)^n dz \quad (73)$$

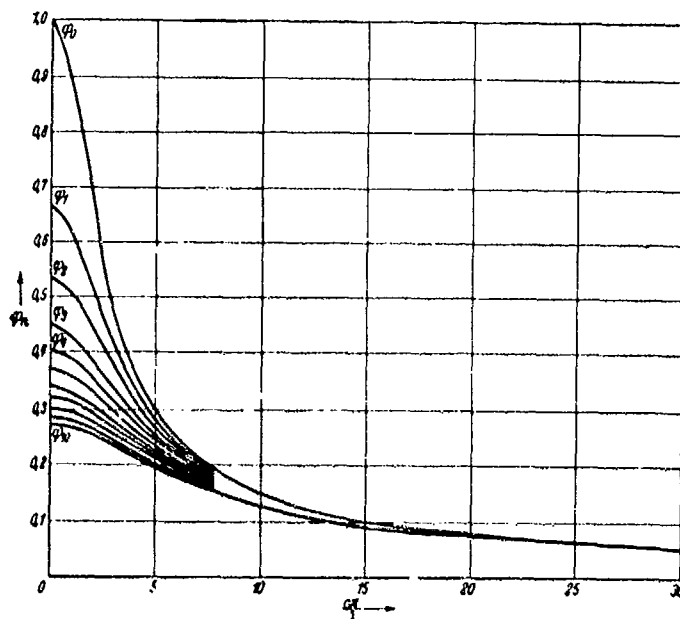


Fig. 37. Functions for the calculation of the radiation factor of the rectangle.

These functions are represented in Fig. 37. Here it is seen that as soon as c/λ becomes greater than 5, $\varphi_1, \varphi_2, \dots$ can be replaced by φ_0 . It then follows from (72) that

¹⁸ Ann. d. Phys., Vol. 7 (1930), pp. 953-957.

$$\mathcal{S} = \varphi_0 \left(\frac{c\pi}{\lambda} \right) \cdot \frac{2}{\pi} \int_0^{\pi/2} \frac{\sin^2 \left(\frac{b\pi}{\lambda} \cos \varphi \right)}{\left(\frac{b\pi}{\lambda} \cos \varphi \right)^2} d\varphi. \quad (74)$$

The integral

$$\psi = \frac{2}{\pi} \int_0^{\pi/2} \frac{\sin^2 \left(\frac{b\pi}{\lambda} \cos \varphi \right)}{\left(\frac{b\pi}{\lambda} \cos \varphi \right)^2} d\varphi \quad (74a)$$

is found by the series development:

$$\psi = 1 - \frac{\left(\frac{b\pi}{\lambda} \right)^2}{3 \cdot 1! \cdot 2!} + \frac{\left(\frac{b\pi}{\lambda} \right)^4}{5 \cdot 2! \cdot 3!} - \frac{\left(\frac{b\pi}{\lambda} \right)^6}{7 \cdot 3! \cdot 4!} + \dots \quad (75)$$

or, for the larger values of $b\pi/\lambda$, better by the Bessel function series

$$\psi = \frac{1}{b\pi/\lambda} \left[J_1 \left(\frac{2\pi b}{\lambda} \right) + 2J_3 \left(\frac{2\pi b}{\lambda} \right) + 2J_5 \left(\frac{2\pi b}{\lambda} \right) + \dots \right]. \quad (76)$$

For the larger values of $b\pi/\lambda$ this series is considerably more convenient to evaluate. It turns out that for $b\pi/\lambda > 3$ the value of the bracketed sum differs from unity only by (a few) percent¹⁹. The value of the function

$$x \cdot \psi(x) = \frac{2}{\pi} \int_0^{\pi/2} \frac{\sin^2(x \cos \varphi)}{x \cos^2 \varphi} d\varphi \quad (77)$$

is represented in Fig. 38.

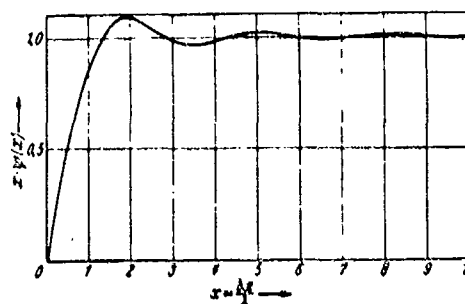


Fig. 38. Auxiliary function for the calculation of the radiation factor.

¹⁹ This is adjudged to be the meaning of the following sentence in which one or more words have apparently been left out: "Und zwar ergibt sich, dass für $b\pi/\lambda > 3$ der Wert der in der eckigen Klammer stehenden Summe nur um Prozente von Eins abweicht."

If we therefore assume that $c/\lambda > 5$ and $b/\lambda > 1$, the condensation factor then becomes

$$f = \frac{c\pi/\lambda \cdot b\pi/\lambda}{\pi/2} = \frac{2\pi F}{\lambda^2}. \quad (78)$$

The condensation factor is represented for values of $b\pi/\lambda$ and $c\pi/\lambda$ between 0 and 10 in Fig. 39. Here are drawn the curves

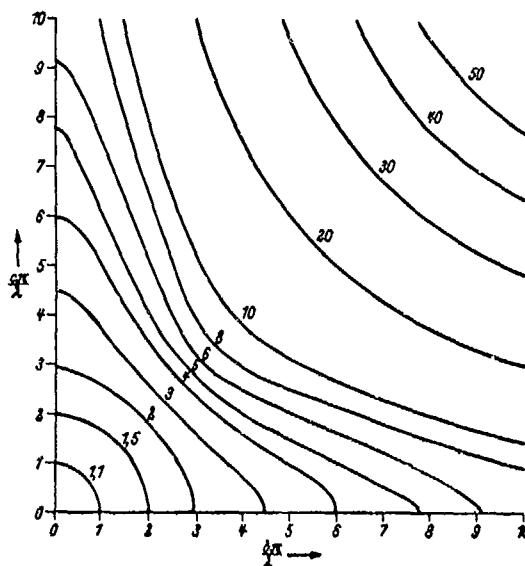


Fig. 39. Condensation factor of the rectangular piston membrane. (The numbers on the curves are the condensation factor.)

for which the condensation factor possesses a constant value. We find, e.g., the same condensation factor $f = 7$ for a square for which $b\pi/\lambda = c\pi/\lambda = 3.15$ as for the rectangle $b\pi/\lambda = 0.5$; $c\pi/\lambda = 10$ even though the surface of the rectangle is only half as large. For $a\pi/\lambda < 1$ and $b\pi/\lambda < 1$ (quarter) circles result. For $f > 10$, (in the more central part) the curves are hyperbolas. This last means that with sufficient accuracy, one can write $f = 2\pi F/\lambda^2$.

In the calculation of directional characteristics, we have remarked that whenever individual parts of the membrane vibrate in opposite phase, the direction effect is substantially affected. This influence must also be effective for radiation factors. As a very simple example, we calculate the radiation factor of two radiators, small compared to the wave length, at the distance d which vibrate in opposite phase. A computation analogous to that on page 43 yields

$$\mathcal{G} = \frac{1}{2} \left(1 - \frac{\sin 2\pi d/\lambda}{2\pi d/\lambda} \right). \quad (79)$$

We obtain the corresponding curve by reflection of the curve

$$\mathcal{G} = \frac{1}{2} \left(1 + \frac{\sin 2\pi d/\lambda}{2\pi d/\lambda} \right), \quad (63)$$

on the horizontal line $y = \frac{1}{2}$ (see Fig. 33).

The maximum of f occurs here for $\frac{2\pi d}{\lambda} = 7.725$, i.e., for $d/\lambda = 1.23$ and it amounts to 2.294. This is the condensation factor at the position where $\mathcal{R} = 1$ and corresponds to $\gamma = 24^\circ$. While, with two in-phase radiators, we could obtain a 2.55-fold condensation (for $\gamma = 0^\circ$), with two oppositely phased radiators there resulted at most a 2.29-fold condensation (for $\gamma = 24^\circ$). For the example on page 30 where w_m vanished, the radiation factor must naturally lose its meaning and we must calculate the total power L_1 by the formula (59). Then from

$$p = \frac{c \cdot \sigma \cdot F}{\lambda \cdot R} (\mathcal{R}_1(x) - \mathcal{R}_0(x)) \quad (80)$$

it follows that

$$\begin{aligned} L_1 &= \frac{1}{2} \frac{c \cdot \sigma}{\lambda^3 R^2} \cdot F^2 \int_K [\mathcal{R}_1(x) - \mathcal{R}_0(x)]^2 dx \quad * \\ &= 4\pi c \sigma \frac{F^2}{\lambda^2} \left[\frac{1}{3x^3} - \frac{J_1(2x)}{x^3} + \frac{4J_3(2x)}{x^3} - \frac{8J_5(2x)}{x^3} \right]. \end{aligned} \quad (81)$$

If the Bessel's functions are replaced by the corresponding power series, there results

$$L_1 = 4\pi c \sigma \frac{F^2}{\lambda^2} \left[\frac{1 \cdot 2 \cdot x^4}{3! 6!} - \frac{2 \cdot 3 x^6}{4! 7!} + \frac{3 \cdot 4 \cdot x^8}{5! 8!} - \dots \right]. \quad (82)$$

If the power radiated by a piston membrane of the same size with the velocity amplitude $w = 1$

$$L_2 = 2\pi \cdot c \cdot \sigma \cdot \frac{F^2}{\lambda^2} \cdot \frac{2}{x^2} \left(1 - \frac{J_1(2x)}{x} \right). \quad (83)$$

is compared with L_1 for small values of x , one finds

$$\frac{L_1}{L_2} = \frac{4x^4}{3! 6!} \quad (83a)$$

* λ^2 should replace λ^3 in the denominator of the fraction preceding the integral sign.

For $x = \frac{\pi d}{\lambda} = \frac{1}{2}$ this becomes

$$L_1/L_2 = 1/17280. \quad (83b)$$

This means that if the membrane for L_1 is to radiate the same power as that for L_2 , then the amplitude of the first membrane must be

$$\sqrt{17280} = 131$$

times that of the latter.

For very large values of d/λ , on the other hand, we have by (81) and (83):

$$\frac{L_1}{L_2} = \frac{1}{3}. \quad (83c)$$

(b) With artificial compensation

From Fig. 27, it is to be seen that the radiation distribution is also substantially changed by artificial compensation. In general, the radiation factor for the group consisting of two radiators is

$$\mathcal{G}_k = \frac{1}{4\pi} \int_0^{2\pi} \int_{-\pi/2}^{+\pi/2} \cos^2 \left[\frac{\pi d}{\lambda} (\sin \gamma - \sin \gamma_k) \right] \cos \gamma d\gamma. \quad (84)$$

If we introduce a new variable of integration x by

$$x = \frac{\pi d}{\lambda} (\sin \gamma - \sin \gamma_k) \quad (84a)$$

it is found that

$$\mathcal{G}_k = \frac{\lambda}{2\pi d} \int_{-\frac{\pi d}{\lambda}(1 - \sin \gamma_k)}^{\frac{\pi d}{\lambda}(1 - \sin \gamma_k)} \cos^2 x dx, \quad (85)$$

$$\mathcal{G}_k = \frac{1}{2} \left\{ 1 + \frac{\sin \frac{2\pi d}{\lambda}}{2\pi d/\lambda} \left[\cos \left(\frac{2\pi d}{\lambda} \sin \gamma_k \right) \right] \right\}.$$

In Fig. 40, \mathcal{E}_k is represented for $\sin \gamma_k = 0, \frac{1}{4}, \frac{1}{2}, \frac{3}{4}, 1$. Since $\sin \gamma_k = 0$ corresponds to the uncompensated case, it is seen that for

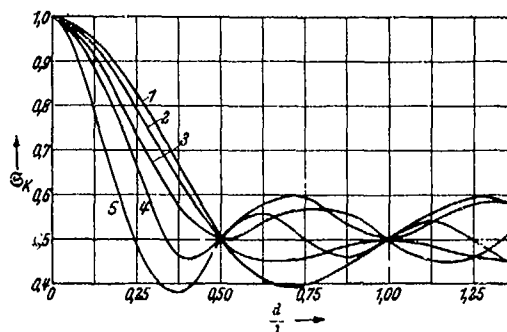


Fig. 40. Radiation factor for two compensated radiators (Distance d , compensation angle γ_k).

1. $\sin \gamma_k = 0$; 2. $\sin \gamma_k = \frac{1}{4}$; 3. $\sin \gamma_k = \frac{1}{2}$; 4. $\sin \gamma_k = \frac{3}{4}$; 5. $\sin \gamma_k = 1$

$d/\lambda < \frac{1}{2}$ the uncompensated case always yields larger values. E.g., for $d/\lambda = \frac{1}{2}$; $\mathcal{E} = 0.83$; $\mathcal{E}_k = 0.5$.

From this it follows that the condensation factor of the compensated group in the direction of the line of the radiators (i.e., $\gamma_k = 90^\circ$) is 1.66 times as great as the condensation factor of the uncompensated group in the maximum direction. If, therefore, with two nondirectional radiators at the distance $d < \lambda/2$, the greatest sound intensity for one definite direction is desired, the best results will be obtained by working with a compensated array.

In general, for a compensated straight line group which consists of n equidistant radiators, the radiation factor turns out to be

$$\mathcal{E}_k = \frac{1}{n} + \frac{2}{n^2} \sum_{m=1}^{n-1} (n-m) \cdot 2 \frac{\sin(m \cdot 2\pi d/\lambda) \cdot \cos(m \cdot 2\pi d/\lambda \sin \gamma_k)}{m \cdot 4\pi d/\lambda} \quad (85a)$$

If the direction of the compensation line coincides with the direction of the array (i.e., $\gamma_k = 90^\circ$), one finds

$$\mathcal{E}_k = \frac{1}{n} + \frac{2}{n^2} \sum_{m=1}^{n-1} (n-m) \frac{\sin(m \cdot 4\pi d/\lambda)}{m \cdot 4\pi d/\lambda} \quad (86)$$

Comparing this with the radiation factor for the uncompensated case (i.e., $\gamma_k = 0$)

$$\mathcal{G} = \frac{1}{n} + \frac{2}{n^2} \sum_{m=1}^{n-1} (n-m) \frac{\sin\left(m \cdot \frac{2\pi d}{\lambda}\right)}{m \cdot 2\pi d/\lambda}. \quad (87)$$

we conclude that the straight line uncompensated group with the receiver distance d has the same radiation factor as the group compensated in the array direction with the receiver distance $d/2$. Or, otherwise expressed, the sound concentration of this straight line uncompensated group on the normal axis is equal to the sound concentration of the group compensated in the array direction with half the receiver distance.

In order to find the radiation factor for the densely covered circular group with a compensation direction $(\alpha_0 \beta_0 \gamma_0)$, we have to calculate the integral

$$\mathcal{G}_k = \frac{1}{2\pi} \int_0^{2\pi} d\varphi \int_0^{\pi/2} d\gamma \mathcal{R}^2 \sin \gamma \quad (88)$$

where, according to (52), \mathcal{R} is given by

$$\mathcal{R} = J_0\left(\frac{\pi d}{\lambda} \sqrt{(\cos \alpha - \cos \alpha_0)^2 + (\cos \beta - \cos \beta_0)^2}\right) \quad (88a)$$

Since $\cos \alpha = \sin \gamma \cos \varphi$, $\cos \beta = \sin \gamma \sin \varphi$ it follows that

$$\mathcal{R} = J_0(kr) \sqrt{\sin^2 \gamma - 2 \sin \gamma \sin \gamma_0 \cos(\varphi - \varphi_0) + \sin^2 \gamma_0}. \quad (88b)$$

If, for abbreviation, we set $u = kr \sin \gamma$, $v = kr \sin \gamma_0$, it then follows by the addition theorem for Bessel functions that

$$\begin{aligned} \mathcal{R} &= J_0(\sqrt{u^2 + v^2 - 2uv \cos(\varphi - \varphi_0)}) \\ &= J_0(u)J_0(v) + 2 \sum_{n=1}^{\infty} J_n(u)J_n(v) \cos n(\varphi - \varphi_0) \end{aligned} \quad (89)$$

If we now form the integral

$$\frac{1}{2\pi} \int_0^{2\pi} \mathcal{R}^2 d\varphi, \quad (89a)$$

then since

$$\int_0^{2\pi} \cos m(\varphi - \varphi_0) \cos n(\varphi - \varphi_0) d\varphi = \begin{cases} 0 & \text{für } m \neq n \\ \pi & \text{für } m = n \end{cases} \quad (89b)$$

the terms with unequal indices fall out and there results

$$\frac{1}{2\pi} \int_0^{2\pi} R^2 d\varphi = J_0^2(u) J_0^2(v) + 2J_1^2(u) J_1^2(v) + \dots \quad (90)$$

It then turns out that

$$\begin{aligned} \mathcal{E}_k &= J_0^2(kr \sin \gamma_0) \cdot \int_0^{\pi/2} J_0^2(kr \sin \gamma) \sin \gamma d\gamma \\ &+ 2J_1^2(kr \sin \gamma_0) \int_0^{\pi/2} J_1^2(kr \sin \gamma) \sin \gamma d\gamma + \dots \end{aligned} \quad (91)$$

or since

$$\int_0^{\pi/2} J_n^2(x \sin \gamma) \sin \gamma d\gamma = \frac{1}{x} \int_0^x J_{2n}(\xi) d\xi \quad (92) \checkmark^{20}$$

it follows that

$$\begin{aligned} \mathcal{E}_k &= J_0^2(kr \sin \gamma_0) \cdot \frac{1}{kr} \int_0^{kr} J_0(2\xi) d\xi + 2J_1^2(kr \sin \gamma_0) \cdot \frac{1}{kr} \int_0^{kr} J_2(2\xi) d\xi \\ &+ 2J_2^2(kr \sin \gamma_0) \cdot \frac{1}{kr} \int_0^{kr} J_4(2\xi) d\xi + \dots \end{aligned} \quad (93)$$

The calculations of the integrals

$$\varphi_n(x) = \int_0^x J_{2n}(2x) dx \quad (93a)$$

may be easily carried out by the relation

$$\int_0^x J_r(2x) dx = 2 \sum_{n=0}^{\infty} J_{r+2n+1}(2x) \quad (94)$$

with the aid of the Bessel function tables.

\checkmark^{20} (92) is obtained if, in the well-known equation

$$J_n^2(x \sin \gamma) = \frac{2}{\pi} \int_0^{\pi/2} J_{2n}(2x \sin \gamma \cos \varphi) d\varphi \quad (a)$$

both sides are multiplied by $\sin \gamma d\gamma$ and are integrated from 0 to $\pi/2$ and the relation given by Nielsen (Handb. der Zylinderfunktionen, p. 380, formula 1, $\nu=0$)

$$\frac{d}{dx} \int_0^{\pi/2} \int_0^{\pi/2} x \sin \omega / (x \sin \omega \sin \varphi) d\omega d\varphi = \frac{\pi}{2} J_0(x) \quad (b)$$

is used.

The corresponding functions

$$\varphi_n(x)$$

are represented in Fig. 41.

In Fig. 42 the radiation factor (for the circular group) $\mathcal{G}_k\left(\frac{2\pi r}{\lambda}\right)$ is drawn as a function of $\frac{2\pi r}{\lambda}$ (r = radius of the circle, λ = wave length). Here:

Curve 1 represents the uncompensated case (i.e., $\gamma_k = \gamma_0 = 0^\circ$),

Curve 2 represents the case $\gamma_k = 30^\circ$,

Curve 3 represents the case $\gamma_k = 90^\circ$.

Besides this, the curves 4, 5, 6:

$$\frac{2\pi r}{\lambda} \mathcal{G}_k\left(\frac{2\pi r}{\lambda}\right)$$

resulting from this are drawn.

From the latter, it is recognized that with increasing

$$\frac{2\pi r}{\lambda}, \quad \frac{2\pi r}{\lambda} \mathcal{G}_k\left(\frac{2\pi r}{\lambda}\right)$$

approaches nearer and nearer to the value $1/2$.

This means that, for larger values of r/λ and with great directivity, the condensation factor $1 = 1/\mathcal{G}_k$ is given by $\frac{2\pi r}{\lambda} \cdot 2$. Otherwise expressed this says: The length of the circumference of the circle measured in λ , when multiplied by 2, gives the size of the condensation factor. In connection with the earlier considerations on the condensation factor for uncompensated radiator arrays, the straight line, a circular line, a circular surface or a rectangular surface, we can formulate the following general theorem:

With great directivity the condensation factor is:

1. Two times the length of the radiating line measured in wave lengths for line-shaped radiator arrays.
2. 2π times the surface of the radiating arrangement measured in λ^2 for surface radiator arrays.

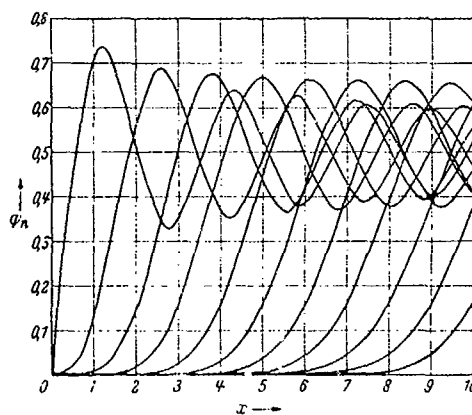


Fig. 41. Auxiliary functions for calculating the radiation factor.

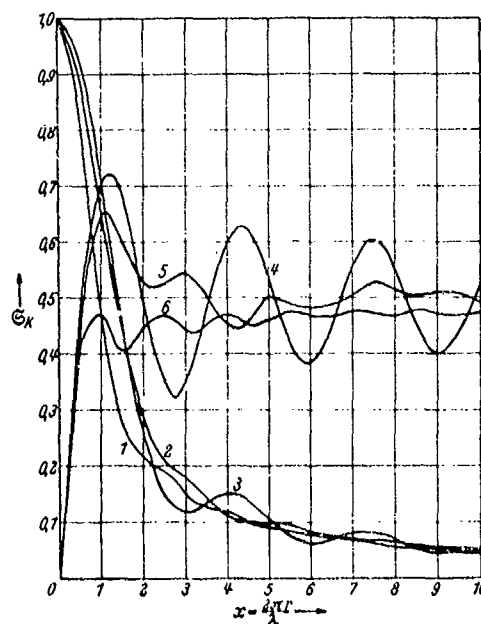


Fig. 42. Radiation factor of the compensated circular group:

1. $\mathcal{Z}_1(x)$ for $\gamma_k = 0$; 2. $\mathcal{Z}_1(x)$ for $\gamma_k = 30^\circ$; 3. $\mathcal{Z}_1(x)$ for $\gamma_k = 90^\circ$; 4. $\mathcal{Z}_1(x)$ for $\gamma_k = 0$; 5. $\mathcal{Z}_1(x)$ for $\gamma_k = 30^\circ$; 6. $\mathcal{Z}_1(x)$ for $\gamma_k = 90^\circ$.

Part Two

THE SOUND FIELD IN THE NEIGHBORHOOD OF THE RADIATOR

3. The group of two radiators

For the previous considerations, the assumption was made that the field point was at a sufficient distance from the radiating surface. For this part of the sound field, which is generally taken into consideration first in the usual practical problems, there results a simple representation when, to the expression which characterizes the nondirectional radiation, a factor is affixed which is independent of the distance of the field point and depends only on the direction of the field point line. Furthermore, this characteristic function (the directional characteristic) was only dependent upon one quantity (e.g., the function

$$x = \frac{2\pi r}{\lambda} \sin \gamma).$$

The sound field was therefore substantially determined by this one function - the determination being quite general for any given frequency (wave length) and for any given dimension of the radiating system (r/λ). The conditions for the calculation and representation of the nearby field are considerably more difficult. First, we are forced to calculate the adjacent field at so great a number of points that the complete field can be obtained by interpolation, and secondly it is necessary to carry out this representation for each particular case which is characterized by the ratio of the geometric dimension to the wave length. The diversity of the problem has now thus become substantially greater. We will, therefore, have to confine the representation of the adjacent field to special cases. The sound field will be represented when we draw curves in the neighborhood of the radiating system which correspond to a constant pressure amplitude.

It must first be made clear when a field point is to be regarded as belonging to the nearby field and when this is not the case. The term "nearby field" could lead to the mistaken idea that it is only a question of the geometry of the radiators so that one could perhaps say that with a radiating circular piston membrane of the radius a , all field points are no longer to be regarded as belonging to the nearby field which, e.g., are at a greater distance from the membrane center than 10 times the radius. Actually, this definition is not sufficient since, besides this, it is also a question of the wave length. In order

to investigate this more closely we must start from the formula generally valid for distant and nearby fields and determine under what conditions this becomes formula (6) given for the distant field.

We assume that the radiating surface of the membrane is in a rigid infinite wall or acts as a double membrane, where the one part vibrates symmetrically to the other part at each instant as is represented in Figs. 1-e and 1-f. Here the radiating surface must consist of several component parts situated in the same rigid wall, or of several individual double membranes all of which have a common symmetry plane. We assume the radiating surface to be at the zero position in the XY-plane and the velocity amplitude given by

$$w = w(x, y)e^{i\omega t} \quad (95)$$

Here we will, in general, assume $w(x, y)$ to be a real function. Physically, this means that all oscillating membrane elements pass through the zero position simultaneously, and reach their extreme positions simultaneously so that (besides nodal lines) only motions of the membrane elements which are in phase or in phase opposition are possible. Basically no difficulties exist in prescribing the velocity amplitude at every point of the membrane with respect to amplitude and phase when

$$w(x, y) = u(x, y) + iv(x, y) \quad (95a)$$

is regarded as a complex function.

Then for an arbitrary field point P in the upper half space (because of the rigid wall, we can confine ourselves to the half-space $z \geq 0$) the behavior of the sound pressure according to Rayleigh²¹ is given by

$$p = e^{i(\omega t + \pi/2)} \cdot \frac{c\sigma}{\lambda} \int_F w(x, y) \frac{e^{-ikr}}{r} dF \quad (96)$$

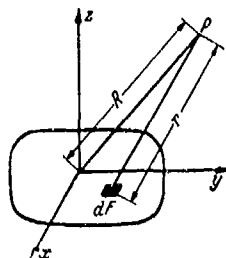


Fig. 43. For the definition of the nearby field.

Here the integration is to extend over the surface F radiating into the half space. r is the distance of the element of integration dF from the field point P and R is the distance of the field point from the coordinate origin (see Fig. 43).

If the field point P has the coordinates, x_0, y_0, z_0 , and the mid-point of the surface element dF has the coordinates x, y , the relation

$$r^2 = R^2 + x^2 + y^2 - 2xx_0 - 2yy_0 \quad (96a)$$

²¹

The theory of sound, Sec. 278.

then follows from

$$\begin{aligned} R^2 &= x_0^2 + y_0^2 + z_0^2, \\ r^2 &= (x - x_0)^2 + (y - y_0)^2 + z_0^2 \end{aligned} \quad (96b)$$

Therefore

$$\begin{aligned} \frac{r}{R} &= \left[1 - \frac{2(x \cos \alpha + y \cos \beta)}{R} + \frac{x^2 + y^2}{R^2} \right]^{\frac{1}{2}}, \\ \frac{r}{R} &= 1 - \frac{x \cos \alpha + y \cos \beta}{R} + \frac{1}{2} \frac{x^2 + y^2}{R^2} - \frac{1}{2} \left(\frac{x \cos \alpha + y \cos \beta}{R} \right)^2. \end{aligned} \quad (97)$$

In this development, terms of higher order than the second are neglected. In place of the earlier formula (which was derived on assuming a sufficient distance of the field point):

$$\varphi = \frac{e \sigma}{\lambda \cdot R} e^{i(\omega t + \pi/2 - kR)} \int_F w(x, y) e^{ik(x \cos \alpha + y \cos \beta)} dF \quad (98)$$

there now follows from (96) and (97):

$$\begin{aligned} \varphi &= \frac{e \cdot \sigma}{\lambda \cdot R} e^{i(\omega t + \pi/2 - kR)} \int_F w(x, y) \cdot e^{ik(x \cos \alpha + y \cos \beta)} \\ &\quad \cdot \frac{1 - \frac{x \cos \alpha + y \cos \beta}{R} + \frac{1}{2} \frac{x^2 + y^2 - (x \cos \alpha + y \cos \beta)^2}{R^2}}{1 - \frac{x \cos \alpha + y \cos \beta}{R} + \frac{1}{2} \frac{x^2 + y^2 - (x \cos \alpha + y \cos \beta)^2}{R^2}} dF. \quad (99) \end{aligned}$$

(99) can therefore be replaced by (98) when

$$\begin{aligned} &\frac{1 - \frac{x \cos \alpha + y \cos \beta}{R} + \frac{1}{2} \frac{x^2 + y^2 - (x \cos \alpha + y \cos \beta)^2}{R^2}}{1 - \frac{x \cos \alpha + y \cos \beta}{R} + \frac{1}{2} \frac{x^2 + y^2 - (x \cos \alpha + y \cos \beta)^2}{R^2}} \\ &= 1. \end{aligned} \quad (99a)$$

can be replaced by 1. Since this is to hold for all values of α and β , it is easy to see that because of the denominator, one must have

$$\frac{x^2 + y^2}{R^2} = 1 \quad (100)$$

and because of the numerator it must be that

$$1 - \frac{x \cos \alpha + y \cos \beta}{R} + \frac{1}{2} \frac{x^2 + y^2 - (x \cos \alpha + y \cos \beta)^2}{R^2} = 1 \quad (101)$$

* Here the exponent of $(x \cos \alpha + y \cos \beta)$ in the second exponential of the integrand should be changed from 3 to 2.

Since in the most unfavorable case

$$x^2 + y^2 = \varrho_m^2 \quad (101a)$$

is the greatest distance of a membrane point from the coordinate origin, (100) asserts that the field point distance R must be large compared to the greatest linear dimension of the radiating surface (in the XY-plane). From (101) it furthermore follows that one must have

$$\frac{\pi \cdot \varrho_m}{\lambda \cdot R} \ll 1 \quad (102)$$

With small values of λ (more precisely, if $\lambda \ll \pi R$) condition (102) is therefore more discriminating. If we assume a piston membrane of 5 cm radius and first use a wave length of 15 cm and then a wave length of 1 cm, then, according to (100), the sufficient distance R would be given by $R \gg 5$ cm while in the second case it would, according to (102), be given by $R \gg 75$ cm.

For two radiators which are small compared to the wave length, a simple addition replaces the integration of formula (10). We obtain the pressure of the resultant field in the following form:

$$p = e^{i(\omega t - \pi/2)} \frac{c \cdot \sigma}{2 \cdot \lambda} \left[w_1 F_1 \frac{e^{-ikr_1}}{r_1} + w_2 F_2 \frac{e^{-ikr_2}}{r_2} \right] \quad (103)$$

Here,

w_1, w_2 are the mean velocity amplitudes of F_1 and F_2 ,
 F_1, F_2 are the radiating surfaces
 r_1, r_2 are the distances of the radiators from the field point.

If, furthermore, we introduce the abbreviations

$$\frac{w_1 F_1}{2 \lambda^2} = a, \quad \frac{w_2 F_2}{2 \lambda^2} = b, \quad \frac{r_1}{\lambda} = x, \quad \frac{r_2}{\lambda} = y, \quad (103a)$$

then there results from (103) the relation

$$\frac{p}{c \cdot \sigma} = \frac{a}{x} e^{-i2\pi x} + \frac{b}{y} e^{-i2\pi y} \quad (104)$$

for the pressure amplitude p .

Since we leave the phase out of consideration, we have to investigate the expression on the right only as regards to its magnitude. By a simple calculation, we obtain

$$\frac{p}{c \sigma} = \left[\left(\frac{a}{x} \right)^2 + \left(\frac{b}{y} \right)^2 \right]^{1/2} \cos^2 \pi(x - y) + \left(\frac{a}{x} - \frac{b}{y} \right)^2 \sin^2 \pi(x - y) \quad (105)$$

or

$$\frac{p}{c \cdot \sigma} = \left\{ \left(\frac{a}{x} \right)^2 + \left(\frac{b}{y} \right)^2 + \frac{2ab}{xy} \cos 2\pi(x - y) \right\}. \quad (105a)$$

For certain values of $(x - y)$, $\cos 2\pi(x - y)$ (and therefore also $\frac{p}{c \cdot \sigma}$) assumes simple values which are shown in the following table:

$x - y$	$2 \cos 2\pi(x - y)$	$\frac{p}{c \sigma}$
0	+ 2	$a/x + b/y$
$\pm \frac{1}{2}$	+ 1	$\{a^2/x^2 + b^2/y^2 + ab/xy\}$
± 1	0	$\{a^2/x^2 + b^2/y^2\}$
$\pm \frac{3}{2}$	- 1	$\{a^2/x^2 + b^2/y^2 - ab/xy\}$
± 2	- 2	$a/x - b/y$
$\pm \frac{5}{2}$	- 1	$\{a^2/x^2 + b^2/y^2 - ab/xy\}$
± 3	0	$\{a^2/x^2 + b^2/y^2\}$
$\pm \frac{7}{2}$	+ 1	$\{a^2/x^2 + b^2/y^2 + ab/xy\}$
1	+ 2	$a/x + b/y$
$\pm (1 + 2)$	+ 1	$\{a^2/x^2 + b^2/y^2 + ab/xy\}$

etc.

The values of $p/(c\sigma)$ corresponding to the points lying on the hyperbolas $x - y = \text{constant}$ can thus be simply calculated and, by interpolation, curves of constant pressure can be constructed for which x and y are the distances measured in wave lengths of the field point from the two radiators.

Of particular importance is the determination of the positions where the pressure amplitude vanishes. For this it is manifestly necessary that $\frac{x}{y} = \frac{a}{b}$ and that $x - y = \frac{2m+1}{2} (m = 0, 1, 2, \dots)$. (without limiting the generality, a can be assumed greater than b .)

From this it follows that

$$\begin{aligned} x &= \frac{a}{b} \cdot \frac{2m+1}{2} \\ y &= \frac{b}{a} \cdot \frac{2m+1}{2} \end{aligned} \quad (105b)$$

Moreover, in order that the circles described by x and y yield a real intersection point, the condition

$$x + y = d \leq x - y, \quad (105c)$$

must be fulfilled for a given distance d of the two radiators.

That is, the condition

$$\frac{a+b}{a-b} \cdot \frac{2m+1}{2} \geq \frac{d}{\lambda} \geq \frac{2m+1}{2} \quad (106)$$

must be satisfied.

To each value of m for which the inequality (106) is fulfilled corresponds a zero position of the pressure. If $d/\lambda < \frac{1}{2}$ there are therefore no zero positions at all. If $a=2$, $b=1$, and $d/\lambda=4$, then from

$$3(2m+1) \geq 8 \geq 2m+1 \quad (106a)$$

there result the solutions $m=1$, $m=2$, $m=3$. If $a=3$, $b=2$, and $d/\lambda=1$ then from

$$5(2m+1) \geq 2 \geq 2m+1 \quad (106b)$$

only the solution $m=0$ results.

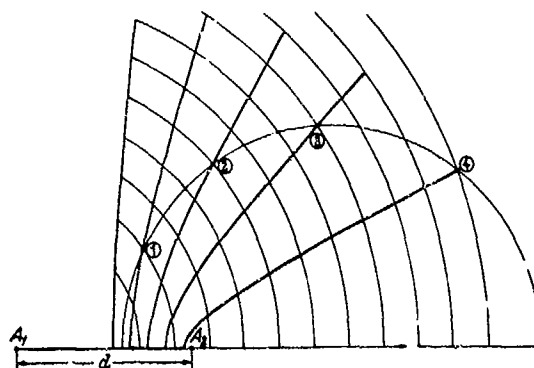


Fig. 44. The zero positions of the sound pressure of two point radiators at the distance $d = 5\lambda$ for different deformation volumes.

Fig. 44 represents the conditions for $d/\lambda=5$, $a=3$ and $b=2$. Here the hyperbola branches

$$r_1 - r_2 = \lambda/2, 3/2\lambda, 5/2\lambda, 7/2\lambda, 9/2\lambda \quad (106c)$$

and the zero positions (1), (2), (3), (4) lying on them are drawn. These zero positions are the points of intersection of the circles which are described about the point radiators A_1 and A_2 with the radii

$$\left. \begin{aligned} \frac{r_1}{\lambda} &= \frac{3(2m+1)}{10} \frac{d}{\lambda} \\ \frac{r_2}{\lambda} &= \frac{2(2m+1)}{10} \frac{d}{\lambda} \end{aligned} \right\} \quad (m=1, 2, 3, 4) \quad (107)$$

Moreover, all the zero positions lie on one circle which divides the distance A_1A_2 harmonically with the ratio $a:b$ and whose center lies on A_1A_2 (see Fig. 44). The radius of this circle is

$$r = \frac{ab}{a^2 - b^2} \frac{d}{\lambda}. \quad (107a)$$

A representation of the curves of equal pressure may be attained by graphical means. For this purpose we draw the locus of the termini of the vector

$$r_1 = a \cdot \frac{e^{-i2\pi x}}{x} \quad (107b)$$

and of the vector

$$r_2 = -b \frac{e^{-i2\pi y}}{y}. \quad (107c)$$

This was done by allowing x or y to increase by 0.05 so that each vector followed from the preceding by a rotation of $2\pi \cdot 0.05 = 18^\circ$. One then needs only to draw the straight lines through the zero point intersecting each other at an angle of 18° and to lay off on them the lengths a/x or b/y as the case may be. Two spirals thus result which wind around the null-point with ever closer windings. If these spirals have been numbered with the corresponding x and y values, all the solutions x, y of the equation

$$\left| a \cdot \frac{e^{-i2\pi x}}{x} + b \frac{e^{-i2\pi y}}{y} \right| = c \quad (108)$$

can be given when a straight line of the length c moves so that the initial point slides on the one (x) spiral and the end point slides on the other (y) spiral. Each position of the line c defines by its initial and end points on the spirals a system of values x, y which satisfies equation (14) ²³.

As an example, we choose $a = b = 1$, i.e., two radiators of equal intensity. In Fig. 45, the spiral $r_1 = e^{i2\pi x}/x$ is represented for all values from $x = 0.5$ to $x = 5$. In order to clarify the drawing, only the spiral points corresponding to the individual values $y = 0.5, y = 0.6, y = 0.7$, etc., to $y = 2.5$ are represented for the second spiral $r_2 = e^{-i2\pi y}/y$. These are obtained very simply by reflecting the corresponding points of the x spiral with respect to the center. These latter points are marked by small round circles near which the corresponding figure is given in a square. If we describe a circle with the radius unity about such a point of the y -spiral (e.g., the point 1), we obtain by the scale given on the x -spiral all the values of x (lying between 0.5 and 5) which satisfy the equation

$$\frac{e^{i2\pi x}}{x} + \frac{e^{-i2\pi y}}{y} = 1 \quad (108a)$$

²³ Apparently, eq. (104) is meant here.

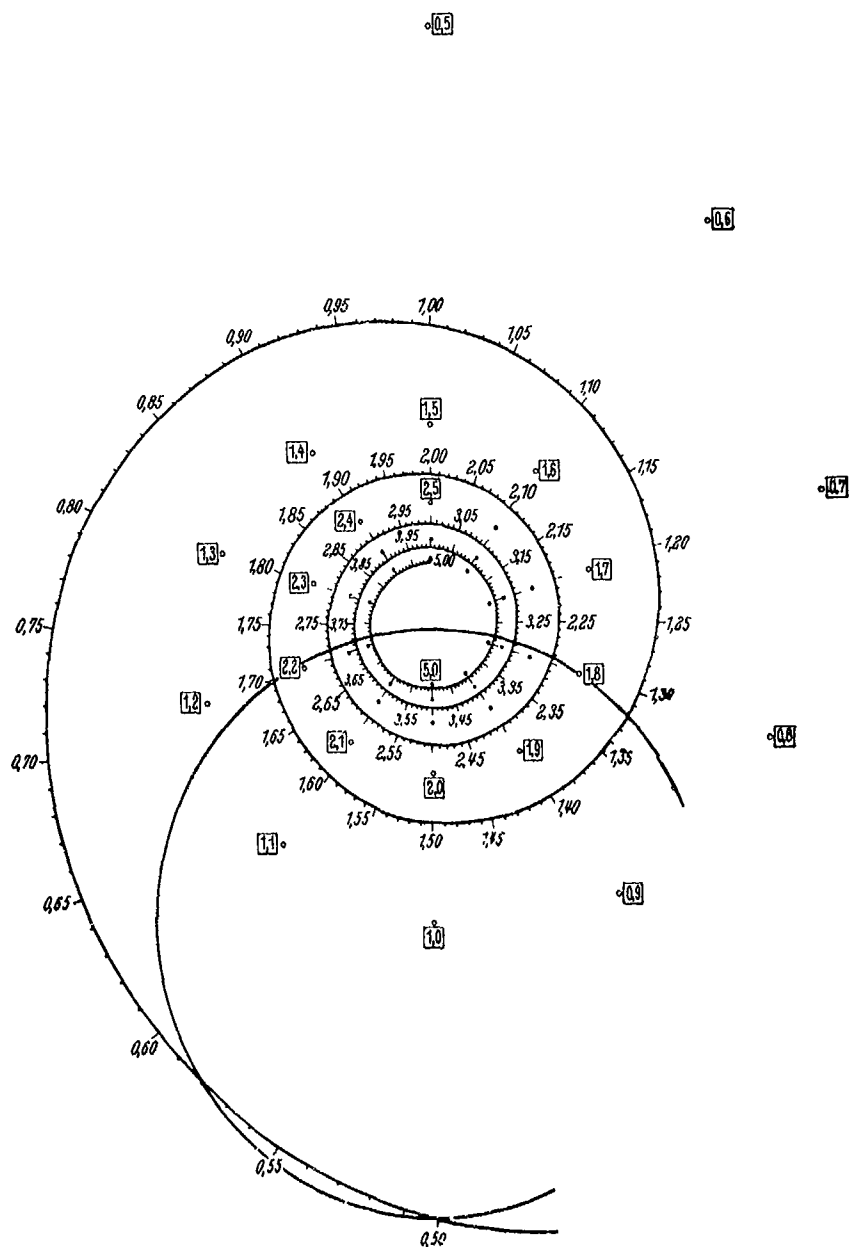


Fig. 45. Spirals for the calculation of the nearby field of two point radiators.

We thus read from Fig. 45 the solutions $x = 0.50; 0.58; 1.32; 1.70; 2.29; 2.71; 3.28; 3.72; 4.29; 4.72$. The relation becomes still clearer if we draw the curve defined by

$$\left| \frac{e^{-i2\pi x}}{x} + \frac{e^{-i2\pi y}}{y} \right| - 1 = 0 \quad (108b)$$

in rectangular coordinates. One half of this curve is given in Fig. 46. The other half is secured by reflecting the first half on the straight line $y - x = 0$. In addition to this the curves for

$$\left| \frac{e^{-i2\pi x}}{x} + \frac{e^{-i2\pi y}}{y} \right| - \frac{1}{2} = 0, \quad \left| \frac{e^{-i2\pi x}}{x} + \frac{e^{-i2\pi y}}{y} \right| - \frac{3}{2} = 0 \quad (109)$$

and

$$\left| \frac{e^{-i2\pi x}}{x} + \frac{e^{-i2\pi y}}{y} \right| - 2 = 0$$

are drawn in Fig. 46²⁴.

In order to obtain from these curves, which are independent of the radiator distance, the corresponding curves of constant pressure for a given radiator distance (e.g., $d/\lambda = 3$), we have to draw the two points A_1 and A_2 at the distance $d/\lambda = 3$ and describe about these points circles whose radii are given by the coordinates x and y of the desired point. Here, however, only the coordinates x and y are to be considered which lead to real intersection points of the two circles. Manifestly, this depends essentially on the radiator distance. From the condition for the intersection of the two circles

$$r_1 + r_2 = d \quad r_2 = r_1 \quad (109a)$$

it follows that

$$y + x = d/\lambda \quad y = x. \quad (109b)$$

²⁴ These curves can be identified as follows: For their intersection with $y - x = 0$, we have, by the given conditions and eq. 108:

$$\frac{1}{x} |2 e^{-kx}| = c$$

or

$$|\cos kx - i \sin kx| = \frac{cx}{2}$$

The value of the expression on the left-hand side is 1. Hence the abscissa of the intersection of the curve with $y - x = 0$ is $x = \frac{2}{c}$

This assumes the values 1, $4/3$, 2 and 4 for $c = 2, 3/2, 1$ and $1/2$ respectively.

If, in Fig. 46, we draw the three straight lines

$$y + x = d/\lambda, \quad y - x = d/\lambda, \quad y - x = 0 \quad (109c)$$

(where, because of symmetry, we assume $r_2 > r_1$ and can confine our-

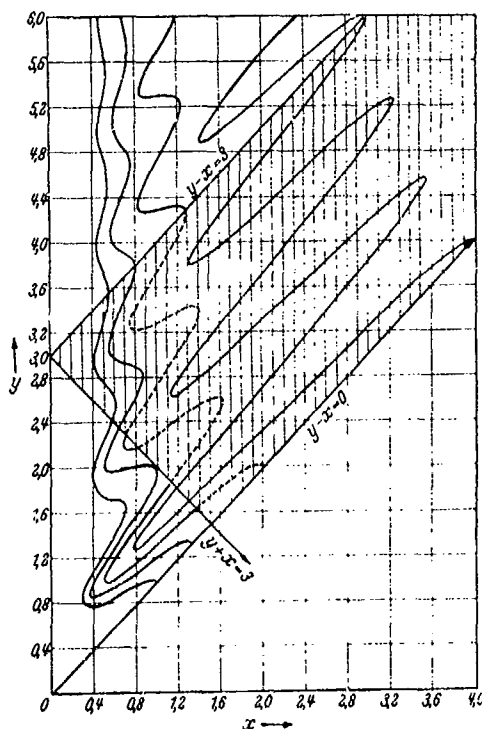


Fig. 46. The functions

$$\frac{e^{-i2\pi x}}{x} + \frac{e^{-i2\pi y}}{y} = c \quad \text{for } c = 1, 1.5, 2.$$

selves to one quadrant), a rectangular strip is then bounded by these lines which contains those and only those points x, y for which the condition

$$y + x \geq d/\lambda \quad y - x \leq 0 \quad (109d)$$

is fulfilled.

The corresponding strip for $d/\lambda = 3$ has been shaded in Fig. 46. One recognizes that, e.g., of the curve

$$\frac{e^{-i2\pi x}}{x} + \frac{e^{-i2\pi y}}{y} = 1 \quad (109e)$$

only the broken part enters into consideration. If we transfer the four curves, insofar as they are contained in the shaded strip, we thus obtain the corresponding curves of constant sound pressure (for one quadrant). Here each point of the curves in Fig. 46 with the coordinates (x, y) yields a corresponding point in Fig. 47 as the intersection point of the circle described about A_1 with the radius x and the circle described

about A_2 with the radius y . It is important that one recognizes from Fig. 46 whether the constant pressure curve consists of one continuous curve or how many separate curve sections result. Thus for $d/\lambda = 3$ the constant pressure curves corresponding to

$$\frac{e^{-i2\pi x}}{x} + \frac{e^{-i2\pi y}}{y} = c \quad (109f)$$

yield two separate curve sections for $c = 0.5$ and three for $c = 1$ while $c = 1.5$ and $c = 2$ each produce one continuous curve section. In Fig. 47 the corresponding curves of constant pressure are represented. The complete spatial distribution is obtained when one allows the whole structure to rotate about A_1, A_2 . Three separate surfaces then result for $c = 0.5$, five for $c = 1$ and two each for $c = 1.5$ and $c = 2$. If we allow d/λ to assume smaller values, the corresponding shaded area in Fig. 46 becomes steadily narrower and the number of

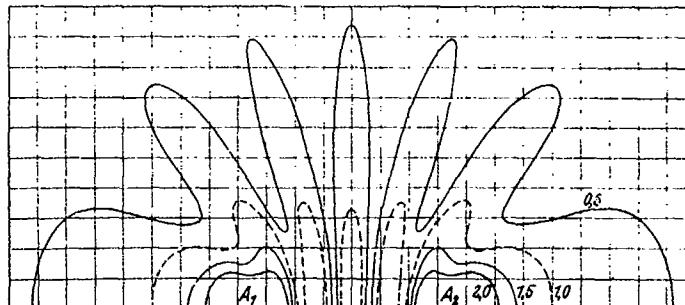


Fig. 47. Curves of constant pressure amplitude for two point radiators at the distance $d = 3\lambda$.

extreme values always decreases until finally for $d/\lambda = \frac{1}{2}$ only one maximum (on the normal axis) remains for all curves.

In Figs. 48 and 49 the sound fields are drawn for $d/\lambda = 1$ and for Fig. 48

$$\frac{w_1 F_1}{2\lambda^2} = \frac{w_2 F_2}{2\lambda^2} = 1$$

while in Fig. 49

$$\frac{w_1 F_1}{2\lambda^2} = 1.2; \quad \frac{w_2 F_2}{2\lambda^2} = 0.8$$

According to previous considerations, a null point (in the spatial sound field, a null circle) must appear²⁵. One sees from Fig. 49 that particularly in the neighborhood of this null position, a fair dissymmetry of the sound field is produced.

²⁵ For these values of a and b (i.e., $a = 1.2, b = 0.8$) condition (106) is satisfied by the single value $m=0$. Consequently, by eq. (105b) $x = 3/2, y = 1$. This point lies within the 0.05 curve of Fig. 49. In the previous example with $a=b$, the condition for a null point can only be satisfied at infinity.

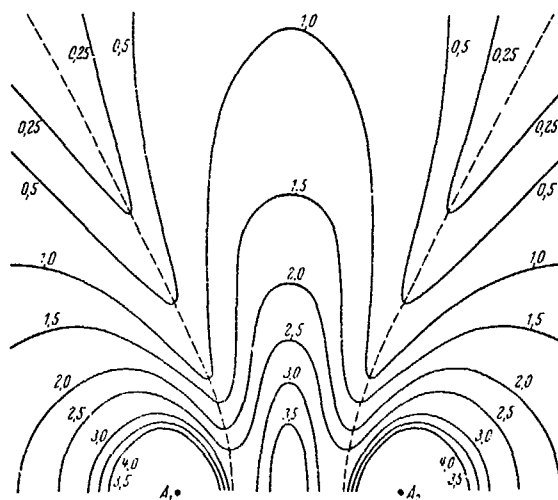


Fig. 48. Curves of constant sound pressure amplitude for two point radiators with equal deformation volumes.

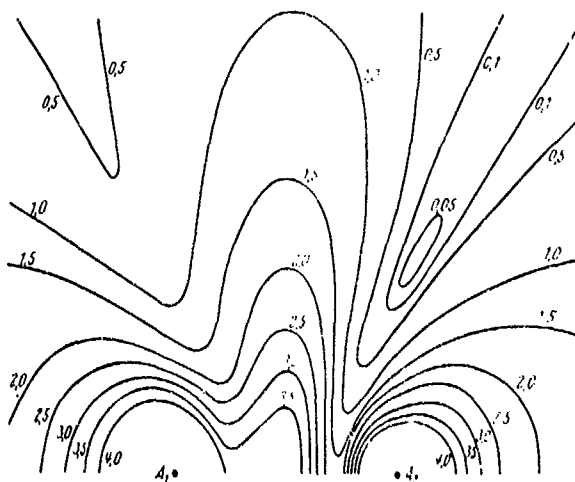
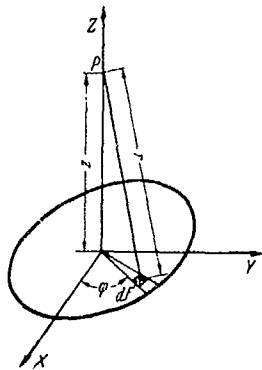


Fig. 49. Curves of constant sound pressure amplitude for two point radiators with different deformation volumes.

4. The circular piston membrane

The calculation of the sound field of a piston membrane for an arbitrary field point in the neighborhood of the membrane raises considerable difficulties. Therefore we first investigate the case where the field point lies on the normal axis of the membrane. Then the calculation may be very simply carried out²⁶. Since $w(x, y)$ is to be constant ($= w_0$), the calculation of the integral



$$J = \int \frac{e^{-ikr}}{r} dF \quad (109g)$$

is necessary.

If we introduce the polar coordinates ρ, φ for the surface element, then $dF = \rho d\rho d\varphi$ and since $r^2 = \rho^2 + z^2$, $\rho d\rho = r dr$. (Fig. 50).

Fig. 50. For the calculation of the circular piston membrane.

It then follows that

$$J = \int_0^{2\pi} d\varphi \int_0^R \rho d\rho \frac{e^{-ikr}}{r} = 2\pi \int_z^{\sqrt{R^2+z^2}} e^{-ikr} dr = -\frac{2\pi}{ik} [e^{-ik\sqrt{R^2+z^2}} - e^{-ikz}]. \quad (110)$$

Using the easily to be derived relation

$$e^{-i\alpha} - e^{-i\beta} = -2i \sin \frac{\alpha + \beta}{2} e^{-i \frac{\alpha + \beta}{2}} \quad (110a)$$

there results:

$$J = 2i \sin \left\{ \frac{k}{2} [\sqrt{R^2+z^2} + z] \right\} e^{-i \frac{k}{2} (\sqrt{R^2+z^2} - z)}. \quad (110b)$$

Upon substitution of this result in (11), there follows:

$$p = 2c \cdot \sigma \cdot w_0 \cdot \sin \left\{ \frac{k}{2} [\sqrt{R^2+z^2} + z] \right\} \cdot e^{i \left[\omega t - \frac{\pi}{2} - \frac{k}{2} (\sqrt{R^2+z^2} - z) \right]}. \quad (111)$$

The relative sound amplitude is therefore,

$$\frac{p}{c \sigma} = 2 \sin \left\{ \frac{k}{2} [\sqrt{R^2+z^2} + z] \right\}. \quad (111a)$$

From this it follows that $p/c \sigma$ has the value zero for

$$k [\sqrt{R^2+z^2} + z] = k z = 2\pi, 4\pi, \dots \quad (111b)$$

²⁶ Backhaus, H., and Trendelenburg, F.: Über die Richtwirkung von Kolbenmembranen, Z. techn. Phys., Vol. 7, p. 630 (1926).

and the value 2 for

$$k\sqrt{R^2 + z^2} - kz = \pi, 3\pi, \dots \quad (111c)$$

If one denotes the values of z corresponding to these extreme values by z_0 and z_m the null positions z_0 are given by

$$z_0 = \frac{\frac{R^2}{\lambda^2} - n^2}{2n/\lambda} \quad (n = 1, 2, \dots) \quad (112)$$

and the "positions of the maximum" by

$$z_m = \frac{\frac{R^2}{\lambda^2} - \left(n + \frac{1}{2}\right)^2}{(2n+1)/\lambda} \quad (n = 0, 1, 2, \dots) \quad (113)$$

With an increasing radius, the number of the zero and maximum positions increases. No extreme values can occur on the normal axis

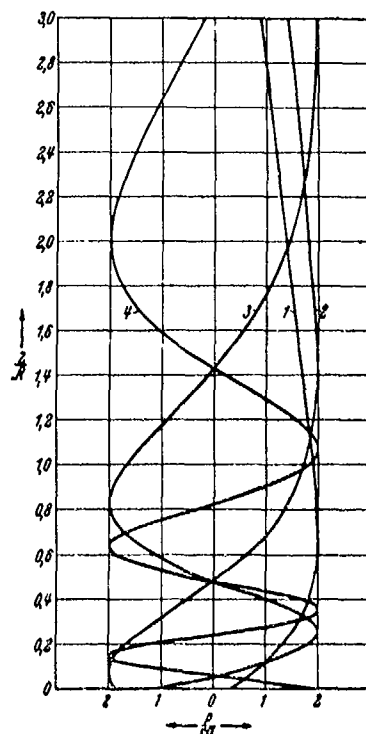


Fig. 51. Pressure amplitude (p/c_0) on the normal axis of the circular piston of the radius R .

1. $kR = 6$. 2. $kR = 10$. 3. $kR = 20$. 4. $kR = 40$.

for membranes whose radius is smaller than λ . The complete behavior of p/c_0 for field points on the normal axis of the piston membrane is represented in Fig. 51. The ordinate is the ratio z/R . The four curves correspond to the values $kR = 6, 10, 20$, and 40 respectively. For points with a sufficiently large value of z , formula (111) transforms into (1) according to a previous conclusion (p.4). By the considerations on page 60, z is sufficiently large if

$$\frac{\pi R^2}{\lambda z} \ll 1 \quad \text{and} \quad \frac{R}{z} \ll 1.$$

Then, however,

$$k\sqrt{R^2 + z^2} - kz = kz \left(1 + \frac{1}{2} \frac{R^2}{z^2}\right) - kz = \frac{\pi R^2}{\lambda z} \quad (113a)$$

and

$$2 \sin \frac{1}{2} \frac{\pi R^2}{\lambda z} = \frac{\pi R^2}{\lambda z} = \frac{R}{\lambda} \frac{R}{z} \quad (113b)$$

so that (111) does in fact transform into (1) (see footnote 1). If the field point distance z is chosen as six times the radius, there then results for

$$\frac{\pi R^2}{\lambda z} \quad (\text{or for } \frac{(kR)^2}{2(kz)}) \quad \text{in the cases}$$

$kR = 6, 10, 20, 40$, the values $\frac{1}{2}, \frac{5}{8}, \frac{3}{4}, \frac{1}{3}$ so that a field point distance greater than three membrane diameters (at most) can be regarded as sufficiently great in the case $kR = 6$. This does not hold by any means for the case $kR = 20$ or for $kR = 40$.

It may be mentioned that formula (111) can be generalized to the case where the radiating surface consists of a sector of a circular ring with the limiting radii R_1 and R_2 and the central angle φ_0 instead of a complete circular surface. If the field point is then located above the center of the circular ring, the formula analogous to (111)

$$p = \frac{\varphi_0}{\pi} \cdot w_0 \cdot c \cdot \sigma \sin \left\{ \frac{k}{2} [\sqrt{z^2 + R_2^2} - \sqrt{z^2 + R_1^2}] \right\} e^{i(\omega t + \frac{\pi}{2} - \frac{k}{2} (\sqrt{z^2 + R_2^2} + \sqrt{z^2 + R_1^2}))} \quad (114)$$

is then valid.

If the pressure at one special point for a piston membrane with an arbitrary boundary is desired, one can, after resolving the radiating surface into the corresponding partial domains, apply this formula and sum up the effects of the individual component surfaces. Here, one has only to see that the neglected parts of the surface are so small that, taken together, they make practically no contribution. The subdivision therefore depends essentially on the magnitude of the wave length.

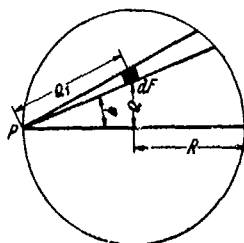


Fig. 52. For the calculation of the sound pressure on the edge of the circular piston membrane.

(Fig. 52):

The calculation of the integral may be simply carried out, if the field point lies on the edge of the membrane. If we choose the field point P at the origin of the coordinate system with the polar coordinates ϱ_1 and φ then

$$\begin{aligned} \int_F \frac{e^{-ikr}}{r} dF &= 2 \int_0^{\pi/2} d\varphi \int_0^{2R \cos \varphi} e^{-ik\varrho_1} d\varrho_1 = \frac{2}{ik} \int_0^{\pi/2} d\varphi [1 - e^{-ik2R \cos \varphi}] \\ &= \frac{\pi}{ik} - \frac{2}{ik} \int_0^{\pi/2} e^{-ik2R \cos \varphi} d\varphi. \end{aligned} \quad (114a)$$

Now

$$\frac{2}{\pi} \int_0^{\pi/2} e^{-ik2R \cos \varphi} d\varphi = J_0(2kR) - iH_0(2kR). \quad (114b)$$

Here J_0 and H_0 indicate respectively the Bessel and Struve functions of zero order. It then follows that²⁷

$$p = c \cdot \sigma e^{i\omega t} \left[\frac{1 - J_0(2kR)}{2} + \frac{i}{2} H_0(2kR) \right]. \quad (115)$$

With the aid of the available tables²⁸ for J_0 and H_0 we can represent the behavior of the pressure amplitude on the edge of the membrane as a function of $2\pi R/\lambda$. In Fig. 53, in addition to this representation, the behavior of the pressure amplitude at the center is indicated which is given by (111) with $z = 0$ by

$$\frac{p}{\sigma c} = 2 \sin \frac{\pi R}{\lambda} \quad (116)$$

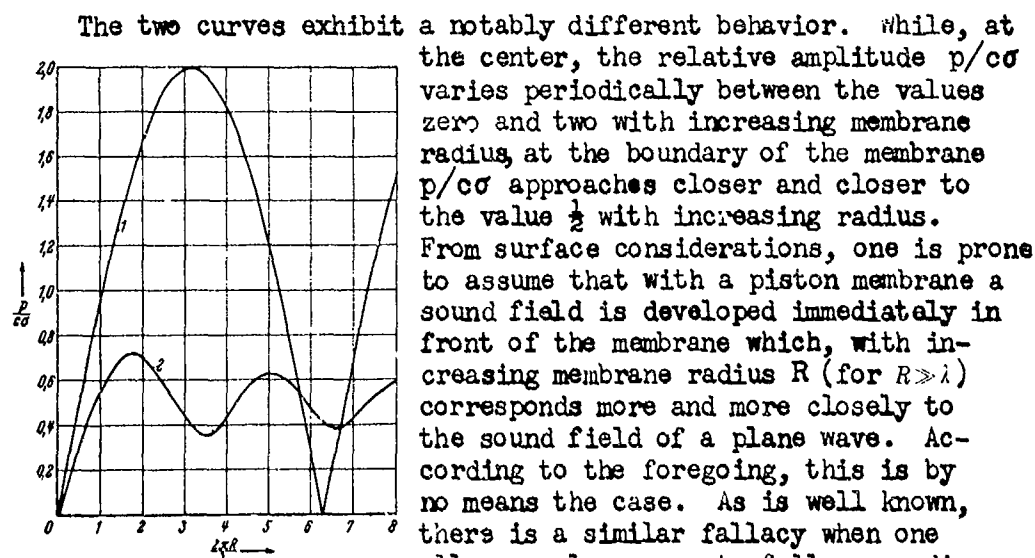


Fig. 53. Pressure amplitude $(p/\sigma c)$ at the center (1) and at the edge (2) of the circular piston membrane of the radius R .

while in actuality with a decreasing radius ρ ($\rho \ll \lambda$) of the opening a more and more nearly hemispherical divergence takes place.

We have already seen that the pressure at a great distance can be simply calculated if the velocity amplitude of the circular membrane $w(\rho)$ is given in the form:

$$w(\rho) = a_0 + a_1 \left(1 - \frac{\rho^2}{R^2}\right) + a_2 \left(1 - \frac{\rho^2}{R^2}\right)^2 + \dots + a_n \left(1 - \frac{\rho^2}{R^2}\right)^n. \quad (116a)$$

²⁷ McLachlan, W.: On the Acoustic and Inertia Pressure on a Vibrating Circular Disk. Phil. Mag. Ser. 7, (1932) p. 1022.

²⁸ Theory of Bessel Functions, Cambridge: G. N. Watson 1922.

Here ϱ is the distance from the center and R is the membrane radius. We will now show that, in the simple case $n = 1$ and for field points on the normal axis and on the edge of the membrane, a simple calculation is also possible. We set

$$w(\varrho) = 1 - f \cdot \frac{\varrho^2}{R^2}. \quad (117)$$

Then the corresponding pressure amplitude p_f is given by

$$p_f = \frac{p}{c\sigma e^{i\omega t}} = \frac{i}{\lambda} \int_0^R \left(1 - f \frac{\varrho^2}{R^2}\right) \frac{e^{-ikr}}{r} dF. \quad (117a)$$

It is sufficient to calculate the pressure amplitudes p_0 (for $f = 0$) and p_1 (for $f = 1$). Then from

$$p_0 = \frac{i}{\lambda} \int_0^R \frac{e^{-ikr}}{r} dF \quad \text{and} \quad p_1 = \frac{i}{\lambda} \int_0^R \left(1 - \frac{\varrho^2}{R^2}\right) \frac{e^{-ikr}}{r} dF \quad (117b)$$

it follows that

$$p_f = (1 - f) p_0 + f p_1. \quad (117c)$$

If the field point lies on the normal axis (Fig. 50) at the distance z then $\varrho^2 = r^2 - z^2$, and, since $dF = r dr d\varphi$, it follows that

$$p_1 = \frac{2\pi i}{\lambda} \left(1 + \frac{z^2}{R^2}\right) \int_z^{\sqrt{R^2+z^2}} e^{-ikr} dr - \frac{2\pi i}{\lambda r^2} \int_z^{\sqrt{R^2+z^2}} r^2 e^{-ikr} dr. \quad (117d)$$

We therefore find for the field point on the normal axis

$$p_1 = e^{-ikz} \left\{1 + \frac{2}{k^2 R^2} + \frac{2ikz}{k^2 R^2}\right\} - e^{-ik\sqrt{R^2+z^2}} \frac{2}{k^2 R^2} \{1 + ik\sqrt{R^2+z^2}\} \quad (118)$$

and by (110)

$$p_0 = e^{-ikz} - e^{-ik\sqrt{R^2+z^2}}. \quad (118a)$$

If the field point is on the edge of the membrane then since (Fig. 52)

$$\varrho^2 = R^2 + \varrho_1^2 - 2\varrho_1 R \cos\varphi, \quad 1 - \frac{\varrho^2}{R^2} = \frac{2\varrho_1}{R} \cos\varphi - \frac{\varrho_1^2}{R^2}, \quad (118b)$$

$$p_1'' = \frac{2i}{\lambda} \int_0^{2\pi} d\varphi \int_0^R e^{-ikr} \left[\frac{2\varrho_1 \cos\varphi}{R} - \frac{\varrho_1^2}{R^2} \right] d\varrho_1. \quad (118c)$$

If we integrate with respect to φ , there results

$$\begin{aligned} p_1^{(r)} &= \frac{1}{kR} \cdot \frac{2}{\pi} \int_0^{\pi/2} \left\{ \frac{1}{kR} - i \cos \varphi - e^{-i2kR \cos \varphi} \left(\frac{1}{kR} + i \cos \varphi \right) \right\} d\varphi, \\ p_1^{(r)} &= \frac{1}{k^2 R^2} - \frac{2i}{\pi kR} - \frac{1}{k^2 R^2} \cdot \frac{2}{\pi} \int_0^{\pi/2} e^{-i2kR \cos \varphi} d\varphi - \frac{i}{kR} \cdot \frac{2}{\pi} \int_0^{\pi/2} \cos \varphi e^{-i2kR \cos \varphi} d\varphi. \end{aligned} \quad (118d)$$

Using the relations²⁹

$$\begin{aligned} \frac{2}{\pi} \int_0^{\pi/2} e^{-ix \cos \theta} d\theta &= J_0(x) - iH_0(x), \\ \frac{2}{\pi} \int_0^{\pi/2} \cos \theta e^{-ix \cos \theta} d\theta &= \frac{2}{\pi} - H_1(x) - iJ_1(x) \end{aligned} \quad (118e)$$

it then follows that for field points on the boundary

$$\begin{aligned} p_1^{(r)} &= \frac{1 - J_0(2kR)}{k^2 R^2} - \frac{J_1(2kR)}{kR} + i \left[\frac{H_0(2kR)}{k^2 R^2} + \frac{H_1(2kR)}{kR} - \frac{4}{\pi} \right], \\ p_0^{(r)} &= \frac{1 - J_0(2kR)}{2} + \frac{i}{2} H_0(2kR). \end{aligned} \quad (119)$$

Here J_0 and J_1 are Bessel functions of the zero and first order and H_0 and H_1 are the Struve functions of the zero and first order. With the aid of the available tables for J_0, J_1, H_0, H_1 the calculation offers no difficulties.

The variation of the pressure on the normal axis for the case $kR = 10$ is represented in Fig. 55 and Fig. 56 for

$$w = 1 - f \cdot \varrho^2 / \lambda^2, \quad (f = 0, \pm \frac{1}{2}, \pm \frac{1}{4}, \pm 1)$$

The corresponding velocity amplitudes

$$w = 1 - f \cdot \varrho^2 / R^2 \quad (f = 0, \pm \frac{1}{2}, \pm \frac{1}{4}, \pm 1)$$

are drawn in Fig. 54. Furthermore the variations of the pressure at the center and on the boundary are represented as a function of kR for $w = 1 - \varrho^2 / R^2$ and $w = 1 - \frac{1}{4} \varrho^2 / R^2$ in Figs. 57 and 58.

²⁹ McLaughlin, W.: Bessel functions for Engineers, p. 167

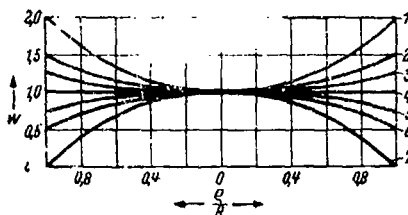


Fig. 54. The velocity amplitudes
 $w = 1 - J \cdot \omega^2 / R^2$ ($J = 0, \pm 1, \pm 1, \pm 1, \pm 1$).

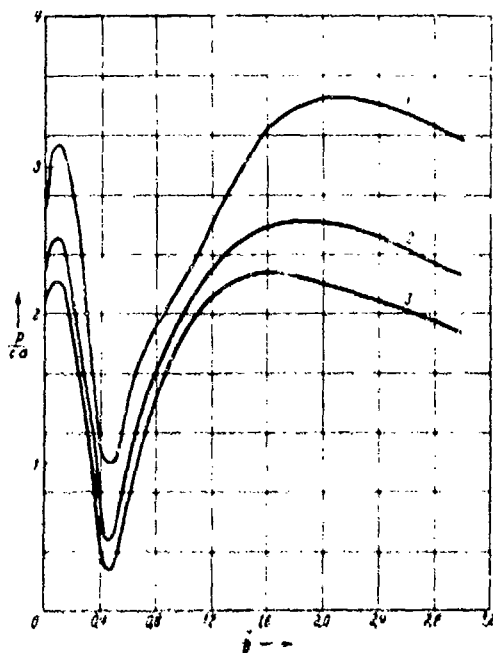


Fig. 55. Pressure amplitude (p/p_0) on the normal axis for the velocity amplitude
 $w = 1 - J \cdot \omega^2 / R^2$ ($J = 0, 1, -1, 1, -1, 1, -1$).

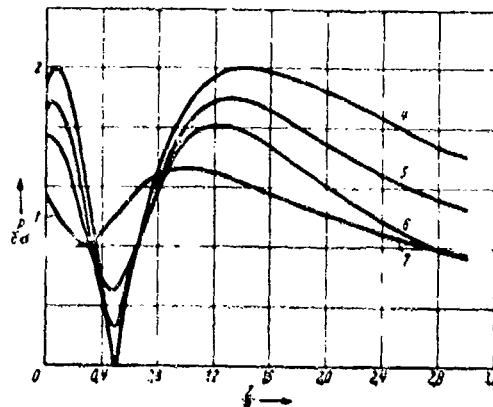


Fig. 56. Pressure amplitude (p/p_0) on the normal axis for the velocity amplitude
 $w = 1 - J \cdot \omega^2 / R^2$ ($J = 0, 1, -1, 1, -1, 1, -1$).

These two cases, where the field point is (a) on the normal axis and (b) on the boundary of the circular piston membrane, are the only ones for which the evaluation of the integral is generally possible, i.e., expressed in terms of well-known functions which are available in tables.

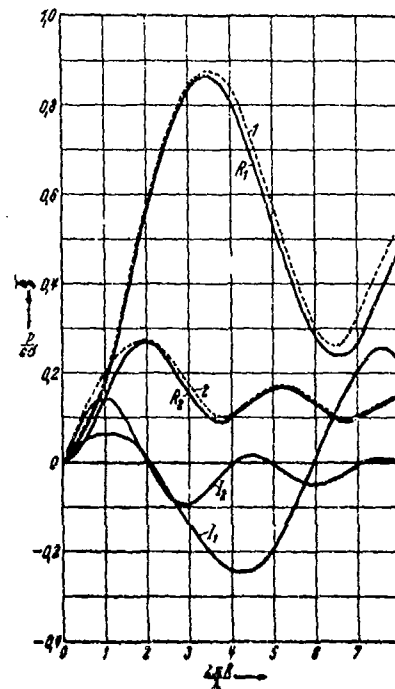


Fig. 57. Pressure amplitude at the center (1) and at the boundary point (2) for the vibration form $w = 1 - e^2/R^2$ and the corresponding components (R_1, J_1) , (R_2, J_2) .

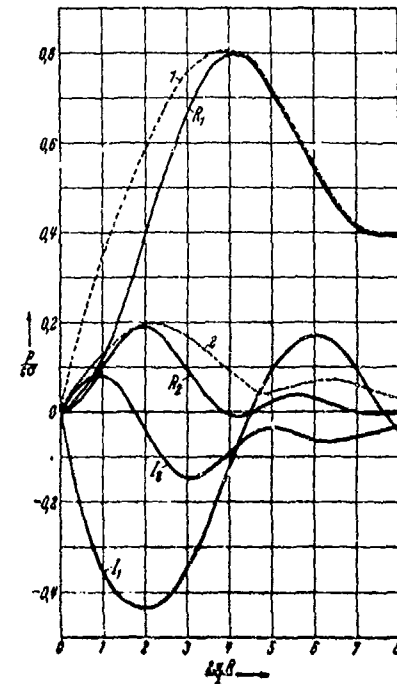


Fig. 58. Pressure amplitude at the center (1) and at the boundary point (2) for the vibration form $w = 1 - \frac{1}{2} e^2/R^2$ with the corresponding components (R_1, J_1) , (R_2, J_2) .

If we now turn to the general calculation of the field of a circular piston membrane³⁰, we will resolve the integral

$$\int \frac{e^{-ikr}}{r} dF$$

into its real and imaginary parts.

We therefore obtain

$$\left. \begin{aligned} p &= c \cdot \sigma \\ &\cdot w_0 e^{i\omega t} (p_a + ip_m) \end{aligned} \right\} \quad (120)$$

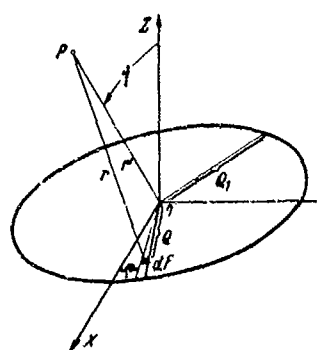
³⁰ Elektr. Nachr. Techn., vol. 12 (1935) pp. 16-30.

wherein

$$\left. \begin{aligned} p_a &= \frac{1}{\lambda} \int_F \frac{\sin kr}{r} dF, \\ p_m &= \frac{1}{\lambda} \int_F \frac{\cos kr}{r} dF \end{aligned} \right\} \quad (121)$$

This is advantageous since the relative pressure components p_a and p_m exhibit an essentially different behavior. If, for example, the wave length is so great that $2\pi r/\lambda \ll 1$, p_a becomes very small, i.e., the component p_m (which, with the velocity amplitude $w = w_0 e^{i\omega t}$ possesses a phase displacement of 90°) predominates. Physically, this means that the membrane works on the field almost wattlessly so that it moves a dead mass back and forth without radiating practically any sound.

In order to be able to evaluate the integrals (121), we must first relate the variable r to the corresponding surface element



(determined by its polar coordinates ϱ, φ). If we denote the angle which the field point line OP forms with the Z-axis by γ , and let the distance of the field point P from O be r_1 while we let r be the distance of the field point from the surface element dF , then one has

$$r = \sqrt{r_1^2 + \varrho^2 - 2r_1\varrho \cos\varphi \sin\gamma}. \quad (122)$$

Fig. 59. For the calculation of the circular piston membrane.

Here the field point P is assumed to be in the X-Z plane in Fig. 59 which, due to symmetry conditions, manifestly does not limit the generality. The integrals (121) then assume the form

$$p_a = \frac{1}{\lambda} \int_0^{2\pi} d\varphi \int_0^{\varrho_1} \varrho d\varrho \frac{\sin kr}{r}, \quad p_m = \frac{1}{\lambda} \int_0^{2\pi} d\varphi \int_0^{\varrho_1} \varrho d\varrho \frac{\cos kr}{r}, \quad (123)$$

where the value of r given by (122) is to be substituted. Since an integration in closed form does not appear generally possible, one will attempt to so transform the integrands by a series development that the variables of integration appear separated. This is done by a series development whose terms are formed from spherical harmonics and Bessel functions. One has the following relations³¹:

$$\frac{\sin \sqrt{x^2 + y^2 - 2xy \cos \theta}}{\sqrt{x^2 + y^2 - 2xy \cos \theta}} = \frac{1}{xy} \sum_{n=0}^{\infty} (2n+1) S_n(x) S_n(y) P_n(\cos \theta), \quad (124)$$

³¹ Watson, G. N.: Theory of Bessel Functions, p. 366, Cambridge 1922.

$$\frac{\cos \sqrt{x^2 + y^2 - 2xy \cos \vartheta}}{\sqrt{x^2 + y^2 - 2xy \cos \vartheta}} = \begin{cases} \frac{1}{xy} \sum_{n=0}^{\infty} (2n+1) S_n(x) C_n(y) P_n(\cos \vartheta), & (x \leq y) \\ \frac{1}{xy} \sum_{n=0}^{\infty} (2n+1) C_n(x) S_n(y) P_n(\cos \vartheta), & (x \geq y) \end{cases} \quad (125)$$

Here $P_n(\cos \vartheta)$ is the Legendre spherical harmonic and

$$S_n(x) = \begin{cases} \frac{\pi}{2} x J_{n+1/2}(x), & C_n(x) = (-1)^n \left[\frac{\pi}{2} x J_{n-1/2}(x), \right] \end{cases} \quad (127)$$

where the J's indicate Bessel's functions. These functions may be relatively simply represented for small values of n as rational functions of x , $\sin x$ and $\cos x$. Thus

$$\left. \begin{aligned} S_0(x) &= \sin x, & C_0(x) &= \cos x, \\ S_1(x) &= \frac{\sin x}{x} - \cos x, & C_1(x) &= \sin x + \frac{\cos x}{x}, \\ S_2(x) &= \left(\frac{3}{x^2} - 1 \right) \sin x - \frac{3}{x} \cos x, & C_2(x) &= \frac{3}{x} \sin x + \left(\frac{3}{x^2} - 1 \right) \cos x, \\ S_3(x) &= \left(\frac{15}{x^3} - \frac{6}{x} \right) \sin x - \left(\frac{15}{x^3} - 1 \right) \cos x, & C_3(x) &= \left(\frac{15}{x^3} - 1 \right) \sin x + \left(\frac{15}{x^3} - \frac{6}{x} \right) \cos x, \end{aligned} \right\} \quad (128)$$

wherein between the $S_n(x)$ and $C_n(x)$ the important relation

$$S_n(x) C_{n+1}(x) - S_{n-1}(x) C_n(x) = 1 \quad (129)$$

exists.

Using the series in (124), (125), and (126) we can now calculate the integrals (123). We first carry out the integration term-wise with respect to φ . Here we use the well-known relation from the theory of spherical harmonics:

$$\int_0^{2\pi} P_{2n+1}(\cos \varphi \sin \gamma) d\varphi = 0, \quad \int_0^{2\pi} P_{2n}(\cos \varphi \sin \gamma) d\varphi = 2\pi P_{2n}(0) P_{2n}(\cos \gamma). \quad (130)$$

From this it follows that all odd terms drop out and there results:

$$p_d = \frac{1}{kr_1} \sum_{n=0}^{\infty} (4n+1) P_{2n}(0) P_{2n}(\cos \gamma) S_{2n}(kr_1) \int_0^{kr_1} S_{2n}(x) dx, \quad (131)$$

$$p_m = \frac{1}{kr_1} \sum_{n=0}^{\infty} (4n+1) P_{2n}(0) P_{2n}(\cos \gamma) C_{2n}(kr_1) \int_0^{kr_1} S_{2n}(x) dx. \quad (132)$$

These term-wise integrations are permissible as long as the series (124) and (125) are uniformly convergent. While this is always the case for (124), it holds for (125) only if $x \leq y$ ³². That is, while the development (131) is valid without any limitation (i.e., for arbitrary positions of the field point), (132) is only valid if the field point distance is greater than the membrane radius. We must, therefore, seek another development for p_m for field points in the neighborhood of the membrane. In order to carry out the calculation when $r_1 < \rho_1$, we imagine the membrane of radius ρ_1 divided into a smaller circle of radius r_1 and a circular ring of the width $\rho_1 - r_1$. If we denote the two resulting regions by F_1 and F_2 , the integral over the surface F breaks down into two summands. The development (132) is valid for the first summand except that kr_1 replaces the upper limit of integration $k\rho_1$. For the region F_2 , formula (126) is now to be applied, however, so that the following development is valid for p_m at a field point distance smaller than the membrane radius:

$$p_m = \frac{1}{kr_1} \sum_{n=0}^{\infty} (4n+1) P_{2n}(0) P_{2n}(\cos \gamma) \times \left[C_{2n}(kr_1) \int_0^{kr_1} S_{2n}(x) dx + S_{2n}(kr_1) \int_{kr_1}^{k\rho_1} C_{2n}(x) dx \right]. \quad (133)$$

For a practical application of the formulae, a tabular computation of the functions

$$P_n, S_n, C_n, \int_0^x S_{2n}(x) dx, \int_{kr_1}^x C_{2n}(x) dx \quad (133a)$$

is necessary. For the spherical harmonics $P_n(\cos \gamma)$, tables for the values of n from 0 to 20 and for $\gamma = 0^\circ, 5^\circ, \dots, 90^\circ$ are given ³³. The functions $S_n(x), C_n(x)$ are available for values of x smaller than 2 ³⁴, for integral values $x = 1, 2, 3, \dots, 10$ ³⁵, and for the intermediate values $x = 2.2, 2.4, \dots, 9.8$ ³⁶. The tables for

$$\int_0^x S_{2n}(x) dx, \quad \text{and} \quad \int_{kr_1}^x C_{2n}(x) dx$$

are given for $n = 0, 1, 2, \dots, 10$ and $x = 1, 1.25, 1.5, \dots, 10$ in the appendix. For the calculation of the latter and for small values

³² The symbols x and y used here refer to eqs. (124) - (127), inclusive, and are to be distinguished from the coordinates (x, y) of the surface element.

³³ Phil. Trans. Roy. Soc. Lond., Vol. 203 (1904), p. 100.

³⁴ Rep. Brit. Assoc. Adv. Sci. 1916, pp. 97-107; 1922, pp. 263-270.

³⁵ Rep. Brit. Assoc. Adv. Sci. 1914, pp. 87-102.

³⁶ Elektr. Nachr.-Techn., Vol. 15, (1938), p. 73.

of x , a series development with respect to x is advantageous. This results at once by a term-wise integration of the well-known series for $S_{2n}(x)$ and $C_{2n}(x)$. Thus it follows that

$$\int_0^x S_{2n}(x) dx = \frac{x^{2n+2}}{1 \cdot 3 \cdot 5 \dots (4n+1)} \times \left(\frac{1}{2n+2} - \frac{x^2}{2(2n+4)(4n+3)} + \frac{x^4}{2 \cdot 4 \cdot (2n+6)(4n+3)(4n+5)} - \dots \right), \quad (134)$$

$$\int_0^x C_{2n}(x) dx = \frac{1 \cdot 3 \cdot 5 \dots (4n-1)}{x^{2n-1}} \times \left(\frac{1}{2n-1} + \frac{x^2}{2(2n-3)(4n-1)} + \frac{x^4}{2 \cdot 4 \cdot (2n-5)(4n-1)(4n-3)} + \dots \right). \quad (135)$$

For the larger values of x it is more advantageous to return to the simple functions $S_n(x)$ and $C_n(x)$. For this we proceed from the equation³⁷.

$$\left(\frac{x}{2}\right)^p J_{\nu-p}(x) = \Gamma(\nu+1) \sum_{s=0}^p (-1)^s \frac{\binom{p}{s} \left(\frac{x}{2}\right)^s J_{\nu+s}(x)}{\Gamma(\nu+s-p+1)}. \quad (136)$$

If we set $\nu = -n - \frac{1}{2}$, $p = n$, $s = m$, we then obtain

$$\begin{aligned} & (-1)^n x^{\frac{1}{2}} J_{-2n-\frac{1}{2}}(x) \\ &= \sum_{m=0}^n \binom{n}{m} (2n+1)(2n+3) \dots (4n-2m-1) x^{m-n+\frac{1}{2}} J_{m-n-\frac{1}{2}}(x) \end{aligned} \quad (136a)$$

From this we find by integrating term-wise considering the relation

$$\int x^{p+1} J_p(x) dx = x^{p+1} J_{p+1}(x) \quad (136b)$$

the desired relation

$$\begin{aligned} (-1)^n \int_0^x C_{2n}(x) dx &= S_0(x) + \binom{n}{1} (2n+1) \frac{C_0(x)}{x} \\ &- \binom{n}{2} (2n+1)(2n+3) \frac{C_1(x)}{x^2} + \dots \\ &- (-1)^n \binom{n}{n} (2n+1)(2n+3) \dots (4n-1) \frac{C_{n-1}(x)}{x^n}. \end{aligned} \quad (137)$$

³⁷ Nielsen, N.: Handbuch der Theorie der Zylinderfunktion, p. 269, Leipzig, 1904.

For the determination of $\int_0^x S_{2n}(x) dx$, we proceed from the formula ³⁸

$$\frac{J_\nu(x)}{p!} = \sum_{s=0}^p \frac{(-1)^{p-s}}{(p-s)!} \binom{p-p-s}{s} \left(\frac{2}{x}\right)^s J_{\nu-2p+s}(x) \quad (137a)$$

and obtain for $\nu = 2n + \frac{1}{2}$, $p = n$, $s = m$

$$J_{2n+\frac{1}{2}}(x) = n! \sum_{m=0}^n \frac{(-1)^{n-m}}{(n-m)!} \binom{n+\frac{1}{2}+m-1}{m} \left(\frac{2}{x}\right)^m J_{2m+\frac{1}{2}}(x); \quad (137b)$$

from which we find by term-wise integration considering

$$\int_0^x x^{-(p+\frac{1}{2})+1} J_{p+\frac{1}{2}}(x) dx = -\frac{J_{p-\frac{1}{2}}(x)}{x^{p-\frac{1}{2}}} \quad (137c)$$

the relation

$$\begin{aligned} (-1)^n \int_0^x S_{2n}(x) dx &= -C_0(x) + \binom{n}{1} (2n+1) \frac{S_0(x)}{x} \\ &\quad - \binom{n}{2} (2n+1)(2n+3) \frac{S_2(x)}{x^2} + \dots \\ &\quad - (-1)^n \binom{n}{n} (2n+1)(2n+3) \dots \frac{(4n-1) S_{n-1}(x)}{x^n} - K. \end{aligned} \quad (138)$$

Here the constant K is to be determined so that the right hand side of (138) vanishes for $x = 0$.

Since

$$C_0(0) = 1 \text{ and } \frac{S_m(x)}{x^m} = \frac{1}{1 \cdot 3 \cdot 5 \dots 2m-1} \text{ (for } x=0) \quad (138a)$$

we then obtain the value of K by the equation

$$\begin{aligned} K &= -1 + \binom{n}{1} (2n+1) - \binom{n}{2} \frac{(2n+1)(2n+3)}{1 \cdot 3} + \dots \\ &\quad + (-1)^n \binom{n}{n} \frac{(2n+1)(2n+3) \dots (4n-1)}{1 \cdot 3 \cdot 5 \dots (2n-1)}. \end{aligned} \quad (139)$$

For the expression on the right-hand side we find the value

$$(-1)^n \frac{2 \cdot 4 \cdot 6 \dots 2n}{1 \cdot 3 \cdot 5 \dots 2n-1} \quad (139a)$$

Therefore, it turns out that

$$\begin{aligned} (-1)^n \int_0^x S_{2n}(x) dx &= (-1)^n \frac{2 \cdot 4 \cdot 6 \dots 2n}{1 \cdot 3 \cdot 5 \dots 2n-1} \\ &\quad - C_0(x) + \binom{n}{1} (2n+1) \frac{S_0(x)}{x} - \binom{n}{2} (2n+1)(2n+3) \frac{S_2(x)}{x^2} + \dots \\ &\quad - (-1)^n \binom{n}{n} (2n+1)(2n+3) \dots (4n-1) \frac{S_{n-1}(x)}{x^n}. \end{aligned} \quad (140)$$

³⁸ Nielsen, N.: Handbuch der Theorie der Zylinderfunktionen, p. 269, Leipzig, 1904.

We will first apply the formulae when the field point is assumed on (i.e., directly in front of) the membrane. Then there is to be substituted:

$$\cos \gamma = 1, \quad P_{2n}(1) = 1 \quad \text{and} \quad P_{2n}(0) = (-1)^n \frac{1 \cdot 3 \cdot 5 \cdots 2n-1}{2 \cdot 4 \cdot 6 \cdots 2n} \quad (140a)$$

Six different values of kq_1 are used (0.5, 2, 4, 6, 8, and 10) while the field point assumes all values from $r_1 = 0$ to $r_1 = q_1$ immediately in front of the membrane for each value of kq_1 . In the calculations we make use of the fact that the portion due to the interior surface elements ($q \leq r_1$) is found by formula (115) so that for p_a and p_m we only have to add the parts

$$\frac{1}{kr_1} \sum_{n=0}^{\infty} (4n+1) P_{2n}(0) P_{2n}(1) S_{2n}(kr_1) \int_{kr_1}^{kq_1} S_{2n}(x) dx \quad (140b)$$

and

$$\frac{1}{kr_1} \sum_{n=0}^{\infty} (4n+1) P_{2n}(0) P_{2n}(1) S_{2n}(kr_1) \int_{kr_1}^{kq_1} C_{2n}(x) dx \quad (140c)$$

due to the ring-shaped region.

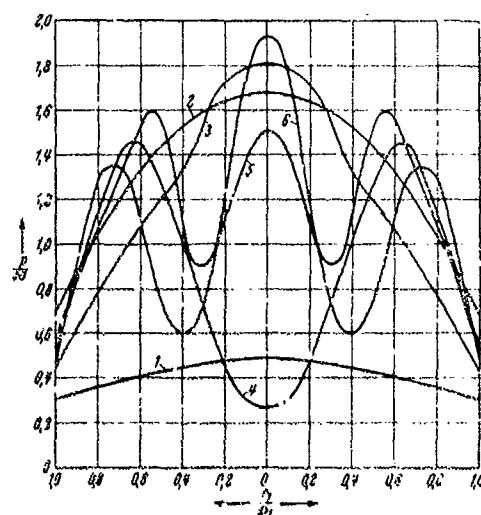


Fig. 60. Sound pressure amplitude ($p(r, 0)$) immediately in front of the circular piston membrane (Radius q_1).

1. $kq_1 = 0.5$, 2. $kq_1 = 2$, 3. $kq_1 = 4$, 4. $kq_1 = 6$
5. $kq_1 = 8$, 6. $kq_1 = 10$.

From the two components p_a and p_m thus obtained $p = \sqrt{p_a^2 + p_m^2}$ is then calculated and a curve is drawn. Here r_1/q_1 is the abscissa so that the abscissa 1 corresponds to the boundary point of the membrane (Fig. 60).

One sees that only for very small values of kq_1 ($kq_1 < 1$) is the pressure amplitude to some degree constant over the whole surface of the membrane and that for larger values of kq_1 an ever increasing waviness makes its appearance while the value at the center continuously oscillates between zero and two and the boundary value, always smaller, fluctuates about the value $\frac{1}{2}$.

39 For the condition as here stated, i.e., the field point on the membrane, the condition would seem to be $\cos \gamma = 0$. This consideration applies likewise to the remainder of equations (140a) and to equations (140b) and (140c).

As an example of the computation with an arbitrary position of the field point, the calculation procedure for the case $k\rho = 10$, $kr = 6$ will be explained. First the quantities

$$a_{2n} = (4n + 1) P_{2n}(0) S_{2n}(kr) \int_0^{k\rho} S_{2n}(x) dx \quad (140d)$$

are easily calculated using the tables in the appendix. Thus one obtains

$2n =$	0	2	4	6	8	10
$a_{2n} =$	-0,086	+0,124	+1,785	-1,694	+0,222	-0,008

From this we find the value on the normal axis ($\gamma = 0$):

$$\sum_{2n=0}^{10} a_{2n} = +0,342. \quad (140e)$$

According to earlier considerations (p. 70) this value is given by $\cos kr - \cos \sqrt{(kr)^2 + (k\rho)^2}$. In fact, this yields

$$\cos 6 - \cos \sqrt{136} = 0,960 - 0,618 = +0,342. \quad (140f)$$

This gives an important control for the correctness of the coefficients a_{2n} . We also calculate the coefficients b_{2n} for

$$p_m = \sum b_{2n} P_{2n}(\cos \gamma)$$

and obtain the following table:

$2n =$	0	2	4	6	8
$(4n + 1) P_{2n}(0) \frac{C_{2n}(kr)}{kr} \int_0^{kr} S_{2n}(x) dx$	+0,006	+1,317	+0,209	-0,631	+0,287
$(4n + 1) P_{2n}(0) \frac{S_{2n}(kr)}{kr} \int_0^{k\rho} C_{2n}(x) dx$	+0,012	+0,093	-1,727	-0,421	+0,640
$b_{2n} =$	+0,018	+1,410	-1,518	-1,052	+0,927
$2n =$	10	12	14	16	18
$(4n + 1) P_{2n}(0) \frac{C_{2n}(kr)}{kr} \int_0^{kr} S_{2n}(x) dx$	-0,171	+0,121	-0,091	+0,074	-0,061
$(4n + 1) P_{2n}(0) \frac{S_{2n}(kr)}{kr} \int_0^{k\rho} C_{2n}(x) dx$	-0,295	+0,174	-0,122	+0,093	-0,076
$b_{2n} =$	-0,466	+0,295	-0,213	+0,167	-0,137

Compared with the coefficients a_{2n} , the last terms of the two series here are, say, larger by a power of 10 so that we have to expect a greater deviation of the sum $\sum b_{2n}$ from the true value p_m . In order to obtain a better control with the directly to be found values:

$$\sin \sqrt{2(kr)^2} - \sin kr = \sum_{n=0}^{\infty} (4n+1) P_{2n}(0) \frac{C_{2n}(kr)}{kr} \int_0^{kr} S_{2n}(x) dx \quad (140g)$$

and

$$\sin \sqrt{(kr)^2 + (kq)^2} - \sin \sqrt{2(kr)^2} = \sum_{n=0}^{\infty} (4n+1) P_{2n}(0) \frac{S_{2n}(kr)}{kr} \int_0^{kq} C_{2n}(x) dx \quad (140h)$$

we observe that the summands of the two series in the tables for the larger values of n oscillate less and less about a mean value. We take account of this by dividing the last term in the two series by 2 and therefore put the value -0.031 in place of -0.061 and the value -0.038 in place of -0.076 . If we denote the thus obtained sums by \sum_1 and \sum_2 , we then have $\sum_1 = +1.091$ and $\sum_2 = -1.591$, while the true values give

$$\sin \sqrt{72} - \sin 6 = 1.087 \quad (140i)$$

and

$$\sin \sqrt{136} - \sin \sqrt{72} = -1.595 \quad (140j)$$

as a result so that a sufficient agreement obtains here. Of course, the device cannot be applied generally ($\gamma \neq 0$) for the calculation of $p_m = \sum b_{2n} P_{2n}(\cos \gamma)$

since, due to the factor $P_{2n}(\cos \gamma)$

regular oscillations are no longer present. But, even here one will be able to count on a deviation of at most 10% from the true value. For acoustic calculations, however, this accuracy is in general to be regarded as quite sufficient. Using

the tables for the spherical harmonics, the quantities $a_{2n} \cdot P_{2n}(\cos \gamma)$ and $b_{2n} \cdot P_{2n}(\cos \gamma)$ are then found for $\gamma = 0^\circ, 5^\circ, 10^\circ$ etc. There thus results the following table (Here, the values given for p_a and p_m are derived from computations originally carried out to four decimal places. Therefore the values of p_a and p_m deviate at times in the last decimal place from the sum of the numbers standing above these values):

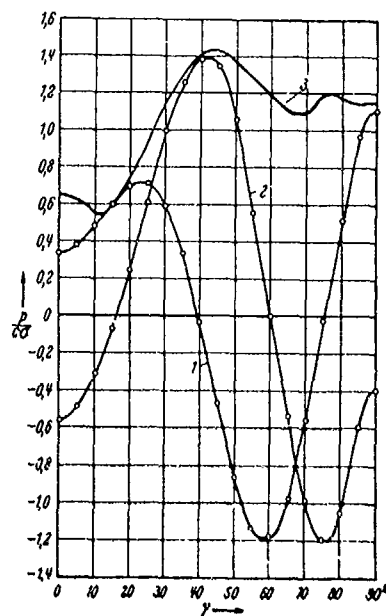


Fig. 61. Sound pressure amplitude (p/c) of the circular piston membrane with the radius a ($ka = 10$) and constant field point distance r ($kr = 6$).

2n	$\gamma = 0^\circ$	$\gamma = 5^\circ$	$\gamma = 10^\circ$	$\gamma = 15^\circ$	$\gamma = 20^\circ$	$\gamma = 25^\circ$	$\gamma = 30^\circ$	$\gamma = 35^\circ$	$\gamma = 40^\circ$	$\gamma = 45^\circ$
0	-0,086	-0,086	-0,086	-0,086	-0,086	-0,086	-0,086	-0,086	-0,086	-0,086
2	+0,124	+0,122	+0,118	+0,111	+0,102	+0,093	+0,077	+0,063	+0,047	+0,031
4	+1,785	+1,717	+1,539	+1,222	+0,847	+0,355	+0,042	-0,305	-0,569	-0,725
6	-1,694	-1,560	-1,191	-0,675	-0,122	+0,319	+0,634	+0,695	+0,548	+0,251
8	+0,222	+0,193	+0,116	+0,021	-0,056	-0,090	-0,075	-0,026	+0,031	+0,066
10	-0,008	-0,007	-0,003	+0,001	+0,003	+0,003	-0,001	-0,002	-0,002	-0,001
$p_n =$	+0,342	+0,379	+0,493	+0,597	+0,688	+0,705	+0,593	+0,339	-0,031	-0,463

2n	$\gamma = 50^\circ$	$\gamma = 55^\circ$	$\gamma = 60^\circ$	$\gamma = 65^\circ$	$\gamma = 70^\circ$	$\gamma = 75^\circ$	$\gamma = 80^\circ$	$\gamma = 85^\circ$	$\gamma = 90^\circ$
0	-0,086	-0,086	-0,086	-0,086	-0,086	-0,086	-0,086	-0,086	-0,086
2	+0,015	-0,001	-0,016	-0,029	-0,040	-0,049	-0,056	-0,064	-0,062
4	-0,762	-0,686	-0,516	-0,277	-0,007	+0,256	+0,474	+0,618	+0,669
6	-0,095	-0,389	-0,548	-0,531	-0,354	-0,073	+0,223	+0,446	+0,529
8	+0,065	+0,032	-0,016	-0,053	-0,062	-0,038	+0,005	+0,045	+0,061
10	+0,001	+0,002	+0,002	—	-0,002	-0,002	-0,001	+0,001	+0,002
$p_n =$	-0,862	-1,128	-1,179	-0,976	-0,551	-0,008	+0,559	+0,960	+1,115

2n	$\gamma = 0^\circ$	$\gamma = 5^\circ$	$\gamma = 10^\circ$	$\gamma = 15^\circ$	$\gamma = 20^\circ$	$\gamma = 25^\circ$	$\gamma = 30^\circ$	$\gamma = 35^\circ$	$\gamma = 40^\circ$	$\gamma = 45^\circ$
0	+0,019	+0,019	+0,019	+0,019	+0,019	+0,019	+0,019	+0,019	+0,019	+0,019
2	+1,410	+1,393	+1,345	+1,265	+1,160	+1,030	+0,880	+0,714	+0,535	+0,355
4	-1,518	+1,460	-1,293	-1,038	-0,721	-0,375	-0,035	+0,270	+0,484	+0,616
6	-1,052	-0,968	-0,740	-0,418	-0,075	+0,214	+0,393	+0,432	+0,340	+0,156
8	+0,927	+0,804	+0,484	+0,089	-0,234	-0,376	-0,314	-0,107	+0,129	+0,276
10	-0,166	-0,373	-0,149	+0,077	+0,187	+0,142	+0,003	-0,118	-0,138	-0,654
12	+0,265	+0,213	+0,035	-0,100	-0,104	-0,007	+0,080	+0,074	-0,006	-0,073
14	-0,214	-0,137	+0,014	+0,086	+0,034	0,050	-0,055	+0,012	+0,055	+0,022
16	+0,167	+0,091	-0,036	-0,060	+0,013	+0,056	+0,001	-0,043	-0,011	+0,036
18	-0,137	-0,061	+0,045	+0,031	-0,035	-0,021	+0,031	+0,016	0,028	0,012
$p_m =$	-0,569	-0,479	-0,276	-0,049	+0,244	+0,626	+1,003	+1,269	+1,379	+1,341

2n	$\gamma = 50^\circ$	$\gamma = 55^\circ$	$\gamma = 60^\circ$	$\gamma = 65^\circ$	$\gamma = 70^\circ$	$\gamma = 75^\circ$	$\gamma = 80^\circ$	$\gamma = 85^\circ$	$\gamma = 90^\circ$
0	+0,019	+0,019	+0,019	+0,019	+0,019	+0,019	+0,019	+0,019	+0,019
2	+0,169	0,009	-0,176	-0,327	-0,457	-0,564	-0,641	-0,688	-0,705
4	+0,651	+0,584	+0,439	+0,235	+0,006	-0,217	-0,408	-0,526	-0,569
6	-0,059	-0,242	-0,339	-0,330	-0,220	0,045	+0,139	+0,278	+0,329
8	+0,274	+0,132	-0,068	-0,224	-0,258	-0,158	+0,022	+0,187	+0,253
10	+0,064	+0,125	+0,088	-0,015	-0,102	-0,108	-0,030	+0,070	+0,114
12	-0,059	+0,015	+0,063	+0,047	-0,623	-0,067	-0,039	+0,031	+0,066
14	-0,039	-0,042	+0,012	+0,047	+0,016	0,036	-0,037	+0,013	+0,045
16	+0,019	-0,029	-0,025	+0,021	+0,029	-0,013	0,032	+0,004	+0,033
18	+0,027	+0,009	-0,026	-0,006	+0,026	+0,003	-0,025	-0,001	+0,025
$p_m =$	+1,068	+0,564	0,007	-0,533	-0,964	-1,186	-1,032	-0,593	-0,393

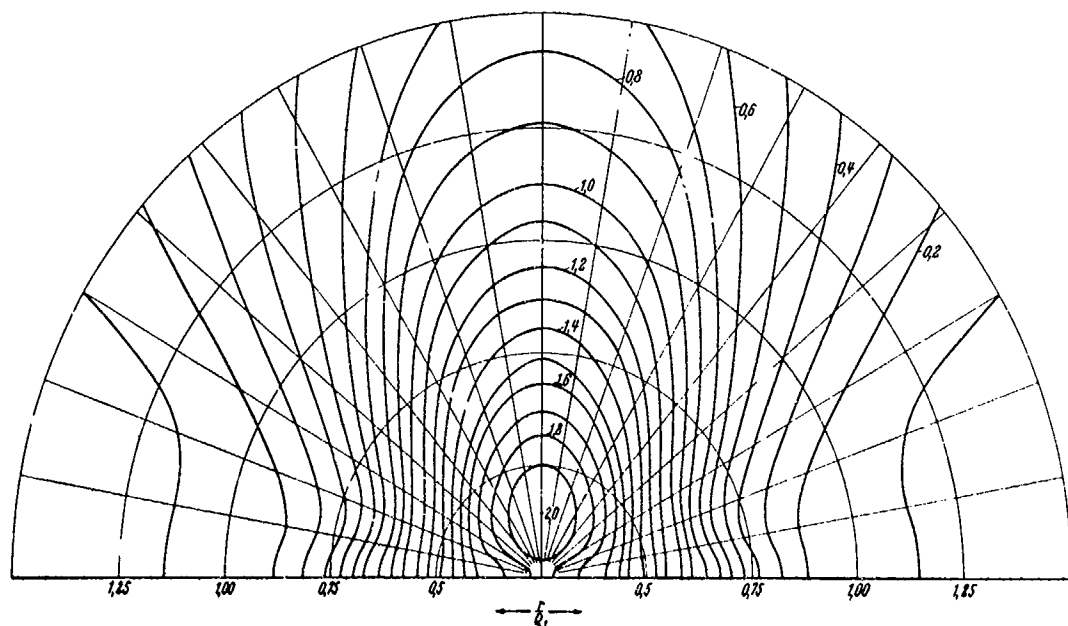


Fig. 62. Sound field ($p, c\sigma$) in the neighborhood of the circular piston membrane ($\mu \rho_1 \approx 4$).

In Fig. 61 the two components p_a and p_m are first represented individually since a valuable control for the results of the calculation is furnished by the continuous sequence of the calculated values. Finally, the complete behavior of the relative pressure amplitude $p = \sqrt{p_a^2 + p_m^2}$ is obtained by geometric addition of the corresponding values of p_a and p_m . (See Fig. 61.)

In this manner, the relative amplitudes $\sqrt{p_a^2 + p_m^2}$ were calculated for three piston membranes (whose radii were given by $\frac{2\pi a_1}{\lambda} = 4, 6, 10$) for such a great number of points of the nearby field that the curves of constant pressure amplitude could be drawn by interpolation. The results are represented in Figs. 62 to 64.

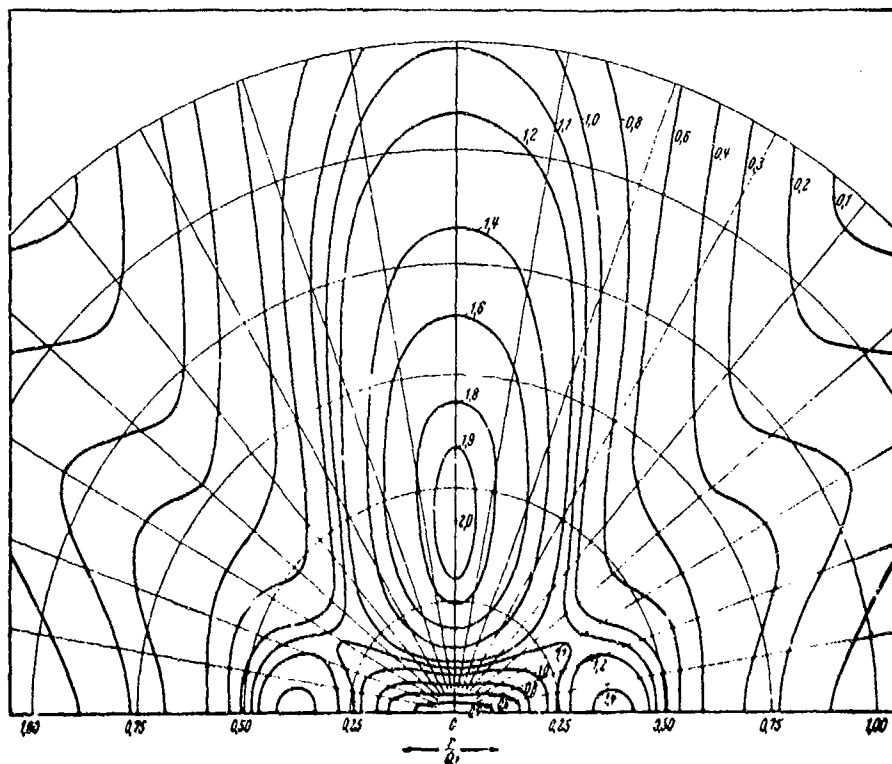


Fig. 63. Sound field (p/c) in the neighborhood of the circular piston membrane ($k a_1 = 0$).

Here the numbers on the horizontal axis are the values r/a_1 , so that the points which are the length of the membrane radius distant from the membrane center lie on the unit semicircle. One recognizes that the essential character of the field is determined by the location of the zero and maximum values (which are found only on the normal axis). If we first consider the case $k a_1 = 0$, we see that the amplitude has approximately the value zero at the center of the

membrane and that on the normal axis with increasing distance, the amplitude first increases rather rapidly and then rises more slowly to the value two, and falls off very gradually from there on. Off of the normal axis lie two peaks at the height of the center which are marked by the high pressure lines 1.4. Beyond these peaks a

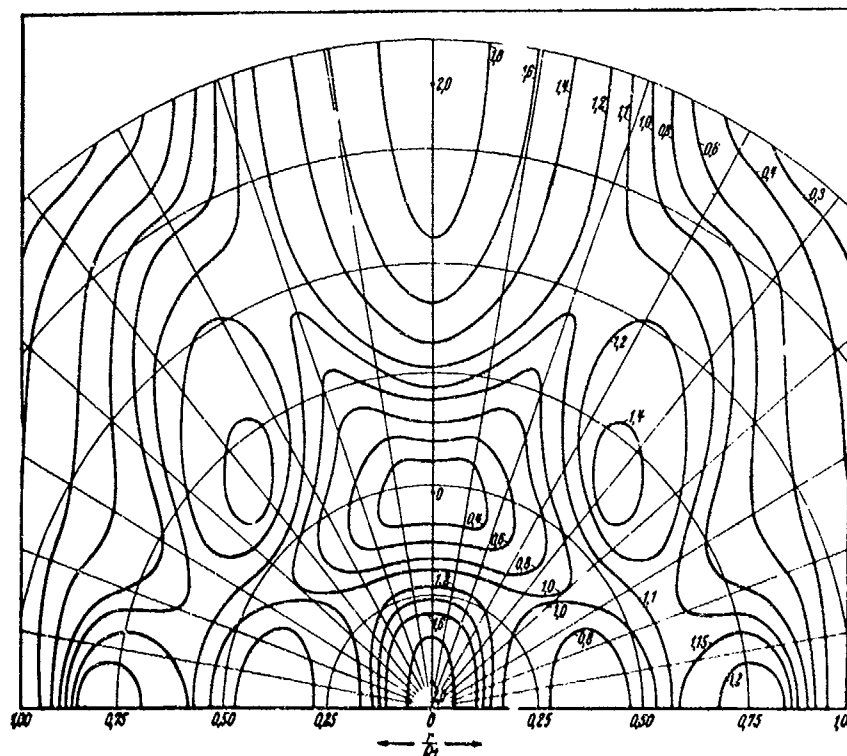


Fig. 64. Sound field (p, c) in the neighborhood of the circular piston membrane ($k_0 = 10$).

uniform drop takes place with increasing radius. If, for comparison, we now consider the field for $k_0 = 10$, a striking similarity of the configuration of the upper part of this sound field with the foregoing appears. If we imagine a horizontal straight line drawn through the zero value on the normal axis, we see that this cuts the field into two parts of which the upper part is extraordinarily similar to the whole field for $k_0 = 6$ as is shown in Fig. 63. The lower part of the field $k_0 = 10$ is essentially different since now a minimum and a maximum have made their appearance both to the right and left of the two-point.

If we now allow the radius of the piston membrane to increase continuously, we then know (from the simple formulae for points on the normal axis) that the maximum and zero values become increasingly

more numerous and progress upwards while new zero and maximum values continually make their appearance at the center of the membrane. According to the above considerations, however, beyond this we have to expect that the constant pressure curves lying to the right and left (of the center) also simply move upwards with the upwardly travelling zero- and two-points of the normal axis without an essential change in their character. If we have a membrane with an arbitrarily great radius and mark the two last two-values of the amplitude on the normal axis, we will then be warranted in expecting that the accompanying field, which lies between the planes parallel to the membrane through these two maximum positions, agrees in character with the field represented in Fig. 64. Moreover, according to Fig. 64, one would suppose that upon travelling from any maximum position on the normal axis in the vertical direction, just as many extreme values will be encountered as if one travelled from the same maximum position in a horizontal direction.

Part Three

THE SOUND FIELD OF THE SPHERICAL RADIATOR

5. The simple spherical radiator of definite order

An essential assumption for the radiators previously discussed was the existence of a sound reflecting rigid infinite plane wall. In its position of rest the radiating surface coincided with this wall. The calculation of the radiation process was then accomplished by the calculation of an integral over the radiating surface. For the problems treated in the following chapters, the radiating surface forms a part of a sound reflecting rigid sphere of fixed radius. Here exists a more general problem since, aside from the amplitude and extent of the radiating surface, the extent of the rigid wall can also be changed. While formerly, for the circular piston membrane e.g., one characteristic function

$$\left(2 \frac{J_1(x)}{x}, x = \frac{2\pi r}{\lambda} \sin \gamma\right)$$

sufficed to completely specify the sound field for an arbitrary field-point position at a great distance and an arbitrary membrane size (in relation to λ) this is now no longer possible. On the other hand there are now quite definite distributions of the velocity amplitude for which the solution becomes conceivable. Here it is also particularly important that the calculation of the neighboring field offers no difficulty. This simple solution

exists if the velocity amplitude is given by one spherical harmonic of definite order. This assumption of the velocity distribution, which at first appears artificial, immediately finds its justification in the fact that an arbitrarily given velocity distribution can generally be reduced to that given by a spherical harmonic. In the computation of practical problems we will limit ourselves to those processes which are rotationally symmetric with respect to an axis through the center of the sphere. The corresponding spherical harmonics are then given by the well-known Legendre functions

$$P_n(\mu), \mu = \cos \gamma \left[P_0(\mu) = 1, P_1(\mu) = \mu, P_2(\mu) = \frac{1 \cdot 3}{2!} \left(\mu^2 - \frac{1}{3} \right) \text{etc.} \right] \quad (140k)$$

By a spherical radiator of zero order, we will understand a pulsating sphere for which the individual elements of the surface vibrate cophasally outwards and inwards with constant velocity amplitudes. (See Fig. 1-a.) The velocity on the sphere is given by

$$w = w_0 e^{i\omega t}. \quad (140m)$$

With a sphere radius r_0 and for a field point distance r , the sound pressure is completely determined by

$$p_0 = p^{(0)} w_0 \frac{1 - i k r_0}{1 + k^2 r_0^2} e^{i[\omega t + \pi/2 - k(r - r_0)]}, \quad (141)$$

where, for abbreviation,

$$p^{(0)} = \frac{c \cdot \sigma \cdot F}{2 \lambda r} \quad (141a)$$

From this follows the pressure amplitude

$$p_0 = p^{(0)} w_0 \frac{1}{\sqrt{1 + k^2 r_0^2}} = \frac{c \sigma w_0}{k r} \frac{k^2 r_0^2}{\sqrt{1 + k^2 r_0^2}}. \quad (142)$$

For $kr_0 \ll 1$ we obtain the formula given previously:

$$p_0 = \frac{c \cdot \sigma \cdot F}{2 \lambda \cdot r} u_0. \quad (142a)$$

The relative pressure amplitude, $p_0 / c \sigma w_0$, is then generally given by

$$\frac{p_0}{c \sigma w_0} = \frac{1}{k r} \frac{k^2 r_0^2}{\sqrt{1 + k^2 r_0^2}} \quad (142b)$$

The curves of constant pressure amplitude are therefore very simply represented in the spatial sound field by concentric spheres. As long as $kr_0 \ll 1$, the pressure increases quadratically with kr_0 . As long as $kr_0 \gg 1$, it increases linearly with kr_0 .

The simple spherical radiator of higher (nth) order⁴⁰ is characterized by the fact that the variation of the velocity amplitude w_n is given by

$$w_n = w_n \cdot P_n(\mu) e^{i\omega t}. \quad (142c)$$

The pressure p_n at the field point determined by the polar coordinates r, γ is then generally given by

$$p_n = p^{(0)} w_n \cdot e^{i\omega t + \pi/2 - k(r-r_0)} \cdot \frac{f_n(ikr)}{F_n(ikr_0)} P_n(\mu). \quad (143)$$

Here

$$F_n(ix) = (1 + ix)f_n(ix) - ix f'_n(ix) \quad (144)$$

and

$$f_n(ix) = 1 + \frac{n(n+1)}{2ix} + \frac{(n-1)(n)(n+1)(n+2)}{2 \cdot 4 (ix)^2} + \dots + \frac{1 \cdot 2 \cdot 3 \dots 2n}{2 \cdot 4 \cdot 6 \dots 2n (ix)^n}. \quad (145)$$

It is better to introduce the Bessel functions $S_n(x)$ and $C_n(x)$ defined by (127) page 79 in place of $F_n(ix)$ and $f_n(ix)$. Due to the relations

$$\begin{aligned} i^{n+1} e^{-ix} f_n(ix) &= S_n(x) + i C_n(x), \\ i^{n+1} e^{-ix} F_n(ix) &= x S_{n+1}(x) - n S_n(x) + i [x C_{n+1}(x) - n C_n(x)], \end{aligned} \quad (145a)$$

we then obtain

$$p_n = p^{(0)} \cdot w_n e^{i(\omega t + \pi/2)} \frac{S_n(kr) + i C_n(kr)}{U_n(kr_0) + i V_n(kr_0)} \cdot P_n(\mu). \quad (146)$$

where, for abbreviation,

$$\begin{aligned} U_n(x) &= x S_{n+1}(x) - n S_n(x), \\ V_n(x) &= x C_{n+1}(x) - n C_n(x). \end{aligned} \quad (147)$$

Then one has

$$\begin{aligned} U_0(x) &= \sin x - x \cos x, & V_0(x) &= \cos x + x \sin x, \\ U_1(x) &= (2/x - x) \sin x - 2 \cos x, & V_1(x) &= 2 \sin x + (2/x - x) \cos x \text{ etc.} \end{aligned} \quad (147a)$$

For the spherical radiator of the first order the velocity amplitude w_1 is given by

$$w_1 = w_1 P_1(\mu) e^{i\omega t} = w_1 \cos \gamma \cdot e^{i\omega t}. \quad (147b)$$

⁴⁰ Rayleigh: Theory of Sound, Sec. 323 and following.

This corresponds to the motion of a sphere vibrating to and fro as a rigid body. Here the pressure p_1 is given by:

$$\frac{p_1}{c\sigma \cdot w_1 \cdot e^{i(\omega t - k(r-r_0))}} = \frac{k^2 r_0^3}{kr} \frac{i + \frac{1}{kr}}{2 + i(kr_0 - \frac{2}{kr})} \cdot \cos \gamma \quad (147c)$$

while the pressure amplitude p_1 is given by

$$\frac{p_1}{c\sigma w_1} = \frac{k^3 r_0^3}{\sqrt{4 + k^4 r_0^4}} \cdot \frac{1}{k^2 r^2} \sqrt{1 + k^2 r^2} \cos \gamma. \quad (147d)$$

As long as $kr_0 \ll 1$, the pressure amplitude increases proportionally to $k^3 r_0^3$. As long as $kr_0 \gg 1$, the pressure amplitude increases proportionally to kr_0 . If we denote the maximum pressure amplitude occurring at the field point $r = r_0$ and $\gamma = 0$ by p_m and require the curves of constant pressure amplitude

$$p_1 = ap_m \quad (a = 1; 0.9; 0.8; \text{ etc.}), \quad (147e)$$

it then follows that

$$\frac{p_1}{p_m} = \cos \gamma \cdot \frac{kr_0}{kr} \sqrt{\frac{1 + \frac{1}{k^2 r^2}}{1 + \frac{1}{k^2 r_0^2}}} = a. \quad (147f)$$

If we choose $kr_0 = 1$ as an example, then for the field points on the symmetry axis ($\gamma = 0$) there results:

$$a = \frac{1}{\sqrt{2}} \cdot \frac{1}{kr} \sqrt{1 + \frac{1}{k^2 r^2}} \quad (147g)$$

and from this:

$$kr = \frac{1}{2a} \sqrt{1 + \sqrt{1 + 8a^2}}. \quad (147h)$$

Accordingly one obtains for the values of p_1/p_m on the normal axis

$p_1/p_m =$	0.1	0.2	0.3	0.4	0.5	0.6	0.7	0.8	0.9	1
$r/r_0 =$	7.14	3.67	2.53	1.98	1.65	1.44	1.28	1.17	1.07	1

If we now imagine the circles

$$r = r_0, r = 1.07 r_0, r = 1.17 r_0, r = 1.28 r_0, \text{ etc.}, \quad (147i)$$

constructed, by calculating the γ values we can easily state the points for the required values of p_1/p_m . For example, on the circle $r = 1.28 r_0$, the values of $\cos \gamma$ for the corresponding values of

p_1/p_m are:

$p_1/p_m =$	0,7	0,6	0,5	0,4	0,3	0,2	0,1
$\cos \gamma =$	1	$\frac{6}{7}$	$\frac{5}{7}$	$\frac{4}{7}$	$\frac{3}{7}$	$\frac{2}{7}$	$\frac{1}{7}$

As an additional example we give the corresponding tables for $kr_0 = 5$:

$p_1/p_m =$	0,1	0,2	0,3	0,4	0,5	0,6	0,7	0,8	0,9	1
$r/r_0 =$	9,81	4,91	3,28	2,46	1,97	1,65	1,42	1,24	1,11	1

For $kr_0 \gg 1$, the corresponding values of r/r_0 are simply given by $1/p_1/p_m$. Therefore, in this case

$p_1/p_m =$	0,1	0,2	0,3	0,4	0,5	0,6	0,7	0,8	0,9	1
$r/r_0 =$	10	5	3,33	2,50	2,00	1,67	1,43	1,25	1,11	1

In Fig. 65 are drawn the curves of constant pressure for the spherical radiator of the first order (with $kr_0 = 1$). Because of the given antisymmetric distribution of the velocity amplitude with respect to the equatorial plane, the character of the field is essentially different as compared with that of the zero radiator since the pressure is now zero in the equatorial plane.

From (143) the pressure amplitude p_n for the spherical radiator of the n th order is given by

$$p_n = p^0 \cdot u_n \left\{ \frac{S_n^2(kr) + C_n^2(kr)}{U_n^2(kr_0) + V_n^2(kr_0)} P_n(\cos \gamma) \right\}, \quad (147j)$$

where

$n =$	0	1	2	3
$S_n^2(x) + C_n^2(x)$	1	$1/x^2 + 1$	$(1 - 3/x^2)^2 + (3/x)^2$	$(1 - 15/x^2)^2 + (6/x + 15/x^3)^2$
$U_n^2(x) + V_n^2(x)$	$1 + x^2$	$x^2 + 4/x^2$	$(4 - 9/x^2)^2 + (x - 9/x)^2$	$(7 - 60/x^2)^2 + (x - 27/x + 60/x^3)^2$

It is noteworthy that the directional influence - i.e., the ratio of the pressure amplitude at an arbitrary field point, (r, γ) to the pressure amplitude at the field point at the same distance r on the symmetry axis ($r, \gamma = 0$) - is given independently of r simply by $P_n(\cos \gamma)$ so that the behavior of the sound field is obtained without difficulty from the values on the symmetry axis. In particular, the nodal lines $P_n(\cos \gamma) = 0$, at which the velocity amplitude

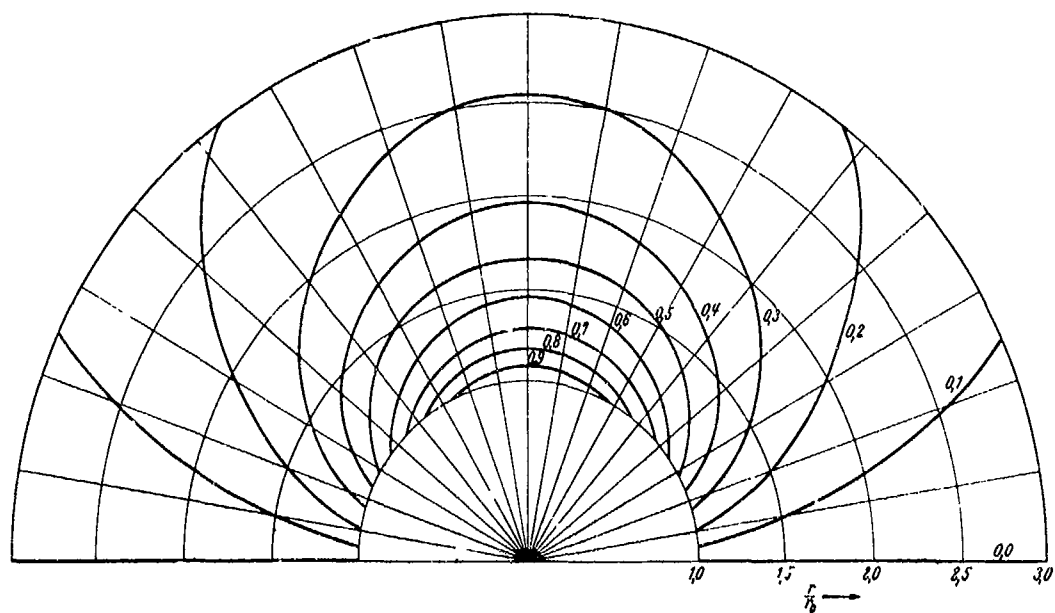


Fig. 65. Curves of constant sound pressure (p_i/p_m) for a radiator of the first order.

on the radiating sphere is equal to zero, determine quite generally the conical surfaces in space for which the pressure amplitude in space vanishes.

Calculations for spherical radiators of a higher order will not be carried out since, from a practical standpoint, scarcely any cases occur in which a radiator behaves as a single radiator of higher order.

6. The compound spherical radiator

Important for the following is the investigation of the sound field which is produced by a combination of a series of spherical radiators of different order. For a sphere with the radius r_0 , whose velocity amplitude w is represented by a superposition of spherical harmonics

$$w = [A_0 P_0(\cos \gamma) + A_1 P_1(\cos \gamma) + \dots + A_n P_n(\cos \gamma)] e^{i\omega t} \quad (148)$$

it turns out that the resulting pressure is given simply by the corresponding superposition of the pressure due to the individual spherical radiators. The pressure p at the field point (r, γ) is then

$$p = p^{(0)} e^{i(\omega t + \pi/2)} \sum_{m=0}^n \frac{S_m(kr) + iC_m(kr)}{U_m(kr_0) + iV_m(kr_0)} A_m P_m(\cos \gamma). \quad (149)$$

Here the A_m 's are constant quantities which, in a given case, may be complex (in order to take account of different phases). The principal significance of this theorem lies, however, in its reversibility. In general the above velocity distribution does not exist in the form (148). The essential thing now is that by the development theorem of spherical harmonics an (to within general continuity requirements) arbitrary function in the form (148) can be represented on the spherical surface.

Thus the calculation of the sound field for an arbitrarily given velocity amplitude on the sphere is then possible. We will illustrate this in a special example.

On the part of a rigid immovable sphere which is characterized by $0 \leq \gamma \leq \gamma_0$ (a spherical cap), a constant velocity amplitude $w = 1$ is given while for the remaining part, $w = 0$ (Fig. 66). We first have the problem to determine the coefficients A_m of the function

$$w = A_0 P_0(\cos \gamma) + A_1 P_1(\cos \gamma) + \dots \quad (150)$$

so that

$$\begin{aligned} w &= 1 \text{ for } 0^\circ \leq \gamma \leq \gamma_0, \\ w &= 0 \text{ for } \gamma_0 < \gamma \leq 180^\circ \end{aligned} \quad (150a)$$

Here the orthogonality relations for spherical harmonics

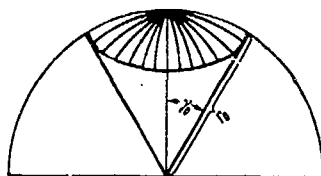


Fig. 66. The radiating spherical cap.

$$\begin{aligned} \int_{-1}^{+1} P_m(\mu) P_n(\mu) d\mu &= 0, & \text{for } m \neq n & \quad (150b) \\ \int_{-1}^{+1} P_n^2(\mu) d\mu &= \frac{2}{2n+1}. \end{aligned}$$

become useful.

When we multiply both sides of equation (150) by $P_n(\mu)$ and integrate from -1 to $+1$, we immediately obtain

$$\int_{-1}^{+1} w P_n(\mu) d\mu = A_n \int_{-1}^{+1} P_n^2(\mu) d\mu = A_n \cdot \frac{2}{2n+1} \quad (150c)$$

and thus generally,

$$A_n = \frac{2n+1}{2} \int_{-1}^{+1} w P_n(\mu) d\mu. \quad (150d)$$

Now in our example w is only different from 0 in the region $\cos \gamma_0 \leq \mu \leq 1$ so that

$$A_n = \frac{2n+1}{2} \int_{\cos \gamma_0}^1 P_n(\mu) d\mu \quad (150e)$$

By the well-known relation of the spherical harmonics

$$(2n+1)P_n(x) = \frac{d}{dx} [P_{n+1}(x) - P_{n-1}(x)] \quad (151)$$

it follows that

$$\begin{aligned} (2n+1) \int_x^1 P_n(\mu) d\mu &= P_{n-1}(x) - P_{n+1}(x), & (n \geq 1) & \quad (152) \\ \int_x^1 P_0(\mu) d\mu &= 1 - x. \end{aligned}$$

Thus there results the required representation for w :

$$w = \frac{1 - \cos \gamma_0}{2} + \frac{1}{2} \sum_{n=1}^{\infty} [P_{n-1}(\cos \gamma_0) - P_{n+1}(\cos \gamma_0)] P_n(\cos \gamma) \quad (153)$$

and therewith also the required pressure by (149) upon substitution of the resulting values for A_n .

If, as a special case, we choose a radiating hemisphere with a constant velocity amplitude $w = 1$ which is completed by a rigid hemisphere on which $w = 0$, we then have to set $\cos \gamma_0 = \cos 90^\circ = 0$. Since

$$P_{2n}(0) = (-1)^n \frac{1 \cdot 3 \cdot 5 \dots (2n-1)}{2 \cdot 4 \cdot 6 \dots 2n} \quad (153a)$$

and $P_{2n+1}(0) = 0$, we find:

$$w = \frac{1}{2} + \frac{3}{4} P_1(\cos \gamma) - \frac{1}{2} \cdot \frac{7}{8} P_3(\cos \gamma) + \frac{1 \cdot 3}{2 \cdot 4} \cdot \frac{11}{12} P_5(\cos \gamma) + \dots \quad (153b)$$

and for a radiating spherical cap with $\gamma_0 = 60^\circ$:

$$\begin{aligned} w = & 0,250 + 0,563 P_1(\cos \gamma) + 0,469 P_2(\cos \gamma) + 0,082 P_3(\cos \gamma) \\ & - 0,264 P_4(\cos \gamma) - 0,306 P_5(\cos \gamma) - 0,067 P_6(\cos \gamma) \\ & + 0,198 P_7(\cos \gamma) + 0,245 P_8(\cos \gamma) + 0,057 P_9(\cos \gamma) - \dots \end{aligned} \quad (153c)$$

In Figs. 67 and 68 the corresponding approximation curves

$$w^{(n)} = \sum_{m=0}^{m=n} a_m P_m(\cos \gamma) \quad (153d)$$

are represented. The deviation of the approximation function from the theoretical value unity may be determined for $\gamma = 0^\circ$. Since $P_m(1) = 1$ in $w^{(n)}$, all terms except the first two and the last two then cancel out so that

$$w_{(\gamma=0^\circ)}^{(n)} = 1 - \frac{P_{n-1}(\cos \gamma_0) + P_n(\cos \gamma_0)}{2} \quad (153e)$$

In the present case, $\gamma_0 = 90^\circ$, the error therefore appears equal to

$$\frac{P_{n-1}(0) + P_n(0)}{2}.$$

Therefore for $n = 0, 1, 2, \dots$ etc. it equals

$$+ \frac{1}{2}, -\frac{1}{2} \cdot \frac{1}{2}, + \frac{1}{2} \cdot \frac{1 \cdot 3}{2 \cdot 4} \text{ etc.}$$

In order to obtain a better agreement with the first formula, we will introduce the radiating surface $F = 2\pi r_0^2(1 - \cos \gamma_0)$ for the representation of the radiating spherical cap defined by γ_0 and having the constant velocity amplitude w , and we will write the pressure p in the form

$$p = c \sigma e^{i(\omega t + \pi/2)} \frac{F \cdot w}{2\lambda r} \cdot \mathfrak{P}(r, r_0, \mu, \mu_0). \quad (153f)$$

Here $p_0 = \frac{c \cdot \sigma F \cdot w}{2\lambda r}$ is the pressure amplitude if the dimensions of the radiator are small compared to the wave length and

$$\begin{aligned} \mathfrak{P}(r, r_0, \mu, \mu_0) = & \frac{S_0(kr) + i C_0(kr)}{U_0(kr_0) + i V_0(kr_0)} \\ & + \frac{1}{1 - \frac{r}{r_0}} \sum_{n=1}^{\infty} P_n(\mu) [P_{n-1}(\mu_0) - P_{n+1}(\mu_0)] \frac{S_n(kr) + i C_n(kr)}{U_n(kr_0) + i V_n(kr_0)} \end{aligned} \quad (154)$$

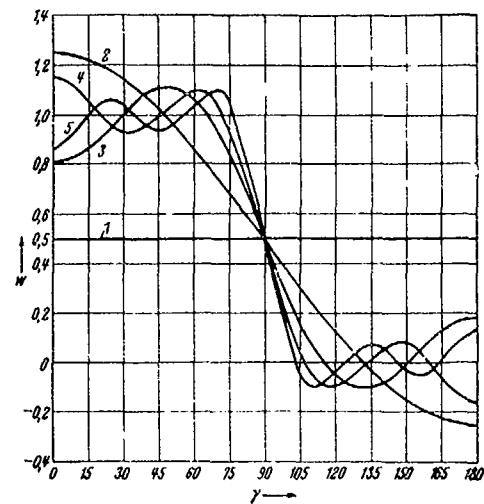


Fig. 67. Approximation of the function $w = \begin{cases} 1 & (0^\circ \leq \gamma < 90^\circ) \\ 0 & (90^\circ \leq \gamma < 180^\circ) \end{cases}$ by spherical harmonics.

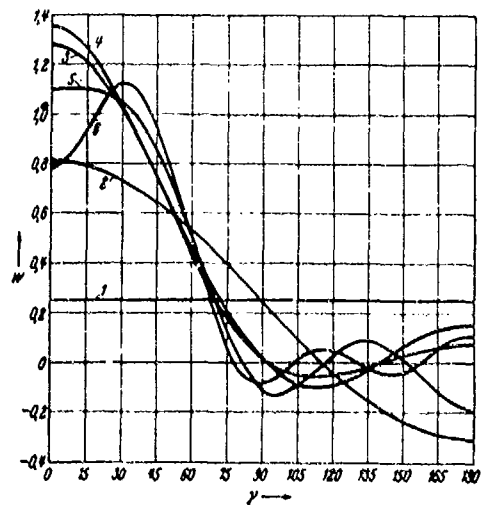


Fig. 68. Approximation of the function $w = \begin{cases} 1 & (0^\circ \leq \gamma < 90^\circ) \\ 0 & (90^\circ \leq \gamma < 180^\circ) \end{cases}$ by spherical harmonics.

A case of practical importance which has been treated by Rayleigh exists when the radiating surface is very small so that $\mu_0 = \cos \gamma_0$ can be replaced by unity. Then formula (154) becomes inapplicable. However, we can easily remove this disadvantage when we consider that by (151)⁴¹:

$$\lim_{\mu_0 \rightarrow 1} \left\{ \frac{1}{1 - \mu_0} [P_{n-1}(\mu_0) - P_{n+1}(\mu_0)] \right\} = 2n + 1 \quad (154a)$$

We then obtain for a point radiator on a rigid sphere

$$p = p_0 \cdot e^{i(\omega t + \pi/2)} \mathfrak{P}(r, r_0, \mu, 1), \quad (155)$$

where

$$\mathfrak{P}(r, r_0, \mu, 1) = \sum_{n=0}^{\infty} (2n+1) P_n(\mu) \frac{S_n(kr) + i C_n(kr)}{U_n(kr_0) + i V_n(kr_0)} \quad (155a)$$

A substantial simplification of the formulae⁴² occurs if the field point is at so great a distance r that one can set $f_n(ikr) = 1$. Since

$$S_n(x) + i C_n(x) = i^{n+1} e^{-ix} f_n(ix) \quad (155b)$$

$S_n(kr) + i C_n(kr)$ becomes $i^{n+1} e^{-ikr}$.

We then obtain

$$p = p_0 \cdot e^{i(\omega t - kr)} f(\gamma, \gamma_0), \quad (155c)$$

where

$$f(\gamma, \gamma_0) = \frac{i}{U_0(kr_0) + i V_0(kr_0)} + \frac{1}{1 - \mu_0} \sum_{n=1}^{\infty} i^{n+1} \frac{P_n(\mu) [P_{n-1}(\mu_0) - P_{n+1}(\mu_0)]}{U_n(kr_0) + i V_n(kr_0)} \quad (156)$$

For practical calculation it is advantageous for the summation to group the terms with the even n and with odd n when we write

$$f(\gamma, \gamma_0) = \frac{i}{U_0(kr_0) + i V_0(kr_0)} + \frac{1}{1 - \mu_0} \mathfrak{S}_1 + \frac{1}{1 - \mu_0} \mathfrak{S}_2, \quad (157)$$

where \mathfrak{S}_1 contains the spherical harmonics $P_2(\mu), P_4(\mu), \dots$ etc. and \mathfrak{S}_2 contains the spherical harmonics $P_1(\mu), P_3(\mu), \dots$ etc. Then since

$$P_{2n}(-\mu) = P_{2n}(\mu) \quad \text{and} \quad P_{2n+1}(-\mu) = -P_{2n+1}(\mu);$$

$$f(180^\circ - \gamma, \gamma_0) = \frac{i}{U_0 + i V_0} + \frac{1}{1 - \mu_0} \mathfrak{S}_1 - \frac{1}{1 - \mu_0} \mathfrak{S}_2 \quad (158)$$

and

$$f(\gamma, 180^\circ - \gamma_0) = \frac{i}{U_0 + i V_0} - \frac{1}{1 + \mu_0} \mathfrak{S}_1 + \frac{1}{1 + \mu_0} \mathfrak{S}_2. \quad (159)$$

⁴¹ Eq. (151) is to be used when L'Hospital's rule is applied in evaluating the indeterminate form on the left of (154a).

⁴² Formulae (153f) and (154) are referred to here.

Manifestly, corresponding relations are also valid for field points which do not lie at a great distance. We need therefore only to carry out the calculation for $0 \leq \gamma \leq 90^\circ$, $0 \leq \gamma_0 \leq 90^\circ$ and the values for $90^\circ \leq \gamma \leq 180^\circ$ and $90^\circ \leq \gamma_0 \leq 180^\circ$ then result from (158) and (159).

Physically (156) and (157) signify that one can replace an arbitrary velocity distribution on the spherical surface by a distribution symmetrical to the equatorial plane and one antisymmetric to the equatorial plane. The first contains the spherical harmonics of even order while the second contains the spherical harmonics of odd order. By (158) one finds the pressure at the image of a field point when one inserts the antisymmetric part with the opposite sign in the formula for the field point. Furthermore, it follows from (158) and (159) that

$$(1 - \mu_0)/(180^\circ - \gamma, \gamma_0) + (1 + \mu_0)/(\gamma, 180^\circ - \gamma_0) = \frac{2i}{U_0 + iV_0}. \quad (159a)$$

This says that the radiations due to (158) and (159) together yield the radiation of a spherical radiator of zero order.

As an example, in the table on page 102, the expressions

$$\frac{i^{n+1}}{U_n(kr_0) + iV_n(kr_0)} [P_n(\cos \gamma_0) - P_{n+1}(\cos \gamma_0)] = A_n + iB_n \quad (159b)$$

are given for $kr_0 = 10$ and $\gamma_0 = 0^\circ, 10^\circ, 20^\circ, \dots, 90^\circ$ and the corresponding values $f(\gamma, \gamma_0)$ for $\gamma = 0^\circ$ and $\gamma = 180^\circ$ are calculated.

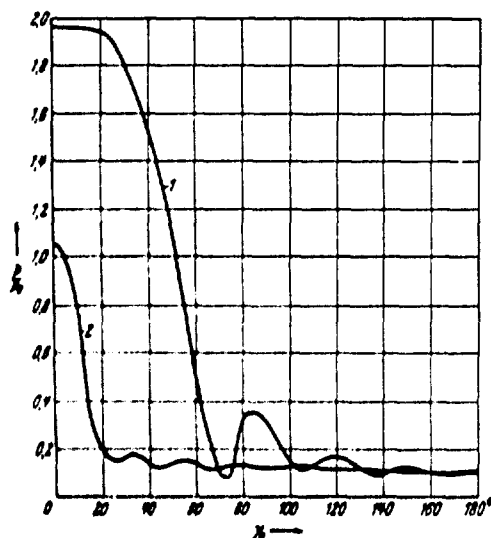


Fig. 69. Pressure amplitude as a function of the central angle of the radiating surface with constant deformation volumes 1. for the principal direction ($\gamma = 0^\circ$), 2. for the opposite direction ($\gamma = 180^\circ$).

In Fig. 69, the magnitudes of $f(0^\circ, \gamma_0)$ and $f(180^\circ, \gamma_0)$ are represented. These curves give a conspectus of the pressure amplitudes in the principal direction ($\gamma = 0^\circ$) and in the opposite direction ($\gamma = 180^\circ$) as a function of the size of the radiating surface (γ_0) with constant deformation volume ($F \cdot w$). We immediately recognize that for small values of γ_0 in the principal direction, the double amplitude occurs as compared with the amplitude for nondirectional radiation

$$(p_0 = \frac{c \cdot \sigma F \cdot w}{2\lambda r}).$$

If one desires the largest possible radiating surface, the greatest possible pressure amplitude in the principal direction and simultaneously the greatest possible extinction for

$$U_{\alpha}(10) + i V_{\alpha}(10) [P_{\alpha-1}(\cos \gamma_0) - P_{\alpha+1}(\cos \gamma_0)]$$

	$\gamma_0 = 10^\circ$	$\gamma_0 = 20^\circ$	$\gamma_0 = 30^\circ$	$\gamma_0 = 40^\circ$	$\gamma_0 = 50^\circ$	$\gamma_0 = 60^\circ$	$\gamma_0 = 70^\circ$	$\gamma_0 = 80^\circ$	$\gamma_0 = 90^\circ$
1	-0.0009 - 0.0012 i	-0.0037 - 0.0047 i	-0.0083 - 0.0104 i	-0.0145 - 0.0182 i	-0.0222 + 0.0277 i	-0.0211 + 0.0288 i	-0.0409 + 0.0511 i	-0.0514 + 0.0642 i	-0.0622 + 0.0777 i
2	-0.0082 - 0.0042 i	-0.0230 - 0.0154 i	-0.0454 - 0.0304 i	-0.0664 - 0.0444 i	-0.0791 + 0.0529 i	-0.0787 + 0.0526 i	-0.0633 + 0.0424 i	-0.0353 + 0.0236 i	-
3	-0.0131 - 0.0018 i	-0.0408 - 0.0057 i	-0.0569 - 0.0080 i	-0.0409 - 0.0058 i	+0.0047 + 0.0007 i	+0.0547 + 0.0077 i	+0.0769 + 0.0108 i	+0.0548 + 0.0077 i	-
4	-0.0043 - 0.0053 i	-0.0097 - 0.0414 i	-0.0048 - 0.0204 i	+0.0082 + 0.0349 i	+0.0139 + 0.0590 i	+0.0034 + 0.0146 i	-0.0123 - 0.0321 i	-0.0145 - 0.0617 i	-
5	-0.0244 - 0.0001 i	-0.0307 - 0.0001 i	-0.0277 + 0.0001 i	-0.0491 + 0.0002 i	+0.0228 - 0.0001 i	+0.0617 - 0.0003 i	-0.0127 + 0.0001 i	-0.0683 + 0.0003 i	-
6	-0.0230 - 0.0006 i	-0.0055 - 0.0020 i	+0.0397 - 0.0149 i	-0.0135 + 0.0051 i	-0.0417 + 0.0157 i	+0.0376 - 0.0141 i	+0.0255 - 0.0099 i	-0.0538 + 0.0202 i	-
7	-0.0071 - 0.0003 i	-0.0048 + 0.0002 i	-0.0053 + 0.0003 i	+0.0131 - 0.0006 i	-0.0093 + 0.0005 i	-0.0037 + 0.0002 i	+0.0150 - 0.0007 i	-0.0125 + 0.0006 i	-
8	-0.0010	+0.0014	-0.0009	-0.0001	+0.0013	-0.0022	+0.0023	-0.0014	-
9	-0.0001	-0.0002	+0.0002	-0.0002	+0.0002	-0.0002	+0.0001	+0.0001	-
10	-0.0171 - 0.0006 i	-0.0357 - 0.0249 i	-0.1095 - 0.0023 i	-0.1634 + 0.0964 i	-0.1096 + 0.1564 i	+0.0416 + 0.0995 i	-0.0084 + 0.0416 i	-0.1832 + 0.0550 i	-0.0622 + 0.0777 i
11	-0.0032 - 0.0032 i	-0.0123 + 0.0125 i	-0.0263 + 0.0267 i	-0.0434 + 0.0442 i	-0.0617 + 0.0628 i	-0.0788 + 0.0802 i	-0.0928 + 0.0945 i	-0.1019 + 0.1037 i	-0.1051 + 0.1069 i
12	-0.0100 - 0.0029 i	-0.0344 - 0.0099 i	-0.0593 + 0.0170 i	-0.0689 + 0.0198 i	-0.0539 + 0.0155 i	-0.0161 + 0.0046 i	+0.0316 - 0.0091 i	+0.0710 - 0.0204 i	+0.0862 - 0.0248 i
13	-0.0125 - 0.0100 i	-0.0339 - 0.0272 i	-0.0335 - 0.0268 i	-0.0004 - 0.0003 i	+0.0407 + 0.0327 i	+0.0516 + 0.0413 i	+0.0179 + 0.0144 i	+0.0335 - 0.0268 i	-0.0579 - 0.0464 i
14	-0.0119 - 0.0181 i	-0.0209 - 0.0320 i	-0.0023 - 0.0035 i	-0.0298 + 0.0457 i	-0.0154 + 0.0236 i	+0.0256 - 0.0393 i	+0.0314 - 0.0482 i	-0.0100 + 0.0154 i	-0.0378 + 0.0580 i
15	-0.0089 - 0.0249 i	-0.0006 - 0.0186 i	-0.0147 - 0.0423 i	-0.0071 - 0.0197 i	+0.0192 + 0.0538 i	+0.0051 + 0.0142 i	-0.0221 - 0.0618 i	-0.0018 - 0.0051 i	+0.0231 + 0.0646 i
16	-0.0026 - 0.0153 i	-0.0006 - 0.0037 i	+0.0037 - 0.0214 i	-0.0042 - 0.0243 i	-0.0008 - 0.0046 i	+0.0055 + 0.0322 i	-0.0039 - 0.0227 i	-0.0026 - 0.0149 i	+0.0062 + 0.0360 i
17	-0.0000 - 0.0029 i	-0.0000 - 0.0029 i	+0.0002 i	+0.0004 i	-0.0058 i	+0.0044 i	-0.0001 i	+0.0001 + 0.0036 i	+0.0001 + 0.0066 i
18	-0.0003 i	+0.0005 i	-0.0005 i	-0.0001 i	-0.0001 i	-0.0002 i	+0.0001 i	-0.0008 i	+0.0001 i
19	-0.0076 - 0.0099 i	-0.0525 - 0.0171 i	-0.1324 + 0.0003 i	-0.1538 + 0.0694 i	-0.0718 + 0.1779 i	-0.0072 + 0.1376 i	-0.0379 - 0.0325 i	-0.0788 + 0.0556 i	-0.0852 + 0.2019 i
20	-0.0247 - 0.0163 i	-0.1083 - 0.0419 i	-0.2419 - 0.0019 i	-0.3172 + 0.1658 i	-0.1815 + 0.3343 i	+0.0345 + 0.2371 i	-0.0463 + 0.0090 i	-0.2620 + 0.1106 i	-0.1474 + 0.2797 i
21	-0.0095 + 0.0032 i	-0.0032 - 0.0078 i	+0.0228 - 0.0024 i	-0.0097 + 0.0289 i	-0.0378 - 0.0214 i	+0.0487 - 0.0380 i	+0.0295 + 0.0741 i	+0.1044 - 0.0006 i	+0.0230 - 0.1243 i
22	-1.625 - 1.084 i	-1.795 - 0.695 i	-1.806 - 0.014 i	-1.366 + 0.709 i	-0.508 + 0.936 i	+0.069 + 0.474 i	-0.070 + 0.014 i	-0.317 + 0.134 i	-0.147 + 0.280 i
23	-0.623 + 0.212 i	-0.052 - 0.128 i	+0.170 - 0.018 i	-0.041 + 0.115 i	-0.106 - 0.061 i	+0.097 - 0.076 i	+0.045 + 0.113 i	+0.126 - 0.001 i	+0.023 - 0.124 i

the opposite direction, the figure shows that this is attained for $\gamma_0 = 20^\circ$ approximately.

With the aid of the tables for $A_n + iB_n$, it is then easy to calculate the complete sound field (for a great distance of the field point) for every value of γ_0 . One needs only to compute the expressions

$$R + iJ = \frac{1}{1 - \mu_0} \sum (A_n + iB_n) P_n(\cos \gamma) \quad (159c)$$

and to plot $\sqrt{R^2 + J^2}$ as a function of γ . The components R, J corresponding to the values $\gamma_0 = 10^\circ, 30^\circ, 60^\circ, 90^\circ, 120^\circ, 150^\circ$, and 170° are plotted in Figs. 70 to 76 and the relative pressure amplitudes obtained therefrom are represented in Figs. 77 to 83.

As long as the radiating surface is small, one may expect a directional effect similar to that of the piston membrane with increasing γ_0 . For the larger values of γ_0 ($\gamma_0 > 90^\circ$) the radiation will gradually approach that of the nondirectional radiator until it becomes identical with that of the spherical radiator of zero order for $\gamma_0 = 180^\circ$. The number of terms which must be calculated to obtain the result with sufficient accuracy increases nearly in proportion to the magnitude of kr_0 . And, indeed, it turns out that the individual terms rapidly decrease as soon as n has become greater than kr_0 so that the necessary number lies between kr_0 and $2kr_0$. This is connected with a general property of the appearing Bessel's functions, which exhibit an essentially different behavior if, with a fixed argument, the function values are plotted with respect to the index n .

As long as $n < x$, $S_n(x)$ and $C_n(x)$ vary between positive and negative values. As soon as n becomes greater than x , $S_n(x)$ decreases sharply and monotonically while $C_n(x)$ increases in the same way. The same thing is true of $U_n(x)$ and $V_n(x)$. In Figs. 84 to 86, $U_n(x)$ and $V_n(x)$ are represented as a function of n for $x = 4, 10, 20$, and 40 .

As an example of the general case when the field point lies in the neighborhood of the radiator we choose

$$kr_0 = 5, r = 2r_0 \text{ (i.e. } kr = 10), \gamma_0 = 30^\circ$$

and calculate the table found on page 110.

For the pressure amplitude p at the field point $r = 2r_0, \gamma = 0$ we obtain from this

$$p = \frac{\sigma \cdot \sigma F \cdot w}{2r \cdot \lambda} |2.03 + 2.24i| = \frac{\sigma \cdot \sigma F \cdot w}{2r \cdot \lambda} \cdot 3.01. \quad (159d)$$

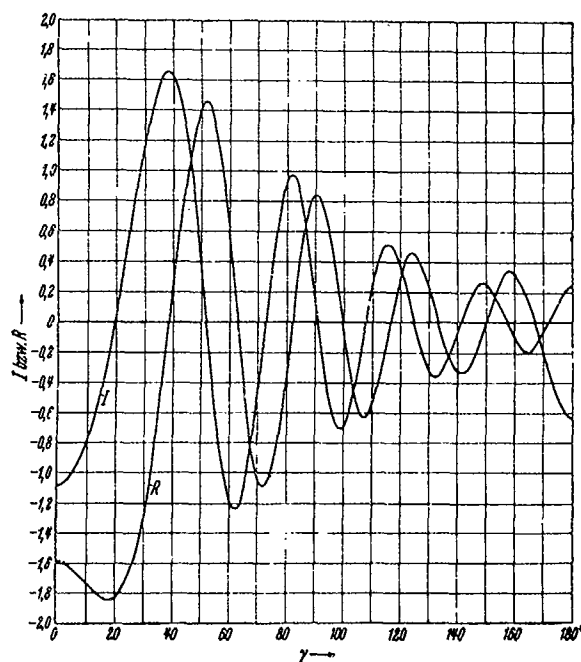


Fig. 70. The components of the sound pressure for $\gamma_0 = 10^\circ$.

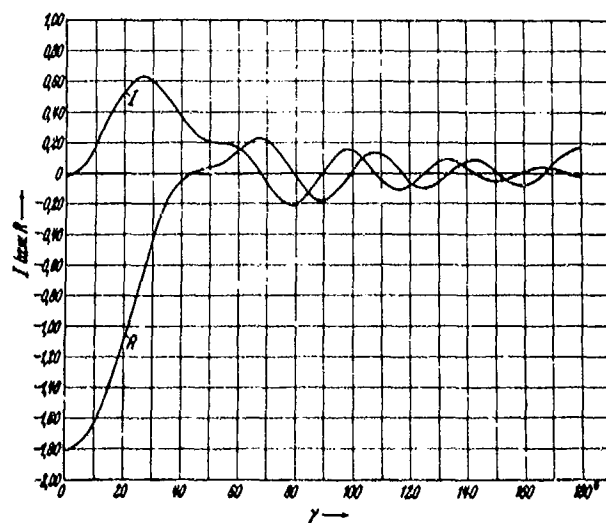


Fig. 71. The components of the sound pressure for $\gamma_0 = 30^\circ$.

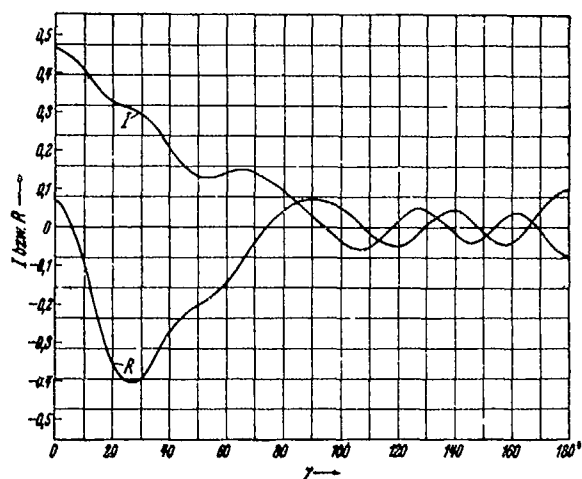


Fig. 72. The components of the sound pressure for $\gamma_0 = 60^\circ$.

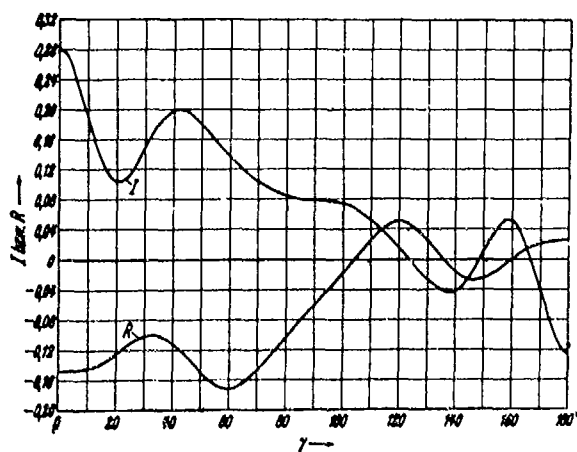


Fig. 73. The components of the sound pressure for $\gamma_0 = 90^\circ$.

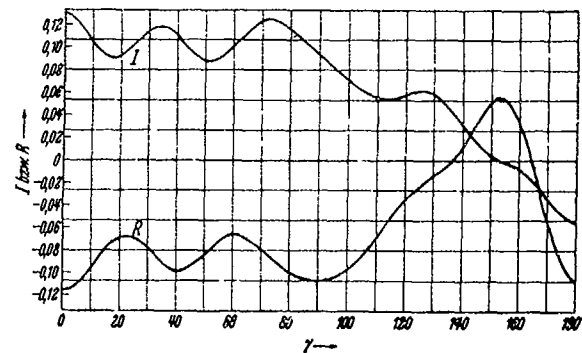


Fig. 74. The components of the sound pressure for $\gamma_0 = 120^\circ$.

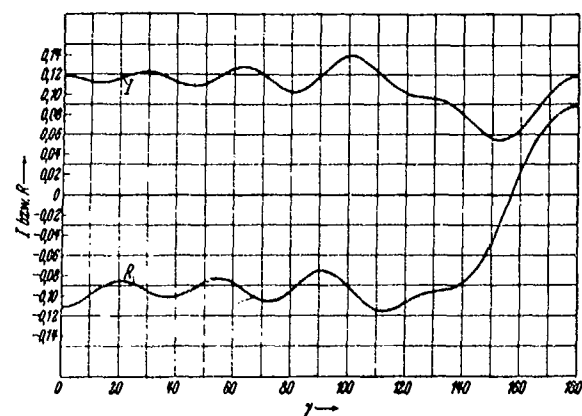


Fig. 75. The components of the sound pressure for $\gamma_0 = 150^\circ$.

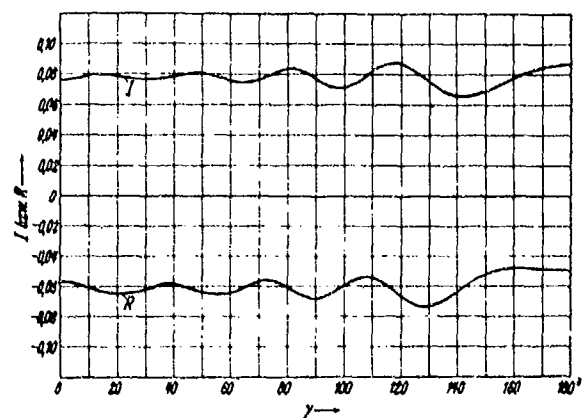


Fig. 76. The components of the sound pressure for $\gamma_0 = 170^\circ$.

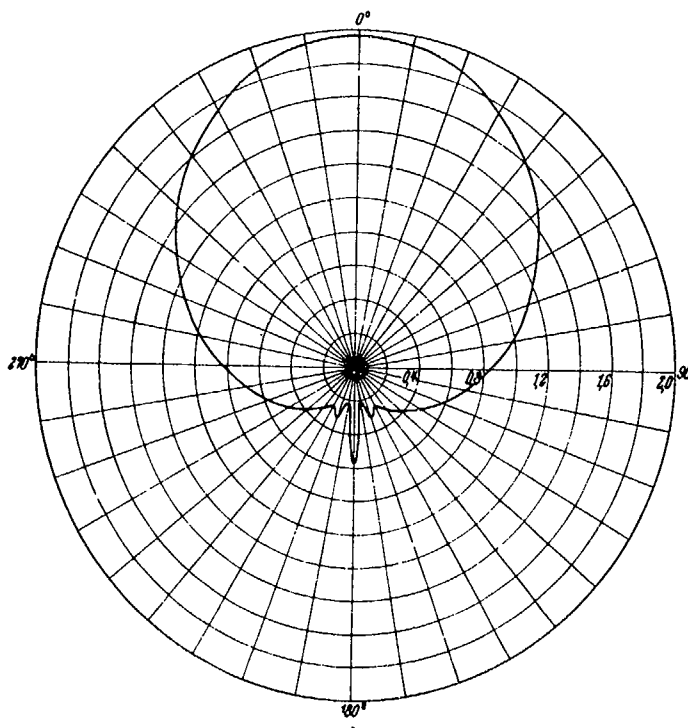


Fig. 77. Sound pressure amplitude (p/p_0) for a radiating spherical cap ($\gamma_s = 10^\circ$).

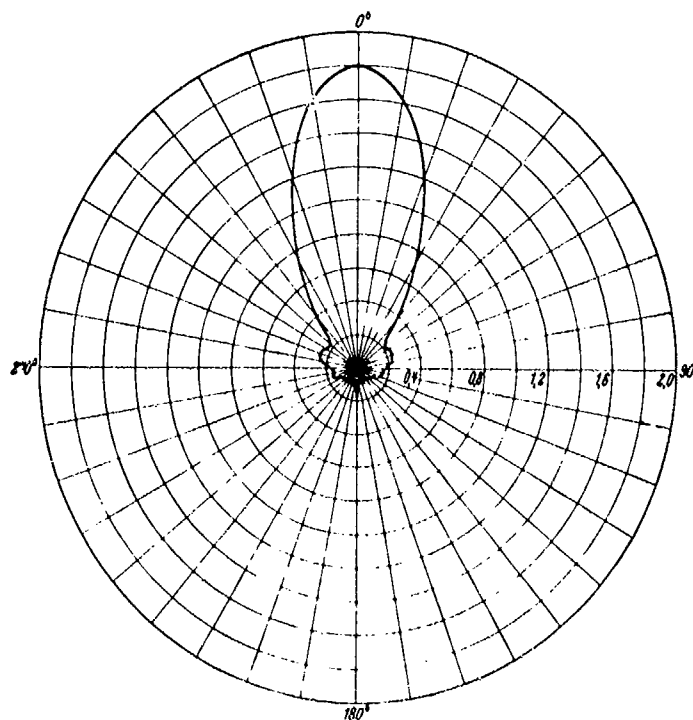


Fig. 78. Sound pressure amplitude (p/p_0) for a radiating spherical cap ($\gamma_s = 30^\circ$).

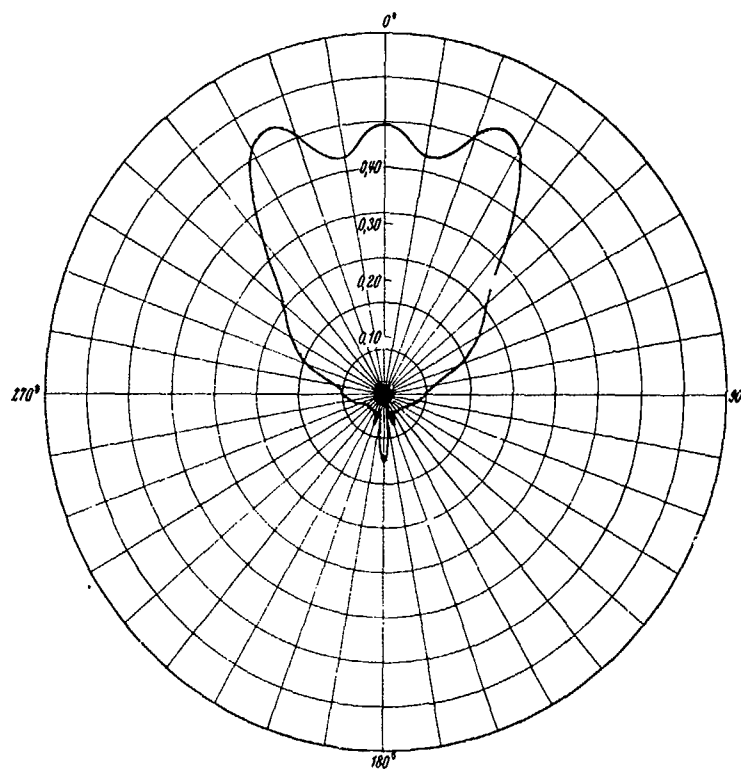


Fig. 79. Sound pressure amplitude (p/p_0) for a radiating spherical cap $(\gamma_0 = 00^\circ)$.

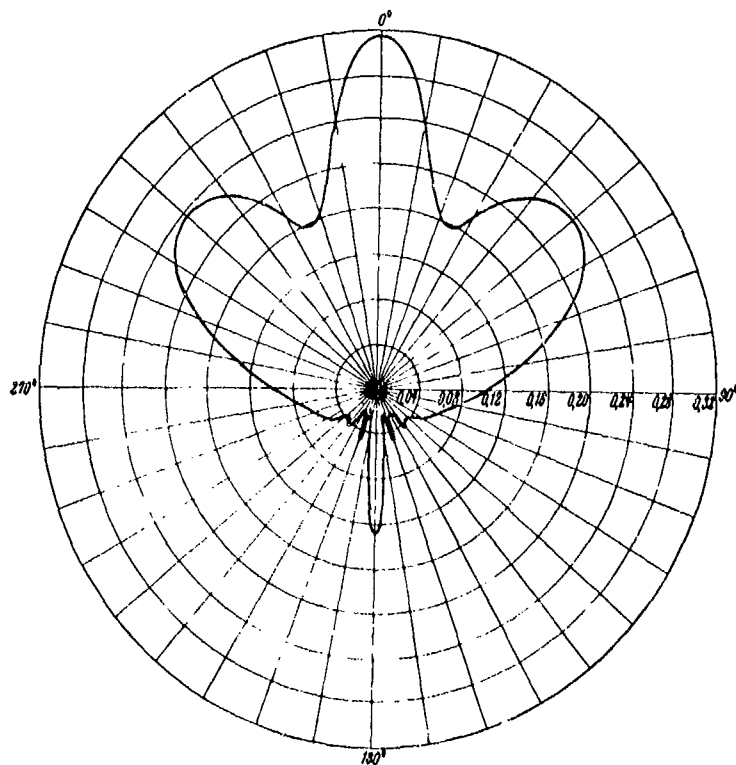


Fig. 80. Sound pressure amplitude (p/p_0) for a radiating spherical cap $(\gamma_0 = 90^\circ)$.

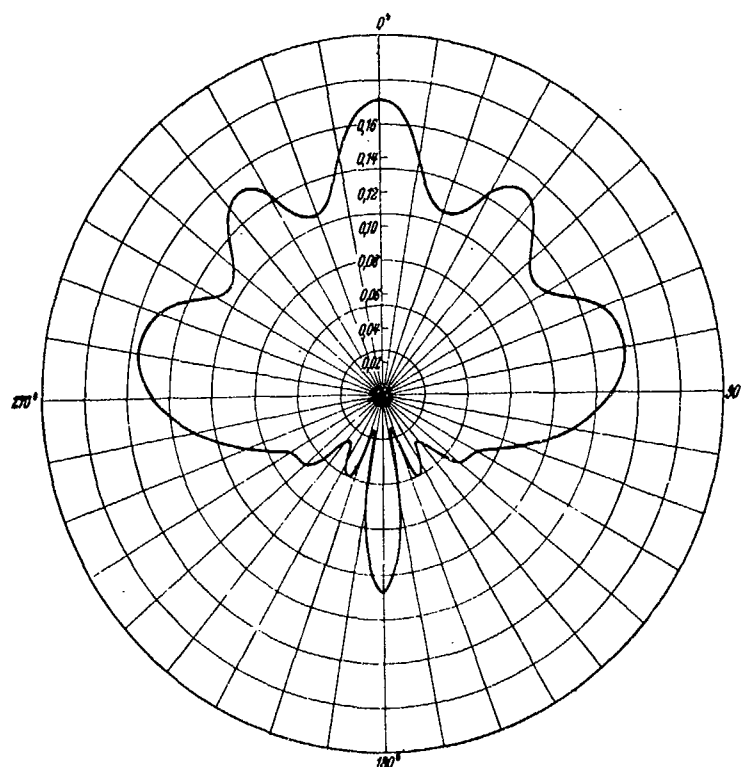


Fig. 81. Sound pressure amplitude (p/p_0) for a radiating spherical cap ($\gamma_s = 120^\circ$).

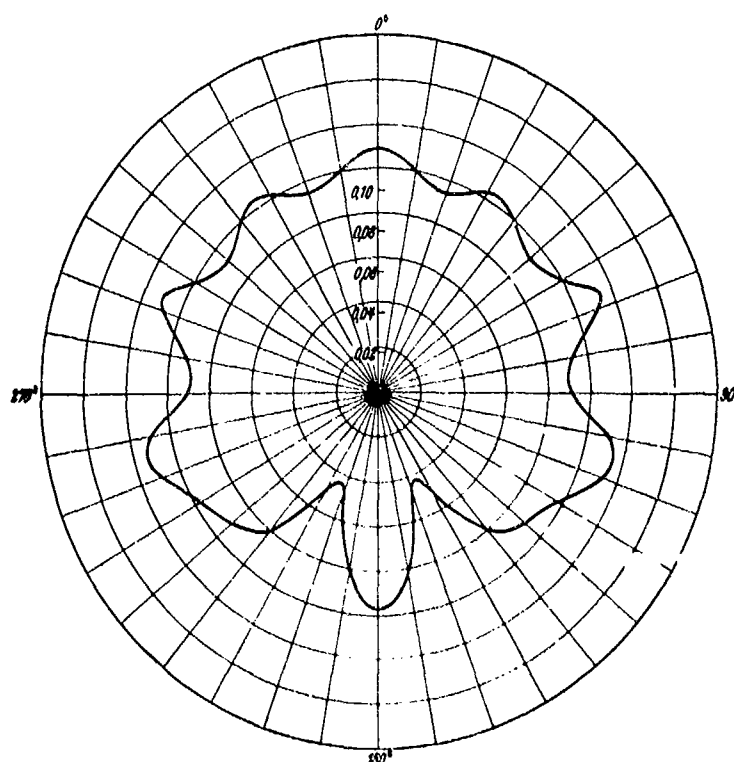


Fig. 82. Sound pressure amplitude (p/p_0) for a radiating spherical cap ($\gamma_s = 160^\circ$).

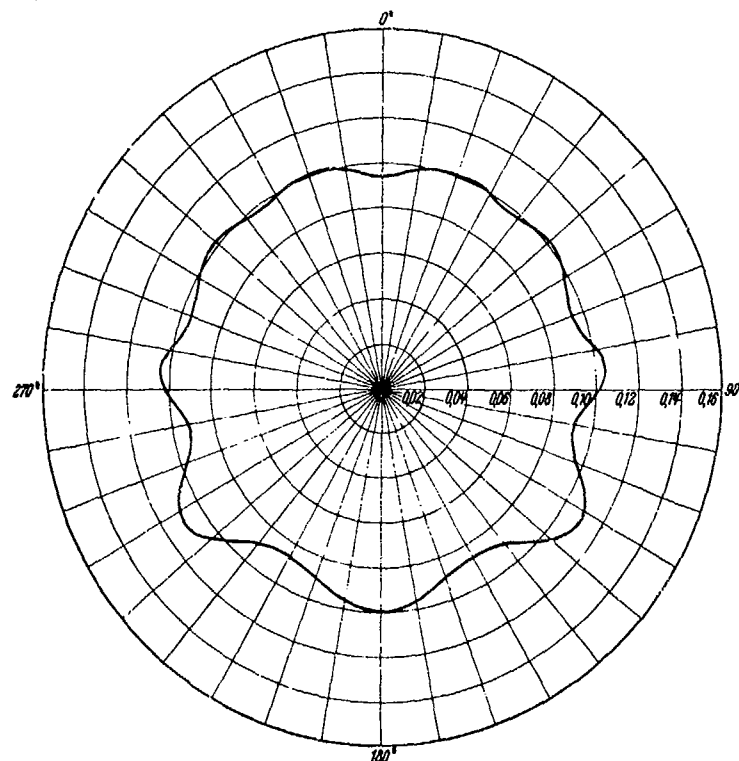


Fig. 83. Sound pressure amplitude (p/p_0) for a radiating spherical cap ($\gamma = 170^\circ$).

n	$\frac{[P_n - 1(\cos 30^\circ) - P_{n+1}(\cos 30^\circ)] [S_n(10) + i C_n(10)]}{(1 - \cos 30^\circ) [U_n(5) + i V_n(5)]}$
0	+0,1953 - 0,0177 i
2	+0,8175 + 0,2193 i
4	+0,2525 + 0,9462 i
6	-0,1490 - 0,0467 i
8	-0,0074 + 0,0228 i
10	-0,0035 + 0,0017 i
12	-0,0002
Σ_1	+1,1052 + 1,1256 i
1	+0,5807 + 0,0128 i
3	+0,7937 + 0,6199 i
5	-0,4259 + 0,4596 i
7	+0,0041 + 0,0109 i
9	-0,0087 + 0,0073 i
11	-0,0009 + 0,0021 i
Σ_2	+0,9330 + 1,1104 i
$\Sigma_1 + \Sigma_2$	+2,0282 + 2,2360 i

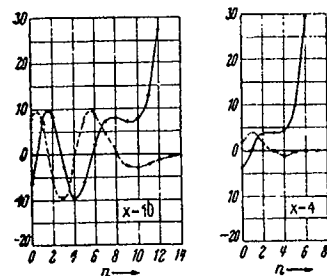


Fig. 84

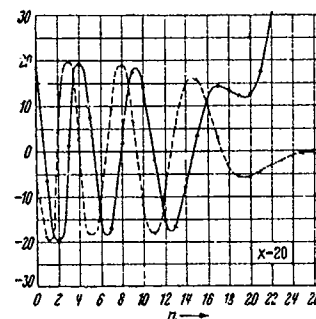


Fig. 85

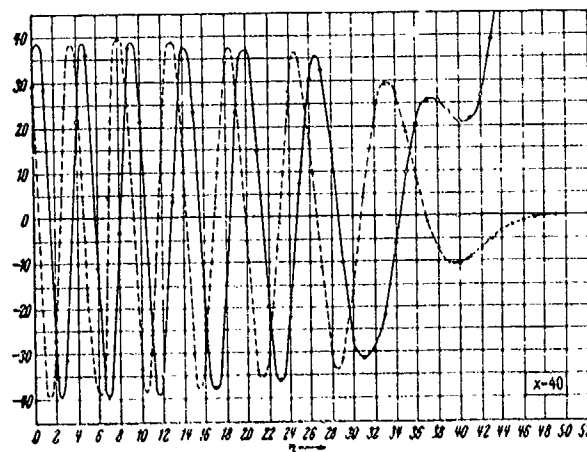


Fig. 86

Figs. 84-86. The auxiliary functions $u_n(x)$ (broken line) and $v_n(x)$ (solid line) for $x = 4, 10, 20, 40$ as a function of n .

$$a_n = (2n + 1) \frac{S_n(kr) + iC_n(kr)}{U_n(1) + iV_n(1)}$$

n	$kr = 1.5$	$kr = 2$	$kr = 3$	$kr = 4$	$kr = 5$
0	+0.1991 -0.6785 i	-0.1506 -0.6909 i	-0.6627 -0.2466 i	-0.5656 +0.4244 i	+0.0516 +0.6997 i
2	+1.1068 -0.1143 i	+0.7754 -0.2198 i	+0.4188 -0.4800 i	-0.0265 -0.5854 i	-0.4416 -0.3517 i
4	+0.4026 -0.0001 i	+0.1466 -0.0005 i	+0.0453 -0.0028 i	+0.0257 -0.0082 i	+0.0153 -0.0154 i
6	+0.1750	+0.0338	+0.0038	+0.0010	+0.0005
8	+0.0774	+0.0082	+0.0004		
10	+0.0344	+0.0020			
12	+0.0153	+0.0005			
14	+0.0068	+0.0001			
16	+0.0030				
18	+0.0013				
Σ_{-1}	+1.9844 -0.7929 i	+0.8160 -0.9112 i	-0.1944 -0.7294 i	-0.5654 -0.1692 i	-0.3742 +0.3326 i
1	+1.3082 -0.9426 i	+0.8104 -1.2622 i	-0.4008 -1.3563 i	-1.2942 -0.4875 i	-1.1353 +0.7637 i
3	+0.6317 -0.0050 i	+0.3299 -0.0136 i	+0.1694 -0.0508 i	+0.0972 -0.1019 i	+0.0085 -0.1277 i
5	+0.2643	+0.0695	+0.0114 -0.0001 i	+0.0050 -0.0004 i	+0.0030 -0.0010 i
7	+0.1163	+0.0166	+0.0012	+0.0002	
9	+0.0516	+0.0041	+0.0001		
11	+0.0229	+0.0010			
13	+0.0102	+0.0003			
15	+0.0045				
17	+0.0020				
19	+0.0009				
Σ_2	+2.4133 -0.9476 i	+1.2318 -1.2758 i	-0.1917 -1.4072 i	-1.1918 -0.5898 i	-1.1237 +0.6350 i

If we imagine a small spherical radiator with the same $F \cdot w$ substituted for the radiating surface, then, in the absence of the rigid sphere, this would produce at the same field point (i.e., field point distance = $r/2$) the pressure amplitude

$$p_0 = \frac{c \cdot \sigma \cdot F \cdot w}{2r\lambda} \cdot 2 \quad (159e)$$

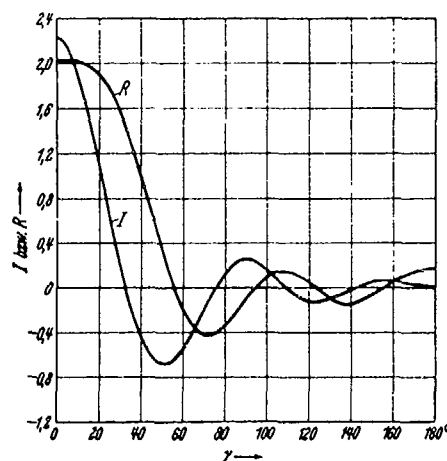


Fig. 87. Sound pressure components of the radiating spherical cap ($\gamma_0 = 30^\circ$) for a small field point distance ($r = 2r_0$, $kr_0 = 5$).

The complete behavior of the pressure amplitude at the distance $r = 2r_0$ is represented as a function of γ in Fig. 88. The corresponding components $[R + iJ = \sum a_n P_n(\cos \gamma)]$ are given in Figure 87.

Finally, we will calculate and illustrate by curves of constant pressure amplitude the sound field of a point radiator located on a rigid sphere - the field being confined in the neighborhood of the sphere. As an example we choose $kr_0 = 1$ and calculate the pressure for the field points whose distances r from the sphere center are determined by

$kr = 1.5, 2, 3, 4$, and 5 . Here, we first calculate the expressions

$$a_n = (2n + 1) \frac{S_n(kr) + iC_n(kr)}{U_n(1) + iV_n(1)} \quad (159f)$$

(see the tables on page 112) and find therefrom $\sum_1 = \sum a_{2n}$ and

$\sum_2 = \sum a_{2n+1}$. If we denote the undistorted (i.e., existing in the absence of the rigid sphere) pressure amplitude by $p_0 = \frac{F \cdot w \cdot c \cdot \sigma}{2\lambda r}$, then the relative pressure amplitude is $p/p_0 = |\sum_1 + \sum_2|$. In the same manner, the relative amplitudes for $\gamma = 5^\circ, 10^\circ$, etc. would be calculated from the quantities $\sum a_n P_n(\cos \gamma)$.

If we collect the values thus found and plot the calculated field points together with the corresponding pressures, we can then draw the curves of constant pressure by interpolation. One recognizes from Figure 89 that the sound field possesses an essentially different character because of the presence of the rigid sphere although the wave length is more than three times the diameter.

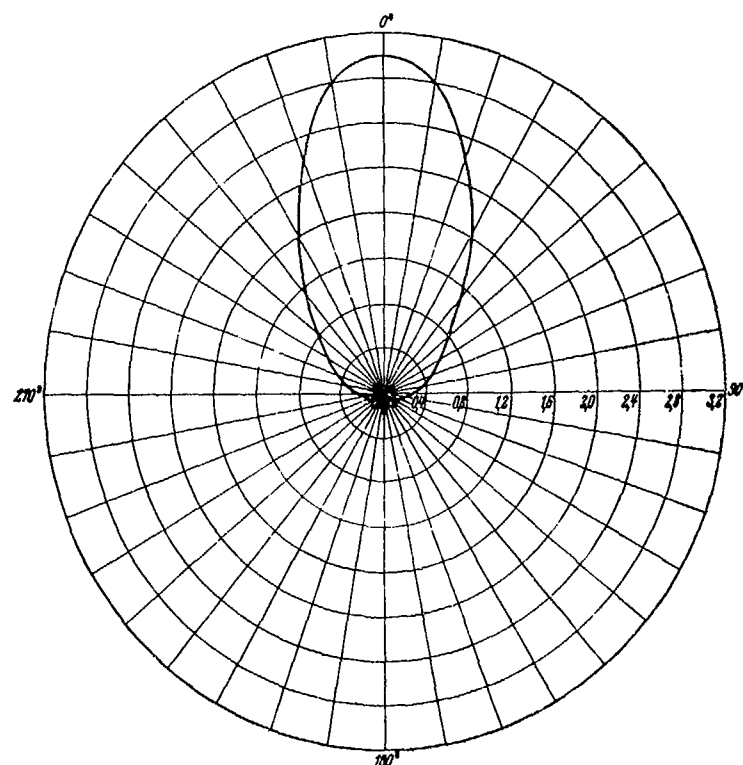


Fig. 88. Sound pressure amplitude (p/p_0) of the radiating spherical cap ($\gamma_0 = 30^\circ$) for a small field point distance ($r = 2r_0$, $kr_0 = 5$).

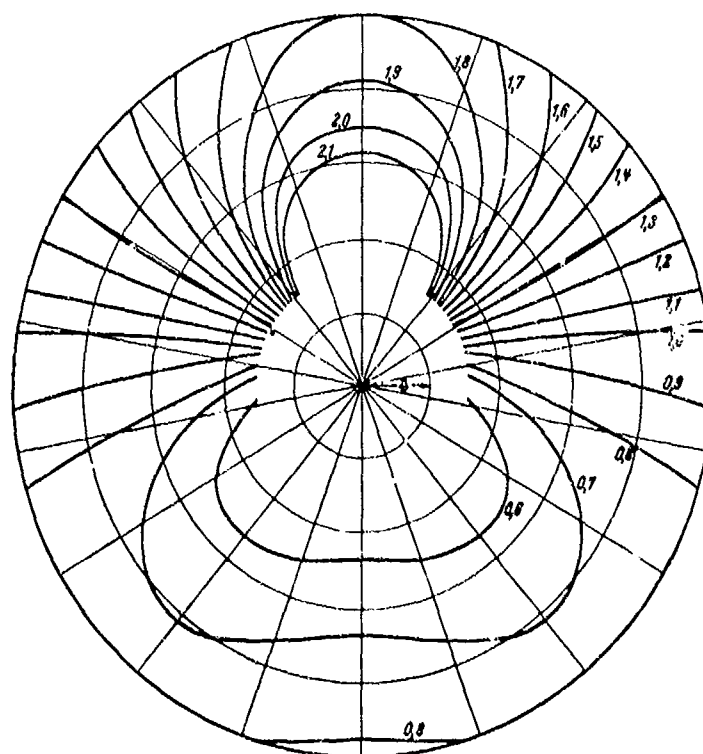


Fig. 89. Sound field (p/p_0) of the point shaped radiator on a rigid sphere ($kr_0 = 1$).

7. The disturbance of a sound field caused by a rigid sphere

(a) The derivation of the general formula

The influence which a plane rigid infinitely extended wall exerts on the sound field produced by a radiator may, as is well known, be easily perceived when a second radiator is introduced which is located at the image position of the original radiator with respect to the wall. The required sound field (lying on the side of the original radiator) then results simply by superposing the two sound fields produced by the individual radiators. In order to prove this, we have to show that the boundary condition for the sound field on the rigid wall (namely, that the velocity component perpendicular to the wall vanishes) is fulfilled. Now, however, it immediately turns out from the symmetrical positions of the radiators that the velocity vector resulting from the two radiators for all field points on the wall lies in the symmetry plane, i.e., possesses no component perpendicular to the wall. More generally, one can state that if, in an arbitrary sound field, a surface is present such that the velocity component perpendicular to this surface vanishes for all field points on this surface, then this surface can be replaced by a rigid, completely reflecting, surface without any change in the sound field. Our problem, to investigate the influence of a rigid sphere on an existing sound field, is then equivalent to the problem of superposing a second field on the existing sound field so that on a prescribed spherical surface the resulting velocity component perpendicular to the spherical surface shall vanish.

We proceed from the undistorted sound field and assume that this is produced by a point radiator located at the point A with the radiating surface F and (constant) velocity amplitude w . Then the sound pressure p_1 for the field point defined by the polar coordinates r, γ is given by

$$p_1 = \frac{c \cdot F \cdot w}{2\lambda R} e^{i(\omega t - kR + \pi/2)} e^{ikr \cos \gamma}. \quad (160)$$

Here R is the distance of the radiator at A from the coordinate origin O. It is assumed to be great compared to r . From (160) with the aid of the relation

$$v_r = \frac{1}{c} \frac{\partial p}{\partial t} \quad (161)$$

there results the radial velocity component

$$v_r = -\frac{F \cdot w}{4\pi R} e^{i(\omega t - kR)} \frac{\partial(e^{ikr \cos \gamma})}{\partial r} \quad (161a)$$

According to the foregoing considerations, we now have to superpose an additional sound field whose radial velocity amplitude v_r^* is equal in magnitude and opposite in sign to v_r on the sphere $r = r_0$. The problem is thus reduced in principle to the earlier calculation where the velocity distribution on a sphere was set forth. By previous considerations, the solution can be stated immediately if the velocity distribution on the sphere is represented by a series of spherical harmonics. In order to bring this about we proceed from the relation ⁴³:

$$e^{ikr \cos \gamma} = \sum_{n=0}^{\infty} i^n \frac{S_n(kr)}{kr} (2n+1) P_n(\cos \gamma). \quad (162)$$

By (161) it then follows that

$$v_r = -\frac{F \cdot w}{4\pi R} e^{i(\omega t - kR)} \cdot k \sum_{n=0}^{\infty} i^n \left(\frac{S_n(kr)}{kr} \right)' (2n+1) P_n(\cos \gamma), \quad (162a)$$

and since

$$\left(\frac{S_n(x)}{x} \right)' = -\frac{U_n(x)}{x^2} \quad (162b)$$

the required velocity represented in the desired form is:

$$v_r^* = -v_r = -\frac{F \cdot w}{2\lambda R} e^{i(\omega t - kR)} \cdot \frac{1}{k^2 r_0^2} \sum_{n=0}^{\infty} (2n+1) i^n U_n(kr_0) P_n(\cos \gamma). \quad (163)$$

By (149) we can immediately specify the sound field produced by v_r^* . The pressure p_2 at the field point r, γ is

$$p_2 = -\frac{c \cdot \sigma \cdot F \cdot w}{2\lambda P} e^{i(\omega t - kR + \pi/2)} \cdot \frac{1}{kr} \sum_{n=0}^{\infty} \frac{(2n+1) i^n U_n(kr_0) \cdot P_n(\cos \gamma)}{U_n(kr_0) + i V_n(kr_0)} [S_n(kr) + i C_n(kr)]. \quad (164)$$

A little manipulation then gives the total sound field existing in the neighborhood of this sphere in the form

$$p_1 + p_2 = \frac{c \cdot \sigma \cdot F \cdot w}{2\lambda R} e^{i(\omega t - kR + \pi/2)} \cdot \frac{1}{kr} \sum_{n=0}^{\infty} \frac{(2n+1) i^{n+1} P_n(\cos \gamma)}{U_n(kr_0) + i V_n(kr_0)} [S_n(kr) V_n(kr_0) - C_n(kr) U_n(kr_0)]. \quad (165)$$

(b) The sound reflection on a rigid sphere

As the simplest case, we first investigate the pressure amplitude produced at the field point A (i.e., at the position of the sound radiator itself) by reflection on the sphere. We will compare this with the sound pressure amplitude which is reflected perpendicularly by a rigid wall at the same distance (as from the sphere). If we introduce the reflection factor $Z = |3|$

⁴³ Rayleigh, Theory of Sound, Sec. 334.

by the relation

$$\beta = \frac{1}{kr_0} \sum_{n=0}^{\infty} (-1)^n \frac{(2n+1) U_n(kr_0)}{U_n(kr_0) + i V_n(kr_0)}, \quad (166)$$

it then follows from (164) that, since $kr \gg 1$, $S_n(kr) + i C_n(kr)$ becomes equal to $i^{n+1} \cdot e^{-ikr}$ and $\cos \gamma$ becomes unity, one has for the reflection amplitude p_r due to the sphere:

$$p_r = \frac{c \sigma F \cdot w}{2 \lambda R^2} r_0 Z, \quad (167)$$

while the reflection amplitude produced by the rigid wall is given by

$$p_r^* = \frac{c \cdot \sigma \cdot F \cdot w}{4 \lambda R} \quad (168)$$

Therefore

$$\frac{p_r}{p_r^*} = \frac{2r_0}{R} Z. \quad (169)$$

A very simple relation for the reflection factor now results. With increasing kr_0 , Z approaches the value $\frac{1}{2}$ so that for the larger values of kr_0 one can with good approximation set the reflection factor equal to $\frac{1}{2}$. (169) therefore states:

The pressure amplitude reflected by a rigid sphere with the radius r_0 at a great distance R is (for the larger values of kr_0) given by r_0/R if the pressure amplitude reflected by an infinite wall placed at the same distance R is set equal to one.

To represent the reflection factor, the two components R and J are computed separately and plotted. The functions $U_n(kr)$ and $V_n(kr)$ necessary for this are easily found by (147) with the aid of the tables for $S_n(x)$ and $C(x)$. The result of the calculation is represented in Fig. 90.

If, furthermore, $R + iJ$ is drawn as a vector in the complex plane, one then has the phase $\chi(\text{tg} \chi = J/R)$ as a function of kr_0 . It turns out that the phase remains practically constant while the reflection factor increases decidedly ($kr_0 = 1, 2$) and later increases uniformly when the reflection factor remains constant (Fig. 91). For the general case ($\gamma \neq 0$), we define the disturbance factor $|\beta(kr_0, \gamma)|$ by

$$\beta(kr_0, \gamma) = \frac{1}{kr_0} \sum_{n=0}^{\infty} (-1)^n \frac{(2n+1) U_n(kr_0)}{U_n(kr_0) + i V_n(kr_0)} P_n(\cos \gamma) \quad (170)$$

and calculate the corresponding components for $kr_0 = 1, 2, \dots, 10$ and can then represent for every value of kr_0 the complete behavior of the disturbance factor as a function of γ (Figs. 92 to 99). It then turns out that for $\gamma = 180^\circ$ (i.e., the direction opposite to that of the sound source) $|\beta|$ increases more and more with kr_0 and for the larger values of kr_0 is very nearly determined by $\frac{1}{2} kr_0$.

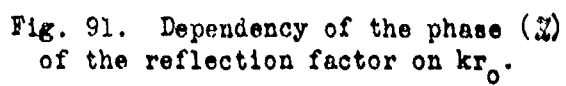
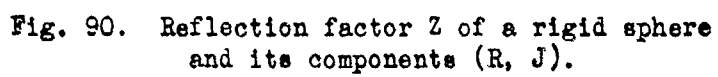


Fig. 92.

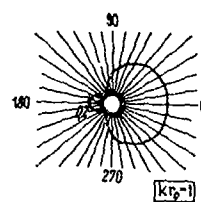


Fig. 93.

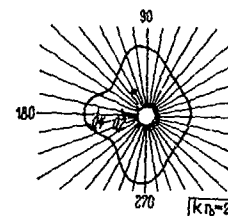


Fig. 94.

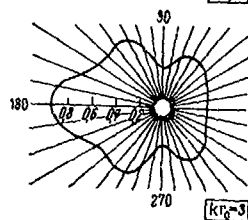


Fig. 95.

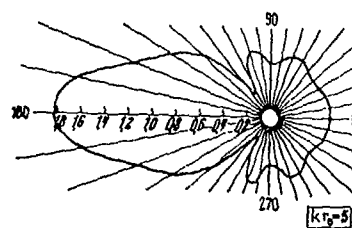
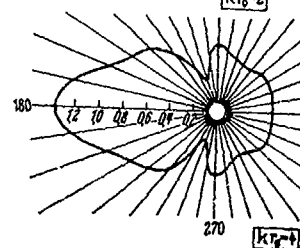


Fig. 96.

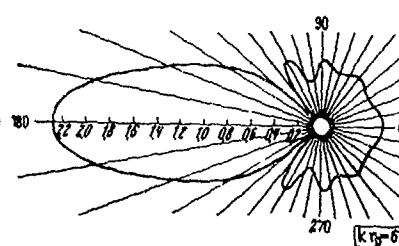


Fig. 97.

Figs. 92-97. The disturbance factor for $k_r = 1$ to $k_r = 6$.

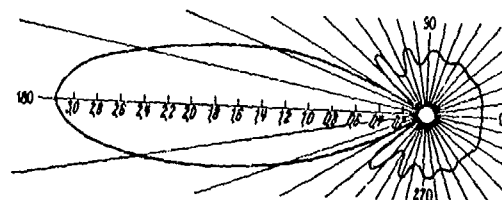


Fig. 98

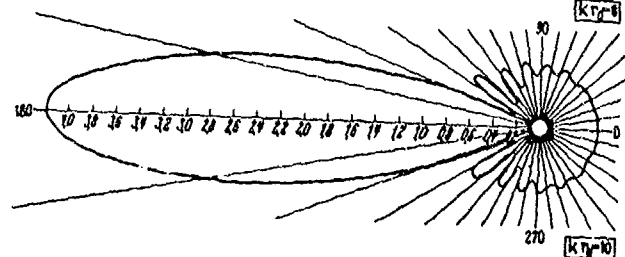


Fig. 99

Figs. 98-99. The disturbance factor for $k_r = 8$ and $k_r = 10$.

However, even for a direction opposite to that of the radiator, the disturbance amplitude is small compared to that of the undistorted field.

(c) The sound field in the neighborhood of the sphere

In the immediate neighborhood of the sphere we will have to expect a substantial distortion of the undistorted field. If we first inquire as to the behavior of the pressure amplitude on the line connecting the radiator with the center of the sphere on the side towards the radiator, then maxima and minima will appear here as they did in front of a rigid plane wall. As an example, we will investigate the case $kr_0 = 2$ when we calculate the pressure for the field points defined by $kr = 2, 3, \dots, 10$. If we set $kr = kr_0$ in (165), then due to the relation (from 129 and 147):

$$S_n(kr_0) V_n(kr_0) - C_n(kr_0) U_n(kr_0) = kr_0, \quad (170a)$$

it follows that

$$p = \frac{c \cdot \sigma}{2 R \lambda} F \cdot w e^{i(\omega t - kR + \pi/2)} \sum_{n=0}^{\infty} (2n+1) \frac{i^{n+1} P_n(\cos \gamma)}{U_n(kr_0) + i V_n(kr_0)}. \quad (171)$$

In accordance with the reciprocity law, this is in agreement with the previously discussed case where the radiator was assumed to be on the spherical surface and the field point was assumed to be at a great distance (Eq. 156).

For convergence reasons, it is better not to calculate the field composed of the original (undistorted) and the distorted field ($p = p_1 + p_2$) by (165) but to first calculate the distorted field p_2 by (164) and to add the undistorted field p_1 from (160).

Therefore, we first calculate the disturbance factor by (164) when we set $P_n(\cos \gamma) = 1$. Then

$$\begin{aligned} \beta(kr_0, kr, 0) &= \frac{1}{kr} \sum_{n=0}^{\infty} \frac{(2n+1) i^n U_n(kr_0)}{U_n(kr_0) + i V_n(kr_0)} [S_n(kr) + i C_n(kr)] \\ &= \sum A_n(kr) + i B_n(kr). \end{aligned} \quad (171a)$$

The quantities $A_n + i B_n$ for $kr_0 = 2$ and $kr = 2, 3, \dots, 10$ are given in the following table:

n	$A_n(kr) - iB_n(kr) = \frac{(2n-1)! U_n(2)}{U_n(2) + iV_n(2)} S_n(kr) - iC_n(kr)$									
	kr=2	kr=3	kr=4	kr=5	kr=6	kr=7	kr=8	kr=9	kr=10	
0	-0.1742 - 0.3483i	-0.1327 - 0.2231i	-0.1946 - 0.0067i	-0.0885 + 0.1281i	+0.0499 + 0.1198i	+0.1096 + 0.0195i	+0.0661 - 0.0714i	-0.0217 - 0.0838i	-0.0740 - 0.1043i	
2	-0.6193 - 0.2959i	-0.1884 - 0.3087i	-0.0581 - 0.2438i	-0.1684 - 0.0927i	-0.1448 + 0.0608i	-0.0322 + 0.1291i	+0.0747 + 0.0882i	+0.1018 - 0.0092i	+0.0451 - 0.0798i	
4	-0.1060 - 0.0607i	-0.0021 - 0.0014i	-0.0693 - 0.0030i	-0.0044 + 0.0046i	-0.0007 + 0.0047i	+0.0022 + 0.0032i	+0.0032 + 0.0005i	+0.0022 - 0.0018i	-0.0025i	
6	-0.0447		+0.0001							
$\sum_{n=0}^{\infty}$	-0.6916 - 0.6435i	-0.0339 - 0.5204i	-0.2569 - 0.2475i	-0.2613 + 0.0399i	-0.0956 + 0.1853i	+0.0796 + 0.1518i	+0.1440 + 0.0173i	+0.0823 - 0.0948i	-0.0289 - 0.1066i	
1	-0.0462 - 0.0347i	-0.0355 - 0.0077i	-0.0112 + 0.0242i	+0.0105 + 0.0183i	+0.0174 + 0.0015i	+0.0083 - 0.0116i	-0.0039 - 0.0124i	-0.0111 - 0.0032i	-0.0079 + 0.0068i	
3	-0.0270 - 0.2371i	-0.0408 - 0.1211i	+0.0571 - 0.0508i	+0.0555 + 0.0018i	+0.0319 - 0.0305i	-0.0017 - 0.0368i	-0.0255 - 0.0188i	-0.0288 + 0.0077i	-0.0087 + 0.0233i	
5	-0.0246i	-0.0029i	-0.0001 - 0.0009i	-0.0001 - 0.0004i	-0.0002 - 0.0002i	-0.0002	-0.0062 + 0.0001i	+0.0002i	+0.0001 + 0.0001i	
$\sum_{n=1}^{\infty}$	-0.0192 - 0.2986i	-0.0453 - 0.1259i	-0.0458 - 0.0741i	-0.0659 + 0.0197i	+0.0491 - 0.0292i	+0.0074 - 0.0484i	-0.0296 - 0.0311i	-0.0379 + 0.0047i	-0.0165 + 0.0302i	
$\sum_{n=0}^{\infty} - e^{-kr}$	-0.6724 - 0.3449i	-0.0392 - 0.4045i	-0.2111 - 0.1734i	+0.1954 + 0.0596i	-0.0465 + 0.1561i	+0.0870 + 0.1034i	+0.1144 - 0.0138i	+0.0444 - 0.0901i	-0.0454 - 0.0764i	
$\sum_{n=0}^{\infty} - e^{-kr} - e^{-kr}$	+0.4162 - 0.9493i	+0.3940 - 0.1411i	-0.6536 + 0.7368i	-0.2837 + 0.9589i	-0.9602 + 0.2794i	-0.7539 - 0.6570i	+0.1455 - 0.9894i	+0.9111 - 0.4121i	+0.8391 + 0.5440i	
$\sum_{n=0}^{\infty} - e^{-kr} - e^{-kr} - e^{-kr}$	-1.0886 - 1.2542i	-1.0292 - 0.5456i	+0.4425 + 0.8834i	-0.4791 + 1.0186i	-1.0067 + 0.4355i	-0.6669 - 0.5536i	+0.2599 - 1.0032i	+0.9565 - 0.5022i	+0.7937 + 0.4676i	
$\sum_{n=0}^{\infty} - e^{-kr} - e^{-kr} - e^{-kr} - e^{-kr}$	+1.660	+1.165	+0.732	+1.110	+1.096	+0.867	+1.036	+1.079	+0.926	

To facilitate later calculations, the sums \sum_1 for even n and \sum_2 for odd n were calculated separately.

The values

$$p = |\sum_1 + \sum_2 - e^{-ikr}| \quad (171b)$$

then give the pressure amplitudes in front of the rigid sphere in the direction of the radiator. Here the undistorted pressure amplitude of the radiator is set equal to unity. We see that the pressure amplitudes in front of the rigid sphere vary in a manner similar to that of

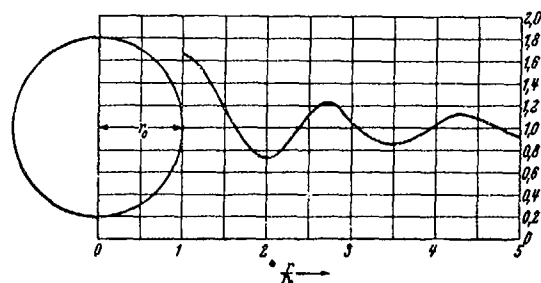


Fig. 100. Reflection on a rigid sphere ($kr_0 = 2$).

the reflection on a plane wall except that the variations with increasing distance from the sphere decrease very rapidly. (See Fig. 100.)

The complete calculation of the distorted sound field is then accomplished with the aid of spherical harmonic tables from

$$\mathcal{B}(kr_0, kr, \gamma) - e^{-ikr \cos \gamma} = \sum (A_n + iB_n) P_n(\cos \gamma) = R + iJ. \quad (171c)$$

The components R and J are first calculated as a function of γ for $kr = 2, 3, 4, \dots, 10$ and are plotted in Figures 101 to 104. The quantities

$$\sqrt{R^2 + J^2}$$

are found from this and their variations about the undistorted value one are represented in Figure 105. Here it is seen that the magnitude of the variations decreases with increasing kr while the number of the variations increases. If the field points given by $kr = 2, 3, 4, \dots, 10$ are numbered corresponding to the values in Figure 105, the curves of constant pressure in the neighborhood of the sphere can be drawn by interpolation. The result is given in Figure 106. The greatest value (1.66) lies on the surface of the sphere opposite the sound source ($\gamma = 0^\circ$). The smallest value (0.66) likewise lies on the sphere ($\gamma = 135^\circ$). For field points at a distance $r > 5r_0$, the difference between the distorted and undistorted amplitudes remains below 10%.

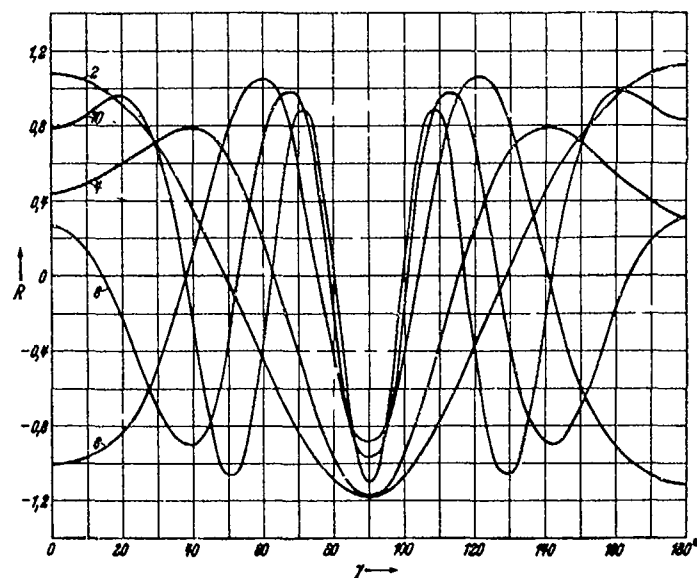


Fig. 101. The components R for
 $kr = 2, 4, 6, 8, 10$.

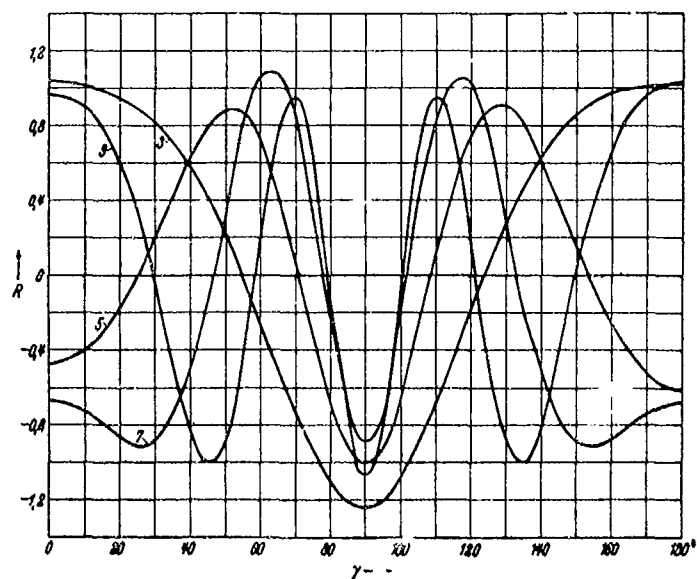


Fig. 102. The components R for
 $kr = 3, 5, 7, 9$.

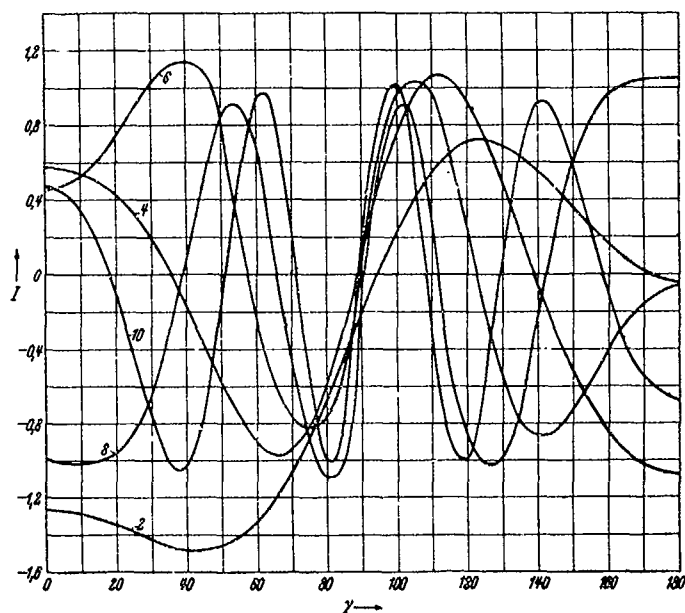


Fig. 103. The components J for
 $kr = 2, 4, 6, 8, 10$.

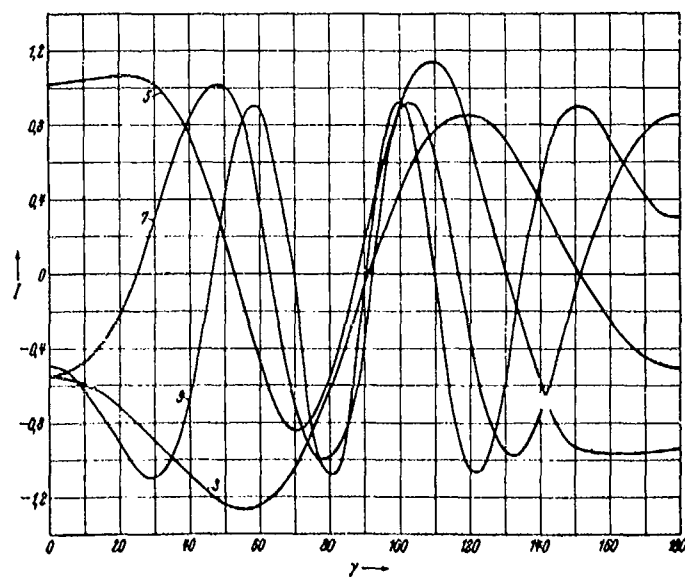


Fig. 104. The components J for
 $kr = 3, 5, 7, 9$.

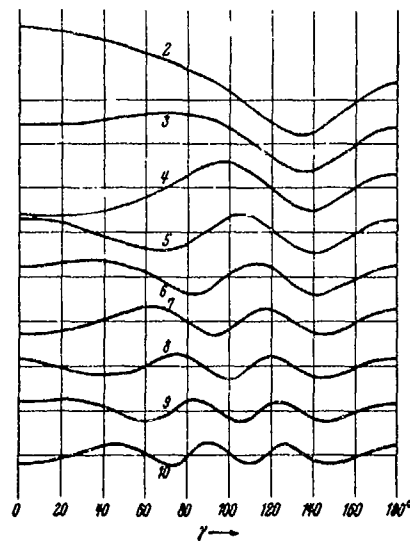


Fig. 105. The deviation of the distorted pressure amplitude in the neighborhood of the sphere (radius r_0) from the undistorted amplitude for the field point (r, γ) $kr_0 = 2$; $kr = 2, 3, 4 \dots 10$.

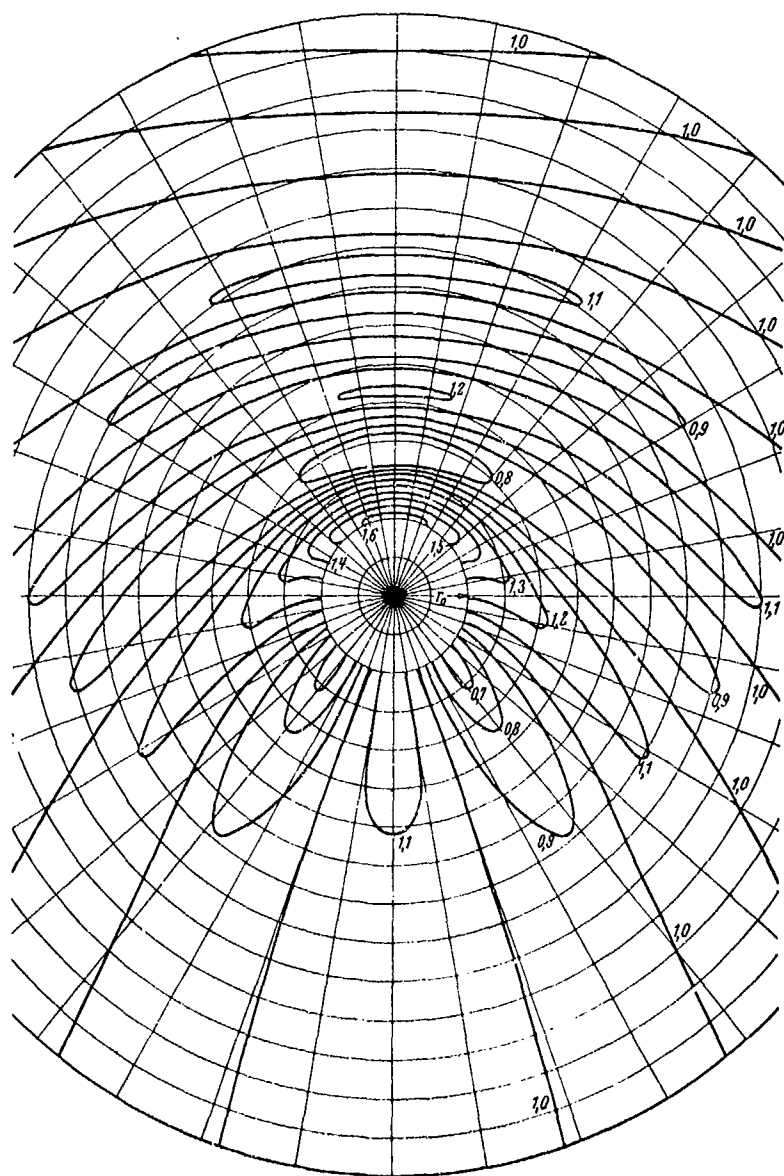


Fig. 106. The curves of constant sound pressure in the neighborhood of a rigid sphere with the radius r_0 when the sound source is at a great distance and $kr_0 = 2$.

$$\sigma_{2n}(x) = (-1)^n \int_0^x S_{2n}(x) dx$$

x	$\sigma_0(x)$	$\sigma_2(x)$	$\sigma_4(x)$	$\sigma_6(x)$
1	$4,5970 \cdot 10^{-1}$	$-1,5889 \cdot 10^{-2}$	$1,7045 \cdot 10^{-4}$	$-9,0064 \cdot 10^{-7}$
1,25	$6,8468 \cdot 10^{-1}$	$-3,776 \cdot 10^{-2}$	$6,3780 \cdot 10^{-4}$	$-5,2881 \cdot 10^{-6}$
1,5	$9,2926 \cdot 10^{-1}$	$-7,575 \cdot 10^{-2}$	$1,8601 \cdot 10^{-3}$	$-2,2323 \cdot 10^{-5}$
1,75	1,1782	$-1,3492 \cdot 10^{-1}$	$4,5611 \cdot 10^{-3}$	$-7,4965 \cdot 10^{-5}$
2	1,4161	$-2,1991 \cdot 10^{-1}$	$9,8396 \cdot 10^{-3}$	$-2,1274 \cdot 10^{-4}$
2,25	1,6282	$-3,3440 \cdot 10^{-1}$	$1,9227 \cdot 10^{-2}$	$-5,3045 \cdot 10^{-4}$
2,5	1,8011	$-4,8070 \cdot 10^{-1}$	$3,4718 \cdot 10^{-2}$	$-1,1934 \cdot 10^{-3}$
2,75	1,9243	$-6,5934 \cdot 10^{-1}$	$5,8749 \cdot 10^{-2}$	$-2,4688 \cdot 10^{-3}$
3	1,9900	$-8,6889 \cdot 10^{-1}$	$9,4155 \cdot 10^{-2}$	$-4,7627 \cdot 10^{-3}$
3,25	1,9641	-1,1057	$1,4412 \cdot 10^{-1}$	$-8,6589 \cdot 10^{-3}$
3,5	1,9365	-1,3642	$2,1165 \cdot 10^{-1}$	$-1,4959 \cdot 10^{-2}$
3,75	1,8208	-1,6367	$3,0013 \cdot 10^{-1}$	$-2,4716 \cdot 10^{-2}$
4	1,6536	-1,9140	$4,1236 \cdot 10^{-1}$	$-3,9266 \cdot 10^{-2}$
4,25	1,4481	-2,1857	$5,5056 \cdot 10^{-1}$	$-6,0232 \cdot 10^{-2}$
4,5	1,2108	-2,4409	$7,1629 \cdot 10^{-1}$	$-8,9529 \cdot 10^{-2}$
4,75	$9,6240 \cdot 10^{-1}$	-2,6687	$9,0998 \cdot 10^{-1}$	$-1,2933 \cdot 10^{-1}$
5	$7,1634 \cdot 10^{-1}$	-2,8590	1,1331	$-1,8231 \cdot 10^{-1}$
5,25	$4,8791 \cdot 10^{-1}$	-3,0029	1,3765	$-2,5010 \cdot 10^{-1}$
5,5	$2,9133 \cdot 10^{-1}$	-3,0935	1,6444	$-3,3609 \cdot 10^{-1}$
5,75	$1,3881 \cdot 10^{-1}$	-3,1264	1,9267	$-4,4243 \cdot 10^{-1}$
6	$3,9829 \cdot 10^{-2}$	-3,0999	2,2196	$-5,7126 \cdot 10^{-1}$
6,25	$0,0506 \cdot 10^{-2}$	-3,0154	2,5144	$-7,2433 \cdot 10^{-1}$
6,5	$2,3414 \cdot 10^{-3}$	-2,8873	2,8026	$-9,0268 \cdot 10^{-1}$
6,75	$1,0700 \cdot 10^{-1}$	-2,6930	3,0750	-1,1068
7	$2,4608 \cdot 10^{-1}$	-2,4580	3,3228	-1,3360
7,25	$4,3208 \cdot 10^{-1}$	-2,2273	3,5368	-1,5888
7,5	$6,5337 \cdot 10^{-1}$	-1,9714	3,7089	-1,8622
7,75	$8,9621 \cdot 10^{-1}$	-1,7188	3,8322	-2,1526
8	1,1455	-1,4835	3,9019	-2,4548
8,25	1,3858	-1,2788	3,9154	-2,7624
8,5	1,6020	-1,1162	3,8731	-3,0696
8,75	1,7808	-1,0050	3,7732	-3,3678
9	1,9111	$-9,5150 \cdot 10^{-1}$	3,6256	-3,6483
9,25	1,9848	$-9,5884 \cdot 10^{-1}$	3,4323	-3,9043
9,5	1,9972	-1,0255	3,2048	-4,1232
9,75	1,9476	-1,1507	2,9517	-4,3118
10	1,8391	-1,3241	2,6878	-4,4467

$$\sigma_n(x) = (-1)^n \int_0^x S_n(x) dx$$

x	$\sigma_0(x)$	$\sigma_{10}(x)$	$\sigma_{11}(x)$	$\sigma_{14}(x)$
1	$2,8390 \cdot 10^{-9}$	$-5,9490 \cdot 10^{-12}$	$8,8897 \cdot 10^{-15}$	$-9,9527 \cdot 10^{-18}$
1,25	$2,6112 \cdot 10^{-8}$	$-8,5647 \cdot 10^{-11}$	$2,0025 \cdot 10^{-13}$	$-3,5068 \cdot 10^{-16}$
1,5	$1,5927 \cdot 10^{-7}$	$-7,5405 \cdot 10^{-10}$	$2,5431 \cdot 10^{-12}$	$-6,4210 \cdot 10^{-15}$
1,75	$7,3086 \cdot 10^{-7}$	$-4,7224 \cdot 10^{-9}$	$2,1722 \cdot 10^{-11}$	$-7,4763 \cdot 10^{-14}$
2	$2,7213 \cdot 10^{-6}$	$-2,3039 \cdot 10^{-8}$	$1,3872 \cdot 10^{-10}$	$-6,2475 \cdot 10^{-13}$
2,25	$8,6320 \cdot 10^{-6}$	$-9,2821 \cdot 10^{-8}$	$7,0921 \cdot 10^{-10}$	$-4,0506 \cdot 10^{-12}$
2,5	$2,4115 \cdot 10^{-5}$	$-3,2141 \cdot 10^{-7}$	$3,0408 \cdot 10^{-9}$	$-2,1489 \cdot 10^{-11}$
2,75	$6,0754 \cdot 10^{-5}$	$-9,8416 \cdot 10^{-7}$	$1,1303 \cdot 10^{-8}$	$-9,6890 \cdot 10^{-11}$
3	$1,4047 \cdot 10^{-4}$	$-2,7214 \cdot 10^{-6}$	$3,7328 \cdot 10^{-8}$	$-3,8185 \cdot 10^{-10}$
3,25	$3,0207 \cdot 10^{-4}$	$-6,9047 \cdot 10^{-6}$	$1,1159 \cdot 10^{-7}$	$-1,3437 \cdot 10^{-9}$
3,5	$6,1037 \cdot 10^{-4}$	$-1,6275 \cdot 10^{-5}$	$3,0635 \cdot 10^{-7}$	$-4,2920 \cdot 10^{-9}$
3,75	$1,1684 \cdot 10^{-3}$	$-3,5991 \cdot 10^{-5}$	$7,8125 \cdot 10^{-7}$	$-1,2609 \cdot 10^{-8}$
4	$2,1331 \cdot 10^{-3}$	$-7,5265 \cdot 10^{-5}$	$1,8679 \cdot 10^{-6}$	$-3,4430 \cdot 10^{-8}$
4,25	$3,7335 \cdot 10^{-3}$	$-1,4980 \cdot 10^{-4}$	$4,2194 \cdot 10^{-6}$	$-8,8147 \cdot 10^{-8}$
4,5	$6,2934 \cdot 10^{-3}$	$-2,8521 \cdot 10^{-4}$	$9,0598 \cdot 10^{-6}$	$-2,1309 \cdot 10^{-7}$
4,75	$1,0254 \cdot 10^{-2}$	$-5,2225 \cdot 10^{-4}$	$1,8589 \cdot 10^{-5}$	$-4,8938 \cdot 10^{-7}$
5	$1,6171 \cdot 10^{-2}$	$-9,2237 \cdot 10^{-4}$	$3,8609 \cdot 10^{-5}$	$-1,0731 \cdot 10^{-6}$
5,25	$2,4890 \cdot 10^{-2}$	$-1,5769 \cdot 10^{-3}$	$6,9466 \cdot 10^{-5}$	$-2,2563 \cdot 10^{-6}$
5,5	$3,7260 \cdot 10^{-2}$	$-2,6104 \cdot 10^{-3}$	$1,2741 \cdot 10^{-4}$	$-4,5663 \cdot 10^{-6}$
5,75	$5,4464 \cdot 10^{-2}$	$-4,2244 \cdot 10^{-3}$	$2,2652 \cdot 10^{-4}$	$-8,9231 \cdot 10^{-6}$
6	$7,7869 \cdot 10^{-2}$	$-6,6497 \cdot 10^{-3}$	$3,9134 \cdot 10^{-4}$	$-1,6886 \cdot 10^{-5}$
6,25	$1,0906 \cdot 10^{-1}$	$-1,224 \cdot 10^{-2}$	$6,5836 \cdot 10^{-4}$	$-3,1017 \cdot 10^{-5}$
6,5	$1,4981 \cdot 10^{-1}$	$-1,6379 \cdot 10^{-2}$	$1,0805 \cdot 10^{-3}$	$-5,5423 \cdot 10^{-5}$
6,75	$2,0209 \cdot 10^{-1}$	$-2,2666 \cdot 10^{-2}$	$1,7332 \cdot 10^{-3}$	$-9,6522 \cdot 10^{-5}$
7	$2,6797 \cdot 10^{-1}$	$-3,2769 \cdot 10^{-2}$	$2,7207 \cdot 10^{-3}$	$-1,6413 \cdot 10^{-4}$
7,25	$3,4960 \cdot 10^{-1}$	$-4,6527 \cdot 10^{-2}$	$4,1857 \cdot 10^{-3}$	$-2,7290 \cdot 10^{-4}$
7,5	$4,4908 \cdot 10^{-1}$	$-6,4934 \cdot 10^{-2}$	$6,3180 \cdot 10^{-3}$	$-4,4431 \cdot 10^{-4}$
7,75	$5,6843 \cdot 10^{-1}$	$-8,9182 \cdot 10^{-2}$	$9,3671 \cdot 10^{-3}$	$-7,0914 \cdot 10^{-4}$
8	$7,0942 \cdot 10^{-1}$	$-1,2077 \cdot 10^{-1}$	$1,3656 \cdot 10^{-2}$	$-1,1109 \cdot 10^{-3}$
8,25	$8,7332 \cdot 10^{-1}$	$-1,6073 \cdot 10^{-1}$	$1,9587 \cdot 10^{-2}$	$-1,7098 \cdot 10^{-3}$
8,5	$1,0613$	$-2,1123 \cdot 10^{-1}$	$2,7667 \cdot 10^{-2}$	$-2,5879 \cdot 10^{-3}$
8,75	$1,2735$	$-2,7391 \cdot 10^{-1}$	$3,8516 \cdot 10^{-2}$	$-3,8543 \cdot 10^{-3}$
9	$1,5095$	$-3,5062 \cdot 10^{-1}$	$5,2873 \cdot 10^{-2}$	$-5,6537 \cdot 10^{-3}$
9,25	$1,7680$	$-4,4325 \cdot 10^{-1}$	$7,1618 \cdot 10^{-2}$	$-8,1741 \cdot 10^{-3}$
9,5	$2,0467$	$-5,5367 \cdot 10^{-1}$	$9,6779 \cdot 10^{-2}$	$-1,1658 \cdot 10^{-2}$
9,75	$2,3427$	$-6,8329 \cdot 10^{-1}$	$1,2649 \cdot 10^{-1}$	$-1,8405 \cdot 10^{-2}$
10	$2,6520$	$-8,3321 \cdot 10^{-1}$	$1,6514 \cdot 10^{-1}$	$-2,2792 \cdot 10^{-2}$

$$\sigma_{2n}(x) = (-1)^n \int_0^x S_{2n}(x) dx$$

x	$\sigma_{10}(x)$	$\sigma_{11}(x)$	$\sigma_{12}(x)$
1	$8,6608 \cdot 10^{-21}$	$-6,0262 \cdot 10^{-24}$	$3,4296 \cdot 10^{-27}$
1,25	$4,7721 \cdot 10^{-19}$	$-5,1906 \cdot 10^{-22}$	$4,6183 \cdot 10^{-25}$
1,5	$1,2596 \cdot 10^{-17}$	$-1,9749 \cdot 10^{-20}$	$2,5326 \cdot 10^{-23}$
1,75	$1,9986 \cdot 10^{-16}$	$-4,2694 \cdot 10^{-19}$	$7,4565 \cdot 10^{-22}$
2	$2,1844 \cdot 10^{-15}$	$-6,1016 \cdot 10^{-18}$	$1,3932 \cdot 10^{-20}$
2,25	$1,7952 \cdot 10^{-14}$	$-6,3555 \cdot 10^{-17}$	$1,8384 \cdot 10^{-19}$
2,5	$1,1779 \cdot 10^{-13}$	$-5,1564 \cdot 10^{-16}$	$1,8433 \cdot 10^{-18}$
2,75	$6,4390 \cdot 10^{-13}$	$-3,4152 \cdot 10^{-15}$	$1,4795 \cdot 10^{-17}$
3	$3,0264 \cdot 10^{-12}$	$-1,9138 \cdot 10^{-14}$	$9,8812 \cdot 10^{-17}$
3,25	$1,2528 \cdot 10^{-11}$	$-9,3150 \cdot 10^{-14}$	$5,6536 \cdot 10^{-16}$
3,5	$4,6530 \cdot 10^{-11}$	$-4,0206 \cdot 10^{-13}$	$2,3348 \cdot 10^{-15}$
3,75	$1,5735 \cdot 10^{-10}$	$-1,5643 \cdot 10^{-12}$	$1,2685 \cdot 10^{-14}$
4	$4,9031 \cdot 10^{-10}$	$-5,5593 \cdot 10^{-12}$	$5,1385 \cdot 10^{-14}$
4,25	$1,4215 \cdot 10^{-9}$	$-1,8242 \cdot 10^{-11}$	$1,9075 \cdot 10^{-13}$
4,5	$3,8658 \cdot 10^{-9}$	$-5,5765 \cdot 10^{-11}$	$6,5529 \cdot 10^{-13}$
4,75	$9,9271 \cdot 10^{-9}$	$-1,6002 \cdot 10^{-10}$	$2,1000 \cdot 10^{-12}$
5	$2,4210 \cdot 10^{-8}$	$-4,3374 \cdot 10^{-10}$	$6,3229 \cdot 10^{-12}$
5,25	$5,6349 \cdot 10^{-8}$	$-1,1165 \cdot 10^{-9}$	$1,7992 \cdot 10^{-11}$
5,5	$1,2568 \cdot 10^{-7}$	$-2,7423 \cdot 10^{-9}$	$4,8637 \cdot 10^{-11}$
5,75	$2,5943 \cdot 10^{-7}$	$-6,4534 \cdot 10^{-9}$	$1,2545 \cdot 10^{-10}$
6	$5,5812 \cdot 10^{-7}$	$-1,4601 \cdot 10^{-8}$	$3,2001 \cdot 10^{-10}$
6,25	$1,1178 \cdot 10^{-6}$	$-3,1849 \cdot 10^{-8}$	$7,3612 \cdot 10^{-10}$
6,5	$2,1713 \cdot 10^{-6}$	$-6,7192 \cdot 10^{-8}$	$1,6853 \cdot 10^{-9}$
6,75	$4,1000 \cdot 10^{-6}$	$-1,3741 \cdot 10^{-7}$	$3,7296 \cdot 10^{-9}$
7	$7,5395 \cdot 10^{-6}$	$-2,7294 \cdot 10^{-7}$	$7,9970 \cdot 10^{-9}$
7,25	$1,3526 \cdot 10^{-5}$	$-5,2771 \cdot 10^{-7}$	$1,6648 \cdot 10^{-8}$
7,5	$2,3708 \cdot 10^{-5}$	$-9,9447 \cdot 10^{-7}$	$3,3716 \cdot 10^{-8}$
7,75	$4,0662 \cdot 10^{-5}$	$-1,8308 \cdot 10^{-6}$	$6,6530 \cdot 10^{-8}$
8	$6,8327 \cdot 10^{-5}$	$-3,2951 \cdot 10^{-6}$	$1,2814 \cdot 10^{-7}$
8,25	$1,1260 \cdot 10^{-4}$	$-5,8063 \cdot 10^{-6}$	$2,4118 \cdot 10^{-7}$
8,5	$1,8218 \cdot 10^{-4}$	$-1,0029 \cdot 10^{-5}$	$4,4324 \cdot 10^{-7}$
8,75	$2,8969 \cdot 10^{-4}$	$-1,6998 \cdot 10^{-5}$	$8,0174 \cdot 10^{-7}$
9	$4,5303 \cdot 10^{-4}$	$-2,8298 \cdot 10^{-5}$	$1,4188 \cdot 10^{-6}$
9,25	$6,9741 \cdot 10^{-4}$	$-4,6307 \cdot 10^{-5}$	$2,4653 \cdot 10^{-6}$
9,5	$1,0577 \cdot 10^{-3}$	$-7,4567 \cdot 10^{-5}$	$4,2097 \cdot 10^{-6}$
9,75	$1,5810 \cdot 10^{-3}$	$-1,1825 \cdot 10^{-4}$	$7,0671 \cdot 10^{-6}$
10	$2,3316 \cdot 10^{-3}$	$-1,8457 \cdot 10^{-4}$	$1,1974 \cdot 10^{-5}$

$$\zeta_{2n}(x) = (-1)^n \int_0^x C_{2n}(x) dx$$

x	$\zeta_0(x)$	$\zeta_2(x)$	$\zeta_4(x)$	$\zeta_6(x)$
1	$+8,4147 \cdot 10^{-1}$	$+2,4624$	$-4,2118 \cdot 10^{-1}$	$+2,2493 \cdot 10^{-2}$
1,25	$+9,4899 \cdot 10^{-1}$	$+1,5168$	$-2,3436 \cdot 10^{-1}$	$+7,7199 \cdot 10^{-2}$
1,5	$+9,9750 \cdot 10^{-1}$	$+1,1390$	$-1,4781 \cdot 10^{-1}$	$+3,2872 \cdot 10^{-2}$
1,75	$+9,8399 \cdot 10^{-1}$	$+6,7842 \cdot 10^{-1}$	$-1,0118 \cdot 10^{-1}$	$+1,6310 \cdot 10^{-2}$
2	$+9,0930 \cdot 10^{-1}$	$+2,8508 \cdot 10^{-1}$	$-7,3071$	$+9,0571 \cdot 10^{-2}$
2,25	$+7,7807 \cdot 10^{-1}$	$-5,9492 \cdot 10^{-2}$	$-5,4629$	$+5,4977 \cdot 10^{-2}$
2,5	$+5,9847 \cdot 10^{-1}$	$-3,6290 \cdot 10^{-1}$	$-4,1630$	$+3,5791 \cdot 10^{-2}$
2,75	$+3,8166 \cdot 10^{-1}$	$-6,2687 \cdot 10^{-2}$	$-3,1903$	$+2,4641 \cdot 10^{-2}$
3	$+1,4112 \cdot 10^{-1}$	$-8,4887 \cdot 10^{-2}$	$-2,4243$	$+1,7740 \cdot 10^{-2}$
3,25	$-1,0820 \cdot 10^{-1}$	$-1,0259$	$-1,7950$	$+1,3230 \cdot 10^{-2}$
3,5	$-3,5078 \cdot 10^{-1}$	$-1,1535$	$-1,2597$	$+1,0140 \cdot 10^{-2}$
3,75	$-5,7158 \cdot 10^{-1}$	$-1,2280$	$-7,9256 \cdot 10^{-2}$	$+7,9299$
4	$-7,5680 \cdot 10^{-1}$	$-1,2470$	$-3,7794 \cdot 10^{-2}$	$+6,2863$
4,25	$-8,9499 \cdot 10^{-1}$	$-1,2099$	$-6,99 \cdot 10^{-3}$	$+5,0190$
4,5	$-9,7753 \cdot 10^{-1}$	$-1,0181$	$+3,2456 \cdot 10^{-2}$	$+4,0091$
4,75	$-9,9929 \cdot 10^{-1}$	$-9,7554 \cdot 10^{-2}$	$+6,1775 \cdot 10^{-2}$	$+3,1796$
5	$-9,5892 \cdot 10^{-1}$	$-7,8873 \cdot 10^{-2}$	$+8,7147 \cdot 10^{-2}$	$+2,4794$
5,25	$-8,5893 \cdot 10^{-1}$	$-5,6631 \cdot 10^{-2}$	$+1,0833$	$+1,8743$
5,5	$-7,0554 \cdot 10^{-1}$	$-3,1869 \cdot 10^{-2}$	$+1,2502$	$+1,3414$
5,75	$-5,0828 \cdot 10^{-1}$	$-1,5896 \cdot 10^{-2}$	$+1,3690$	$+8,6521 \cdot 10^{-2}$
6	$-2,7841 \cdot 10^{-1}$	$+2,0067 \cdot 10^{-2}$	$+1,4369$	$+4,3590 \cdot 10^{-2}$
6,25	$-3,3177 \cdot 10^{-2}$	$+4,4655 \cdot 10^{-2}$	$+1,4524$	$+4,7489 \cdot 10^{-2}$
6,5	$+2,1512 \cdot 10^{-2}$	$+6,6586 \cdot 10^{-2}$	$+1,4149$	$-3,0500 \cdot 10^{-2}$
6,75	$+4,5005 \cdot 10^{-2}$	$+8,4694 \cdot 10^{-2}$	$+1,3257$	$-6,1638 \cdot 10^{-2}$
7	$+6,5009 \cdot 10^{-2}$	$+9,8009 \cdot 10^{-2}$	$+1,1878$	$-8,9189 \cdot 10^{-2}$
7,25	$+8,2308 \cdot 10^{-2}$	$+1,0581$	$+1,0062$	$-1,1276$
7,5	$+9,3798 \cdot 10^{-2}$	$+1,0766$	$+7,8777 \cdot 10^{-2}$	$-1,3211$
7,75	$+9,9405 \cdot 10^{-2}$	$+1,0348$	$+5,4163 \cdot 10^{-2}$	$-1,4697$
8	$+9,8936 \cdot 10^{-2}$	$+9,3482 \cdot 10^{-2}$	$+2,7643 \cdot 10^{-2}$	$-1,5707$
8,25	$+9,2260 \cdot 10^{-2}$	$+7,8233 \cdot 10^{-2}$	$+4,64 \cdot 10^{-3}$	$-1,6223$
8,5	$+7,9849 \cdot 10^{-2}$	$+5,8601 \cdot 10^{-2}$	$-2,6226 \cdot 10^{-2}$	$-1,6232$
8,75	$+6,2472 \cdot 10^{-2}$	$+3,5701 \cdot 10^{-2}$	$-5,1247 \cdot 10^{-2}$	$-1,5735$
9	$+4,1212 \cdot 10^{-2}$	$+1,0841 \cdot 10^{-2}$	$-7,3459 \cdot 10^{-2}$	$-1,4746$
9,25	$+1,7390 \cdot 10^{-2}$	$-1,4549 \cdot 10^{-2}$	$-9,1830 \cdot 10^{-2}$	$-1,3293$
9,5	$-7,5152 \cdot 10^{-3}$	$-3,9003 \cdot 10^{-2}$	$-1,0550$	$-1,1422$
9,75	$-3,1952 \cdot 10^{-3}$	$-1,1109 \cdot 10^{-2}$	$-1,1380$	$-9,1915 \cdot 10^{-2}$
10	$-5,4402 \cdot 10^{-4}$	$-7,9575 \cdot 10^{-3}$	$-1,1633$	$-6,6835 \cdot 10^{-2}$

$$\zeta_{2n}(x) = (-1)^n \int_0^x C_{2n}(x) dx$$

x	$\zeta_0(x)$	$\zeta_2(x)$	$\zeta_4(x)$	$\zeta_6(x)$
1	$-3,0354 \cdot 10^{+5}$	$+7,5261 \cdot 10^{+7}$	$-2,9522 \cdot 10^{+10}$	$+1,0784 \cdot 10^{+13}$
1,25	$-6,5399 \cdot 10^{+4}$	$+1,0297 \cdot 10^{+7}$	$-2,5745 \cdot 10^{+9}$	$+9,3415 \cdot 10^{+11}$
1,5	$-1,8869 \cdot 10^{+4}$	$+2,0434 \cdot 10^{+6}$	$-3,5286 \cdot 10^{+8}$	$+8,8621 \cdot 10^{+10}$
1,75	$-6,6759 \cdot 10^{+3}$	$+5,2483 \cdot 10^{+5}$	$-6,6184 \cdot 10^{+7}$	$+1,2165 \cdot 10^{+10}$
2	$-2,7480 \cdot 10^{+3}$	$+1,6303 \cdot 10^{+5}$	$-1,5625 \cdot 10^{+7}$	$+2,1887 \cdot 10^{+9}$
2,25	$-1,2724 \cdot 10^{+3}$	$+5,8628 \cdot 10^{+4}$	$-4,4020 \cdot 10^{+6}$	$+4,8465 \cdot 10^{+8}$
2,5	$-6,4771 \cdot 10^{+2}$	$+2,3692 \cdot 10^{+4}$	$-1,4268 \cdot 10^{+6}$	$+1,2649 \cdot 10^{+8}$
2,75	$-3,5659 \cdot 10^{+2}$	$+1,0534 \cdot 10^{+4}$	$-5,1846 \cdot 10^{+5}$	$+3,7726 \cdot 10^{+7}$
3	$-2,0976 \cdot 10^{+2}$	$+5,0730 \cdot 10^{+3}$	$-2,0711 \cdot 10^{+5}$	$+1,2571 \cdot 10^{+7}$
3,25	$-1,3062 \cdot 10^{+2}$	$+2,6156 \cdot 10^{+3}$	$-8,9675 \cdot 10^{+4}$	$+4,5995 \cdot 10^{+6}$
3,5	$-8,5442 \cdot 10^{+1}$	$+1,4308 \cdot 10^{+3}$	$-4,1608 \cdot 10^{+4}$	$+1,8233 \cdot 10^{+6}$
3,75	$-5,8347 \cdot 10^{+1}$	$+8,2447 \cdot 10^{+2}$	$-2,0506 \cdot 10^{+4}$	$+7,7485 \cdot 10^{+5}$
4	$-4,1365 \cdot 10^{+1}$	$+4,9763 \cdot 10^{+2}$	$-1,0657 \cdot 10^{+4}$	$+3,4999 \cdot 10^{+5}$
4,25	$-3,0295 \cdot 10^{+1}$	$+3,1312 \cdot 10^{+2}$	$-5,8075 \cdot 10^{+3}$	$+1,6687 \cdot 10^{+5}$
4,5	$-2,2817 \cdot 10^{+1}$	$+2,0460 \cdot 10^{+2}$	$-3,3024 \cdot 10^{+3}$	$+8,3497 \cdot 10^{+4}$
4,75	$-1,7597 \cdot 10^{+1}$	$+1,3836 \cdot 10^{+2}$	$-1,9518 \cdot 10^{+3}$	$+4,3637 \cdot 10^{+4}$
5	$-1,3841 \cdot 10^{+1}$	$+9,6546 \cdot 10^{+1}$	$-1,1654 \cdot 10^{+3}$	$+2,3724 \cdot 10^{+4}$
5,25	$-1,1061 \cdot 10^{+1}$	$+6,9320 \cdot 10^{+1}$	$-7,5630 \cdot 10^{+2}$	$+1,3371 \cdot 10^{+4}$
5,5	$-8,9456$	$+5,1082 \cdot 10^{+1}$	$-4,9318 \cdot 10^{+2}$	$+7,7908 \cdot 10^{+3}$
5,75	$-7,2947$	$+3,8536 \cdot 10^{+1}$	$-3,3080 \cdot 10^{+2}$	$+4,6806 \cdot 10^{+3}$
6	$-5,9738$	$+2,9689 \cdot 10^{+1}$	$-2,2759 \cdot 10^{+2}$	$+2,8934 \cdot 10^{+3}$
6,25	$-4,8918$	$+2,3299 \cdot 10^{+1}$	$-1,6079 \cdot 10^{+2}$	$+1,8370 \cdot 10^{+3}$
6,5	$-3,9857$	$+1,8588 \cdot 10^{+1}$	$-1,1615 \cdot 10^{+2}$	$+1,1959 \cdot 10^{+3}$
6,75	$-3,2109$	$+1,5031 \cdot 10^{+1}$	$-8,5730 \cdot 10^{+1}$	$+7,9717 \cdot 10^{+2}$
7	$-2,5361$	$+1,2294 \cdot 10^{+1}$	$-6,4568 \cdot 10^{+1}$	$+5,4343 \cdot 10^{+2}$
7,25	$-1,9390$	$+1,0143 \cdot 10^{+1}$	$-4,9548 \cdot 10^{+1}$	$+3,7843 \cdot 10^{+2}$
7,5	$-1,4037$	$+8,4194$	$-3,8399 \cdot 10^{+1}$	$+2,6893 \cdot 10^{+2}$
7,75	$-9,1932 \cdot 10^{-1}$	$+7,0128$	$-3,0674 \cdot 10^{+1}$	$+1,9485 \cdot 10^{+2}$
8	$-4,7857 \cdot 10^{-1}$	$+5,8421$	$-2,4661 \cdot 10^{+1}$	$+1,4376 \cdot 10^{+2}$
8,25	$-7,665 \cdot 10^{-2}$	$+4,8507$	$-2,0087 \cdot 10^{+1}$	$+1,0799 \cdot 10^{+2}$
8,5	$+2,8840 \cdot 10^{-1}$	$+3,9971$	$-1,6529 \cdot 10^{+1}$	$+8,2461 \cdot 10^{+1}$
8,75	$+6,1739 \cdot 10^{-1}$	$+3,2503$	$-1,3726 \cdot 10^{+1}$	$+6,3981 \cdot 10^{+1}$
9	$+9,0970 \cdot 10^{-1}$	$+2,5877$	$-1,1479 \cdot 10^{+1}$	$+5,0346 \cdot 10^{+1}$
9,25	$+1,1638$	$+1,9934$	$-9,6504$	$+4,0173 \cdot 10^{+1}$
9,5	$+1,3776$	$+1,4545$	$-8,1358$	$+3,2463 \cdot 10^{+1}$
9,75	$+1,5487$	$+9,8266 \cdot 10^{-1}$	$-6,8048$	$+2,6533 \cdot 10^{+1}$
10	$+1,6747$	$+5,1225 \cdot 10^{-1}$	$-5,7808$	$+2,1910 \cdot 10^{+1}$

$$\zeta_{2n}(x) = (-1)^n \int_0^x C_{2n}(x) dx$$

x	$\zeta_{16}(x)$	$\zeta_{18}(x)$	$\zeta_{20}(x)$
1	$-1,3034 \cdot 10^{+16}$	$+1,3251 \cdot 10^{+19}$	$-1,7076 \cdot 10^{+22}$
1,25	$-4,6343 \cdot 10^{+14}$	$+3,0111 \cdot 10^{+17}$	$-2,4809 \cdot 10^{+20}$
1,5	$-3,0468 \cdot 10^{+13}$	$+1,3722 \cdot 10^{+16}$	$-7,8401 \cdot 10^{+18}$
1,75	$-3,0636 \cdot 10^{+12}$	$+1,0119 \cdot 10^{+15}$	$-4,2417 \cdot 10^{+17}$
2	$-4,2070 \cdot 10^{+11}$	$+1,0614 \cdot 10^{+14}$	$-3,4005 \cdot 10^{+16}$
2,25	$-7,3339 \cdot 10^{+10}$	$+1,4582 \cdot 10^{+13}$	$-3,6836 \cdot 10^{+15}$
2,5	$-1,5441 \cdot 10^{+10}$	$+2,4794 \cdot 10^{+12}$	$-5,0619 \cdot 10^{+14}$
2,75	$-3,7891 \cdot 10^{+9}$	$+5,0118 \cdot 10^{+11}$	$-8,4349 \cdot 10^{+13}$
3	$-1,0556 \cdot 10^{+9}$	$+1,1690 \cdot 10^{+11}$	$-1,6486 \cdot 10^{+13}$
3,25	$-3,2729 \cdot 10^{+8}$	$+3,0759 \cdot 10^{+10}$	$-3,6852 \cdot 10^{+12}$
3,5	$-1,1120 \cdot 10^{+8}$	$+8,9712 \cdot 10^{+9}$	$-9,2379 \cdot 10^{+11}$
3,75	$-4,0893 \cdot 10^{+7}$	$+2,8608 \cdot 10^{+9}$	$-2,5568 \cdot 10^{+11}$
4	$-1,6119 \cdot 10^{+7}$	$+9,8604 \cdot 10^{+8}$	$-7,7161 \cdot 10^{+10}$
4,25	$-6,7547 \cdot 10^{+6}$	$+3,6404 \cdot 10^{+8}$	$-2,5132 \cdot 10^{+10}$
4,5	$-2,9895 \cdot 10^{+6}$	$+1,4287 \cdot 10^{+8}$	$-8,7597 \cdot 10^{+9}$
4,75	$-1,3895 \cdot 10^{+6}$	$+5,9224 \cdot 10^{+7}$	$-3,2435 \cdot 10^{+9}$
5	$-6,7511 \cdot 10^{+5}$	$+2,5794 \cdot 10^{+7}$	$-1,2685 \cdot 10^{+9}$
5,25	$-3,4148 \cdot 10^{+5}$	$+1,1749 \cdot 10^{+7}$	$-5,2131 \cdot 10^{+8}$
5,5	$-1,7919 \cdot 10^{+5}$	$+5,5745 \cdot 10^{+6}$	$-2,2411 \cdot 10^{+8}$
5,75	$-9,7272 \cdot 10^{+4}$	$+2,7460 \cdot 10^{+6}$	$-1,0041 \cdot 10^{+8}$
6	$-5,4483 \cdot 10^{+4}$	$+1,4002 \cdot 10^{+6}$	$-4,8724 \cdot 10^{+7}$
6,25	$-3,1415 \cdot 10^{+4}$	$+7,3712 \cdot 10^{+5}$	$-2,2519 \cdot 10^{+7}$
6,5	$-1,8611 \cdot 10^{+4}$	$+3,9972 \cdot 10^{+5}$	$-1,1211 \cdot 10^{+7}$
6,75	$-1,1309 \cdot 10^{+4}$	$+2,2283 \cdot 10^{+5}$	$-5,7521 \cdot 10^{+6}$
7	$-7,0377 \cdot 10^{+3}$	$+1,2748 \cdot 10^{+5}$	$-3,0360 \cdot 10^{+6}$
7,25	$-4,4794 \cdot 10^{+3}$	$+7,4719 \cdot 10^{+4}$	$-1,6449 \cdot 10^{+6}$
7,5	$-2,9127 \cdot 10^{+3}$	$+4,4808 \cdot 10^{+4}$	$-9,1369 \cdot 10^{+5}$
7,75	$-1,9327 \cdot 10^{+3}$	$+2,7457 \cdot 10^{+4}$	$-5,1947 \cdot 10^{+5}$
8	$-1,3073 \cdot 10^{+3}$	$+1,7173 \cdot 10^{+4}$	$-3,0191 \cdot 10^{+5}$
8,25	$-9,0123 \cdot 10^{+2}$	$+1,0952 \cdot 10^{+4}$	$-1,7917 \cdot 10^{+5}$
8,5	$-6,3233 \cdot 10^{+2}$	$+7,1157 \cdot 10^{+3}$	$-1,0844 \cdot 10^{+5}$
8,75	$-4,5133 \cdot 10^{+2}$	$+4,7059 \cdot 10^{+3}$	$-6,6883 \cdot 10^{+4}$
9	$-3,2751 \cdot 10^{+2}$	$+3,1657 \cdot 10^{+3}$	$-4,1998 \cdot 10^{+4}$
9,25	$-2,4147 \cdot 10^{+2}$	$+2,1647 \cdot 10^{+3}$	$-2,0827 \cdot 10^{+4}$
9,5	$-1,8079 \cdot 10^{+2}$	$+1,5039 \cdot 10^{+3}$	$-1,7421 \cdot 10^{+4}$
9,75	$-1,3737 \cdot 10^{+2}$	$+1,0009 \cdot 10^{+3}$	$-1,1487 \cdot 10^{+4}$
10	$-1,0588 \cdot 10^{+2}$	$+7,5950 \cdot 10^{+2}$	$-7,6970 \cdot 10^{+3}$

LITERATURE

1. Books and comprehensive reports

- LORD RAYLEIGH: The theory of sound. London 1929.
HAHNEMANN, W., u. H. HECHT: Schallfelder und Schallantennen I II. Phys. Z. Bd. 17 (1916) S. 601; Bd. 18 (1917) S. 261.
HAHNEMANN, W., u. H. HECHT: Schallgeber und Schallempfänger I—IV. Phys. Z. Bd. 20 (1919) S. 104, 245; Bd. 21 (1920) S. 264, 426.
AIGNER, F.: Unterwasserschalltechnik. Berlin 1922.
LAMB, H.: The dynamical theory of sound. London 1925.
CRANDALL, J. B.: Theory of vibrating systems and sound. New York 1926.
BACKHAUS, H.: Theorie akustischer Schwingungen. Handbuch der Physik von GEIGER-SCHEEL Bd. 8. Berlin 1927.
SCHOTTKY, W.: Elektroakustik. Die wissenschaftlichen Grundlagen des Rundfunkempfangs von K. W. WAGNER. Berlin 1927.
KÜPFMÜLLER, K.: Schwachstromtechnik. Handbuch der Experimentalphysik von WIEN-HARMS Bd. 11, 3. Teil. Leipzig 1931.
TRENDELENBURG, F.: Fortschritte der physikalischen und technischen Akustik. Leipzig 1932.
McLACHLAN, N. W.: Bessel functions for engineers. Oxford 1934.
HECHT, H., u. F. A. FISCHER: Anwendungen der Ausbreitung des Schalles in freien Medien. Handbuch der Experimentalphysik von WIEN-HARMS Bd. 17. Technische Akustik. Leipzig 1934.
BERGMANN, L.: Der Ultraschall. Berlin 1939.
HIEDEMANN, E.: Grundlagen und Ergebnisse der Ultraschallforschung. Berlin 1939.

2. Papers

- LORD RAYLEIGH: On the acoustic shadow of a sphere. Phil. Trans. roy. Soc. Lond. Bd. 203 A (1904) S. 87.
NICHOLSON, J. W.: On the diffraction of short waves by a rigid sphere. Phil Mag. Bd. 11 (1906) S. 193.
STEWART, S. W.: The acoustic shadow of a rigid sphere, with certain applications in architectural acoustics and audition. Phys. Rev. 1911 S. 467.
BACKHAUS, H., u. F. TRENDLENBURG: Über die Richtwirkung von Kolbenmembranen. Z. techn. Phys. Bd. 7 (1926) S. 630.
STENZEL, H.: Über die Richtwirkung von Schallstrahlern. Elektr. Nachr.-Techn. Bd. 4 (1927) S. 239.
BALLANTINE, S.: Effect of diffraction around the microphone in sound measurements. Phys. Rev. 1928 S. 988.
LINDSAY, R. B.: High frequency sound radiation from a diaphragm. Phys. Rev. (2) Bd. 32 (1928) S. 515.
BACKHAUS, H.: Über die Strahlungs- und Richtwirkungseigenschaften von Schallstrahlern. Z. techn. Phys. Bd. 19 (1928) S. 491.
BACKHAUS, H.: Über die Strahlungs- und Richtwirkungseigenschaften von Schallstrahlern. Z. angew. Math. Mech. Bd. 8 (1928) S. 456.
McLACHLAN: Sound distribution from vibrating rigid disk. Proc. roy. Soc., Lond. Bd. 122 (1929) S. 604.
STENZEL, H.: Über die Richtcharakteristik von in einer Ebene angeordneten Strahlern. Elektr. Nachr.-Techn. Bd. 6 (1929) S. 165.
STENZEL, H.: Interferenzen durch Kolbenmembranen von besonderer Form. Z. techn. Phys. Bd. 10 (1929) S. 567.
WOLFF, J., u. L. MALTER: Sound radiation from a system of vibrating circular diaphragms. Phys. Rev. (2) Bd. 33 (1929) S. 282.

- STRUTT, M. J. O.: The effect of a finite baffle on the emission of sound by a double source. *Phil. Mag.* (7) Bd. 7 (1929) S. 537.
- STRUTT, M. J. O.: Die Wirkung einer endlichen Schirmplatte auf die Schallstrahlung eines Dipols. *Z. techn. Phys.* Bd. 10 (1929) S. 124.
- BACKHAUS, H.: Das Schallfeld der kreisförmigen Kolbenmembran. *Ann. Phys., Lpz.* (5) Bd. 5 (1930) S. 1.
- STENZEL, H.: Über die Berechnung und Bewertung der Frequenzkurven von Membranen. *Elektr.-Nachr.-Techn.* Bd. 7 (1930) S. 87.
- STENZEL, H.: Über die akustische Strahlung von Membranen. *Ann. Phys., Lpz.* (5) Bd. 7 (1930) S. 947.
- FISCHER, F. A.: Über die künstliche Charakteristik der Kugelgruppe. *Elektr. Nachr.-Techn.* Bd. 7 (1930) S. 369.
- STENZEL, H.: Akustische Strahlung von punktförmigen Systemen und Membranen. *Forsch. u. Techn.* 1930 S. 349.
- STRUTT, M. J. O.: Über die Schallstrahlung einer mit Knotenlinie schwingenden Kreismembran. *Ann. Phys., Lpz.* (5) Bd. 11 (1931) S. 129.
- RUEDY: Sound field near quartz oscillators. *Canad. J. Res.* Bd. 5 (1931) S. 297.
- MCLACHLAN, N. W.: The distribution of sound radiation from a sphere vibrating in various ways; with applications to Loudspeaker diaphragms. *Phil. Mag.* Bd. 13 (1932) S. 747.
- MCLACHLAN, N. W.: Accession to of flexible disks vibrating in a fluid. *Proc. phys. Soc., Lond.* Bd. 44 (1932) S. 546.
- MCLACHLAN, N. W.: Sound distribution from disks with nodal lines. *Ann. Phys., Lpz.* Bd. 15 (1932) S. 422.
- MCLACHLAN, N. W.: Power radiated by disks with nodal lines. *Ann. Phys., Lpz.* Bd. 15 (1932) S. 440.
- MCLACHLAN, N. W.: Sound pressure at any point on vibrating disk. *Phil. Mag.* Bd. 14 (1932) S. 1012.
- SIVIAN and O'NEILL: Sound diffraction due to a rigid disk, square plate, and semi-infinite screen. *J. acoust. Soc. Amer.* Bd. 3 (1932) S. 483.
- FISCHER, F. A.: Über die akustische Strahlungsleistung von Strahlergruppen, insbesondere der Kreis- und Kugelgruppen. *Elektr. Nachr.-Techn.* Bd. 9 (1932) S. 147.
- MCLACHLAN, N. W.: Accession to inertia of and power radiated by a sphere vibrating in various ways; with applications to hornless loudspeakers. *Phil. Mag.* Bd. 15 (1933) S. 443.
- MASAAKI SASAO: On the sound emission by a vibrating membrane. *Proc. phys.-mat. Soc., Japan* 1933 S. 86.
- FISCHER, F. A.: Richtwirkung und Strahlungsleistung von akustischen Strahlern und Strahlergruppen in der Nähe einer reflektierenden ebenen Fläche. *Elektr. Nachr.-Techn.* Bd. 10 (1933) S. 19.
- KING, L. V.: On the acoustic radiation field of the piezo-electric oscillator and the effect of viscosity on transmission. *Canad. J. Res.* Bd. 11 (1934) S. 484.
- GROSSMANN, E.: Ultraakustik. *Handbuch der Experimentalphysik von WIEN-HARMS* Bd. 17, 1. Teil, Schallbeugungserscheinungen S. 486.
- STENZEL, H.: Über die Berechnung des Schallfeldes einer kreisförmigen Kolbenmembran. *Elektr. Nachr. Techn.* Bd. 12 (1935) S. 16.
- KING, L. V.: On the acoustic radiation pressure on circular discs. Inertia and diffraction corrections. *Proc. roy. Soc., Lond.* Bd. 153 (1935) S. 17—40.
- STENZEL, H.: Über die von einer starren Kugel hervorgerufene Störung des Schallfeldes. *Elektr. Nachr.-Techn.* Bd. 15 (1938) S. 72.